UNIVERSITÀ DEGLI STUDI DI NAPOLI

"FEDERICO II"

Scuola di Dottorato in Medicina Molecolare

Dottorato di Ricerca in Genetica e Medicina Molecolare

OA1: AN INTRACELLULAR GPCR INVOLVED IN MEMBRANE TRAFFICKING DURING MELANOSOME BIOGENESIS

Coordinatore:
Prof. Carmelo Bruno Bruni

Candidato:
Dott. ssa Francesca Giordano

ANNO ACCADEMICO 2003/2007

UNIVERSITÀ DEGLI STUDI DI NAPOLI

"FEDERICO II"

TIGEM Telethon Institute of Genetics and Medicine

Dottorato di Ricerca in Genetica e Medicina Molecolare

Coordinatore Prof. Carmelo Bruno Bruni

Dipartimento di Biologia e Patologia Cellulare e Molecolare "Luigi Califano"

UNIVERSITÀ DEGLI STUDI DI NAPOLI

"FEDERICO II"

TIGEM Telethon Institute of Genetics and Medicine

Tesi di Dottorato di Ricerca in Genetica e Medicina Molecolare
XIX ciclo

OA1: AN INTRACELLULAR GPCR INVOLVED IN MEMBRANE TRAFFICKING DURING MELANOSOME BIOGENESIS

Docente guida:
Prof. ssa Valeria Marigo

Candidato:
Dott. ssa Francesca Giordano

TABLE OF CONTENTS

1. INTRODUCTION

1.1 Melanogenesis

Eye, hair and skin colour is one of the most obvious phenotype in individuals and it is the result of the presence and distribution of melanins. Melanins are complex pigments exclusively synthesized in a population of highly specialized cells including the epidermal and choroidal melanocytes (Hearing and Tsunkamoto, 1991) and the cells of the pigment epithelium of the retina (RPE), iris and ciliar body of the eye. Melanins tipically consist of copolymers of black and brown melanins (eumelanins) -unsoluble in all the solvents- and red and yellow melanins (pheomelanins) -soluble in alkalis and containing sulphur.

Both types of melanins are synthesized in sequential reactions, initiated by the conversion of tyrosine to L-DOPA (Aroca et al., 1993), catalyzed by a key enzyme, Tyrosinase (TYR), that mediates also the next oxidation of L-DOPA in dopaquinone (Hearing et al., 1992), (Winder et al., 1994); (Jimenez et al., 1991). Pheomelanins are synthesized under certain conditions by subsequent reduction reactions requiring cysteine (Hearing et al., 1999). Eumelanins result from sequential oxidation and hydroxylation reactions, mediated in part by tyrosinase and the related enzymes, Tyrp1 and Tyrp2 (TRP1 and TRP2) (Jackson et al., 1992). Reactive indoles are the end-result of these reactions (Figure 1).

Specialized cell types often require unique organelle to fulfil their specific function. Indeed, in pigmented cells melanin synthesis is confined within unique organelles termed melanosomes (Marks and Seabra, 2001). Sequestration within melanosomes protects component of the cytosol and other membranous organelles from oxidative attack during melanin synthesis,

and concentrates melanin for storage (in eye pigment cells) or cell transfer (from epidermal melanocytes to keratinocytes in the skin and hair).

Melanosomes transfer to keratinocytes provides colour but also photoprotection from ionizing radiations.

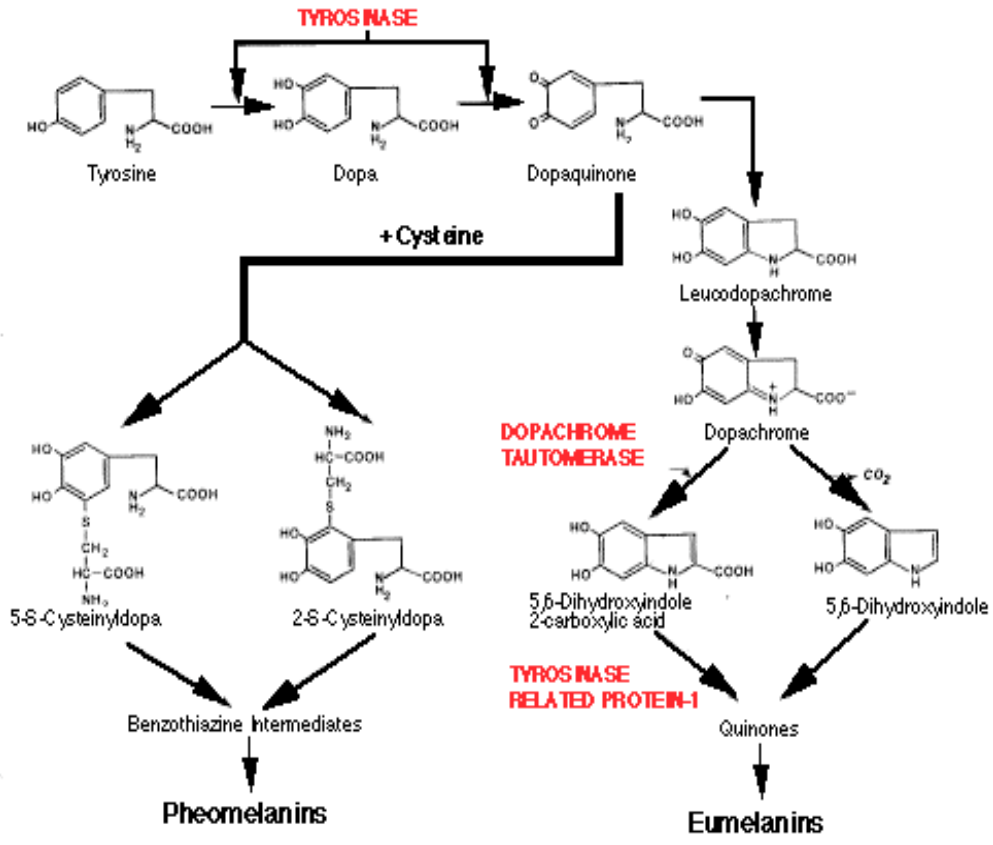

Figure 1. ***The main steps of melanin biosynthesis.*** The enzymes (Tyrosinase, Tyrp-1 and DCT) that catalyze different steps of melanin synthesis are labelled in red.

Melanosomes are not simply pigment-filled granules, but rather organelles that mature from unpigmented premelanosome to fully pigmented melanosomes through four morphologically distinct stages (Seiji et al., 1963) (Figure 2).

The first stage is an endosomal intermediate containing internal vesicles - similar to early multivesicular endosomes (MVBs)- in which amyloid-like fibers begin to form and organize in the typical striation of the stage II

premelanosomes (Piper RC, Luzio JP, 2001). Melanins begin to be deposited on the amyloid-fibers as they are synthesized, in stage III melanosomes, until the entire luminal space is filled, and the organelle reaches its final stage: stage IV.

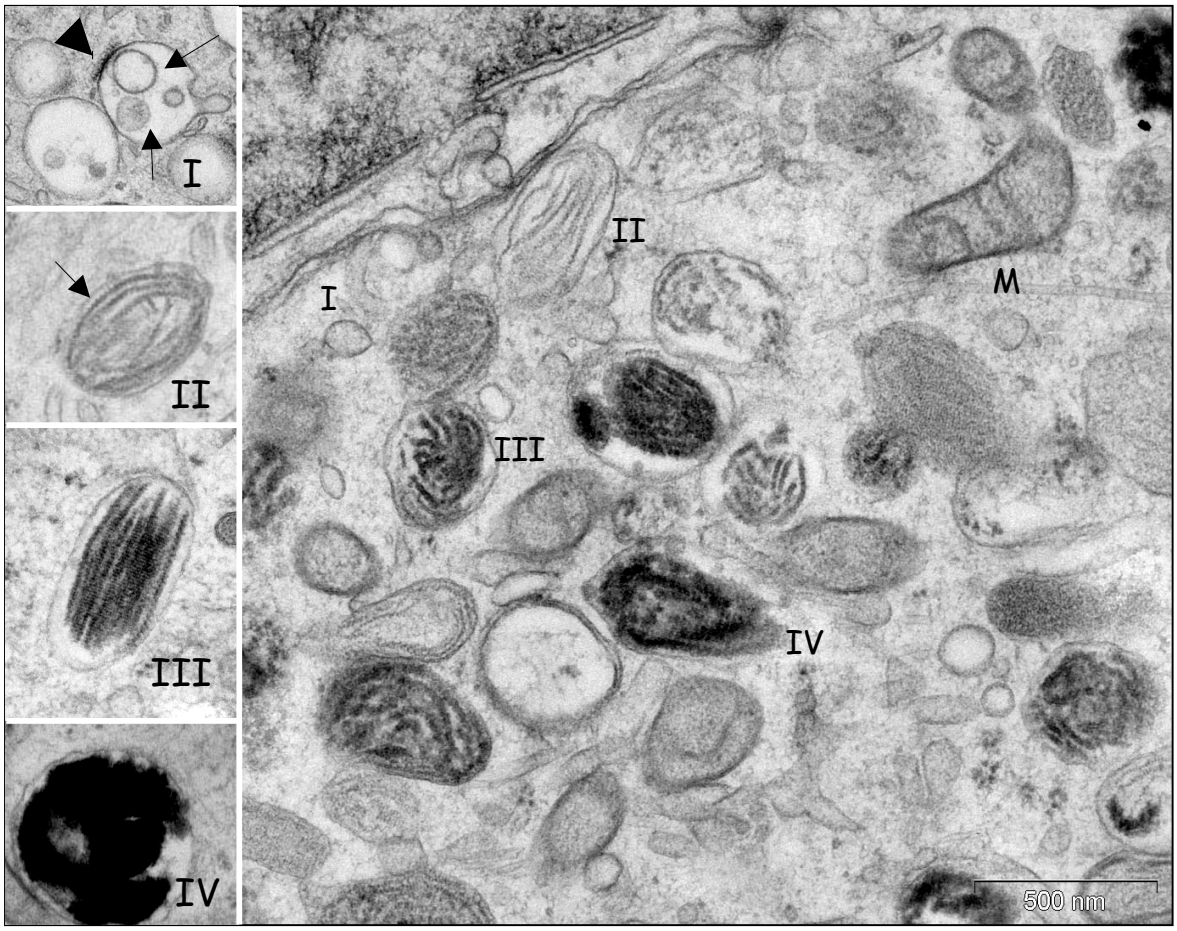

Figure 2 : Ultrastructural characterization of melanosomes. *E*lectron microscopy analyses of a MNT-1 human melanoma cells (from Raposo and Marks, Nat.Rev.Mol.Cell., 2007). The four stages of melanosome development are shown also in detail in the lateral panels. Note the dense bilayered coat (arrowhead) and intralumenal vesicles (arrow) of stage I premelanosomes, the proteinaceous fibrils (arrow) of stage II, and the melanin deposition (black) in stage III and IV. The main panel shows a typical field of MNT-1 cytoplasm, which contain all four stages melanosomes. M, mitocondria. Scale bar represent 500 nm.

In eye pigment cells, stage IV melanosomes are retained and absorb stray light and probably trap free radicals (Futter C.E. 2006). In epidermal melanocytes, stage IV melanosomes are translocated along microtubules from the cell centre to actin-rich dendritic tips, and then transferred in a still-

unresolved manner to neighbouring keratinocytes (Van Den Bossche et al., 2006). Melanosome translocation in these cells involves bidirectional transport along microtubules, facilitated by both dynein and kinesin motors, and peripheral capture on actin filaments (Seabra M and Coudrier E. 2004). Capture on actin filament is mediated, at least in part, by a complex that consists of myosinVa, the small GTPase RAB27a and the linker protein melanophilin (Seabra M and Coudrier E. 2004).

1.2 Melanosome composition and biogenesis

Melanosomes are classified as Lysosome Related Organelles because of their shared features with lysosomes such as: acidic pH, presence of Lysosomal membrane proteins and lysosomal hydrolases, accessibility to endocytic tracers. Nevertheless these organelles have distinct morphological and functional features that are likely to be acquired during their biogenetic process. Melanosomes generate by a multistep process in which an immature organelle forms within the endocytic system and matures by acquisition of additional cargo and effectors proteins. Although they find their origin within the endocytic pathway they coexist and remain distinct from conventional bona fide late endosome/lysosomes (Raposo et al., JCB 2001).

The melanogenic enzymes and structural components of melanosomes (Box 1) are synthesized by pigment cells and must be appropriately targeted to the newly forming melanosomes. Most known components are integral membrane proteins that are uniquely expressed in pigment cells, and mutation in the genes that encode them often cause albinism in humans or coat-colour dilution in animals (Bennett D.C. et al, 2003). For example Pmel17 serves as the structural foundation of the fibrils in stage I and II melanosomes, whereas the melanin biosynthetic enzymes Tyrosinase, Tyrosinase-related protein and

DOPAcrome tautomerase (DCT) are enriched in stage II and IV melanosomes (Raposo et al. 2001; Theos et al. 2005). Melanosomes also harbour ubiquitous components of lysosomes and late endosomes, one example is Lamp-1 (Orlow S.J., 1995; Chi A. et al., 2006). Melanosomal proteins must be also appropriately sorted from the macromolecules destined for conventional lysosomes.

Studies in skin melanocytes from the human patients or mouse models for these pigmentary disorders (e.g. Hermansky Pudlak Syndrome (HPS), a complex genetic disease in which melanosomal protein sorting is defective (Wei M.L., 2006)) begun to elucidate the cellular and molecular mechanisms involved in the trafficking of melanosomal matrix proteins and melanosomal enzymes. All these studies lead to propose a model (Figure 3) in which melanosome biogenesis requires firstly the generation of unpigmented premelanosomes and their Pmel17 driven intraluminal fibers and secondly the transfer of the key enzymes involved in melanin synthesis (Tyrosinase and Tyrp1) (Raposo et al. 2001). In the first event, the transmembrane protein Pmel17 is sorted in endosomal compartments with hallmark of MVBs (Berson et al., 2001; Berson et al., 2003). Pmel17 sorting to the intralumenal vesicles does not require ubiquitination and is not dependent on the ESCRT machinery (Endosomal Sorting Complex responsible for Transport) (Theos et al., 2006) involved in MVB biogenesis (Williams et al., 2007). In these MVBs, Pmel17 is cleaved by a prohormone convertase liberating a fibrillogenetic fragment in its luminal domain, which leads the generation of the striations by a still poorly understood mechanism (Berson et al., 2003). Once premelanosomes are formed, melanogenetic enzymes are transferred to the maturing organelle. It has been recently shown that Tyrosinase traffics through the early endocytic pathway to the maturing melanosome and its sorting requires the recognition of its cytoplasmatic tail by two heterotetrameric adaptors AP-3 and AP-1 (Theos et al., 2005). Altogether these studies indicate that multiple sorting

events participate to the creation of the optimal environment for the melanogenesis, the targeting of melanosomal components and the maintenance of melanosomal identity (Raposo and Marks, 2007). The biosynthetic and endocytic transport in melanocytes requires requires a tight regulation by ubiquitous mechanisms of trafficking (Adaptors, SNAREs, small GTPases of the Rab superfamily) but also additional levels of specialization that are fulfilled by other proteins with still unknown functions in which mutations affect pigmentation (e.g. Biogenesis of Lysosome-related Organelles Complexes -BLOCs- mutated in HPS) or by the melanosomal protein themselves (Raposo et al., 2002).

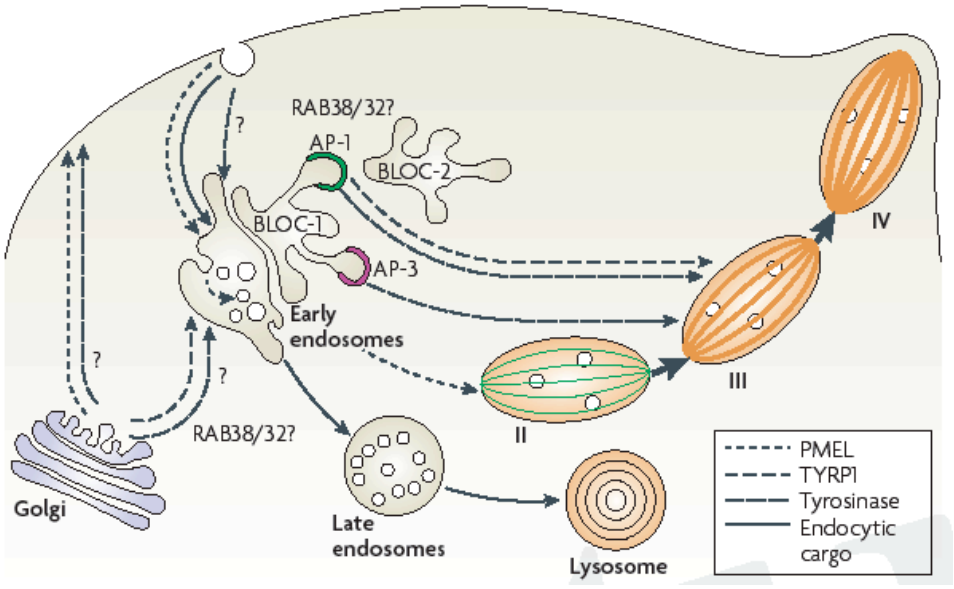

Figure 3: Model for melanosome maturation (from Raposo and Marks, Nat.Rev.Mol.Cell., 2007). Schematic diagram of endosomal and melanosomal stages, and the biosynthetic transport pathways among them for three representative melanosome cargoes – PMEL, tyrosinase and tyrosinase-related protein-1 (TYRP1). The divergence of endocytic cargo that is internalized by fluid phase and destined for lysosomes is also shown. Transport pathways for each cargo are indicated by solid or dashed lines as indicated in the key. All melanosome cargoes derive from the Golgi and traverse vacuolar and/or tubular elements of early endosomes either directly or through the cell surface. From vacuolar elements, PMEL fibrils (green) segregate to stage II melanosomes, and endocytic cargo segregates to late endosomes and eventually lysosomes. From tubular elements of early endosomes, tyrosinase and TYRP1 are targeted to maturing melanosomes where they promote melanin deposition (orange). Adaptor protein-3 (AP-3) coats initiate one endosome-to-melanosome pathway for a cohort of tyrosinase; biogenesis of lysosome-related organelle complex-1 (BLOC-1), BLOC-2 and perhaps AP-1 regulate a second pathway that is traversed by a separate cohort of tyrosinase and by TYRP1.

1.3 Albinism

The melanogenic function of pigmented cells can be altered in some inherited and acquired disorders, with consequent hypopigmentation. In addition to the serious esthetical problems, the melanocyte malfunction may expose the skin to the dangerous effects of UV radiations and increase the risk of melanoma (Sober, 1991). The "pigmentation diseases" include a wide heterogeneous range of pathological conditions. Among these, **albinism** –a genetical disease with a frequency of 1:20000 births- comprises a group of hereditary conditions in which the skin, hair and eye pigment cells show an altered melanin synthesis and/or distribution. Albinism was one of the first genetic inherited diseases to be noted in humans (for the obvious hypopigmented phenotype of hair, eyes and skin), but until relatively recently, little was known about the molecular mechanisms involved in its pathogenesis. Mutations in at least five different genes (Box 1) can cause a reduction in melanin pigment biosynthesis, producing the various clinical features associated with albinism, including hypopigmentation of the skin, hair, and eyes; optic tract misrouting; foveal hypoplasia; and reduced visual acuity.

Two main categories of albinism have been described:

- **Oculocutaneous albinism** (OCA), whose phenotypical alterations affect skin, eyes and hair
- **Ocular albinism** (OA), that involves primarily the eyes, while skin and hair appear normal.

There are several types of oculocutaneous albinism (and multisystem disorders characterized by partial albinism) while there is only one major type of ocular albinism. Many genetic loci that affect melanosome function have been identified by their phenotype in mice with coat colour dilution or in human OCA patients. The function of the proteins affected in albinism is strictly related and specific to melanosome function, in fact are all expressed

only in pigment cells. In the mouse mutations have been found in ubiquitous proteins involved in the motility (rab27/myosinV) (Seabra M and Coudrier E. 2004) and/or formation of melanosomes (P, Matp) and other LROs in various tissues (Wei et al., 2006). A correlation with pigment defects in humans is still under investigation for these latter proteins.

Only one gene mutated in Ocular Albinism (OA) patients has been cloned so far and is called OA1 (GPR143) (Bassi et al. 1995).

Box 1: ***PIGMENTATION GENES AND THEIR PROTEINS.***

Gene	Mouse model	Disease	Protein/function	melanosomal defect
TYR	Albino (*c*)	OCA1	Tyrosinase Melanin enzyme	-Absence of melanin -Melanosome block at stage II
TRP1	Brown (*b*)	OCA3	TRP-1 Melanin enzyme	-reduction of melanin content
MATP	Underwhite (*uw*)	OCA4	MATP Putative membrane transporter	-hypopigmentation due to an abnormal trafficking of Tyrosinase -Small and irregular melanosomes blocked at stage III
P	Pink-eyed dilution (*p*)	OCA2	P-protein Putative anion transporter	-reduction of melanin content -alteration of melanosome architecture -mislocalization of melanin enzymes
OA1	Oa1 KO	OA1	OA1 Intracellular GPCR	-Pigmented macromelanosomes

Mouse models of pigmentary disorders have been of great value for the elucidation of the molecular mechanisms underlying the biogenesis of melanosome. Hermansky-Pudlack syndrome (HPS) is one example of another kind of human pigmentary disease that have helped to highlight novel trafficking steps operating in specialized cell types by the study of its several mouse models. HPS is a complex disorder characterized by partial albinism and bleeding defects, lung fibrosis and ceroid accumulation in lysosomes and major defects are observed in melanosomes and platelet dense granules (Wei

M.L., 2006). HPS results from mutations in any of at least eight genes, and a similar disorder in mouse results from mutations in at least 15 different genes. Most of the genes encode subunits of multimeric protein complexes. Some of the complexes, such as the adaptor protein complex AP3, that are known to be involved in vesicular transport, are also involved in the sorting of melanosomal cargo, whereas others, such as the biogenesis of lysosome-related organelles complex-1 (BLOC-1, BLOC-2 and BLOC-3), that consist of a subunits that lack common structural motif or homology to protein of known function, give specificity to this transport. In fact cargo sorted by AP3 is destined for late endosomes and lysosomes in several cell types; instead, in pigment cells, tyr and tyrp-1 are destined for melanosomes, which indicated that additional effectors must participate in their sorting. Some of these effectors may include BLOCs and other complexes that are also defective in HPS (Wei et al., 2006; Di Pietro e Dell'Angelica, 2005).

1.4 Role of components of the secretory system in melanosome biogenesis.

The secretory system of eukaryotic cells is organized as a series of membrane-enclosed compartments that include the endoplasmic reticulum (ER), Golgi cisternae, the *trans*-Golgi network (TGN), various types of secretory vesicle and the plasma membrane (Bonifacino et al., 2004). This system interconnects at several junctures with the endosomal-lysosomal system, another array of membrane-enclosed compartments, that comprise different types of endosomes (for example, early, late and recycling endosomes) and lysosomes, as well as cell-type specific lysosome-related organelles (for example, melanosomes). Newly synthesized proteins that are destined for secretion into the extracellular space or for residence within organelles of the secretory and endosomal-lysosomal system move from the ER to their final destinations.

This outward flow is counterbalanced by an influx of protein that follow the endocytic pathway and by various retrograde-transport pathways. Among the organelles of the secretory pathway the TGN has a central role as a site of protein sorting (Griffiths et al., 1986) (Bonifacino et al., 2004). Once proteins coming from the ER reach the TGN, the TGN sorts them to each of their possible destinations (extracellular space, different domains of the plasma membrane, secretory vesicles and endosomes) into specific sets of membrane-enclosed carriers. This role of the TGN as a traffic hub is not limited to forward-transport pathways, because the TGN also receives proteins by retrograde transport from more distal organelles, most notably endosomes (Rohn et al., 2000). The movement of proteins between these different compartments is a highly regulated process mediated by many different factors, including SNARE and SNARE attachment proteins (Gerst, 1999), small GTP-binding proteins (Pfeffer, 1996) and vesicle tethering factors (Whyte and Munro, 2002). Tethering factors can be categorized as long, coiled-coil proteins (e.g. GM130/Golgin-95) or multisubunit protein complexes (e.g. TRAPPI, II and COG) that physically link the vesicles and the target membranes upstream of membrane fusion and are believed to significantly contribute to the specificity of the transport reaction (Lowe, 2000; Whyte and Munro, 2002). How the different types of tethering factors contribute to the overall specificity of this process is presently unknown.

Recently, a new mouse model, for mosaic hypopigmentation (*mhyp)* has been identified, in which the mutated gene is *Trappc6*, a subunit of the TRAPP tethering complex, that has been implicate in control of pigmentation and melanosomal size. In fact *Trappc6* mutant RPE shows patchy areas of depigmentation and irregular smaller, incompletely melanized, melanosomes (Gwynn B. et al., 2006). *Trappc6*, the mammalian homologue of the yeast trs33, is a subunit of the TRAPP (transport protein particle) I and II multiprotein complexes (Figure 4), required for tethering ER-derived vesicles

to Golgi membranes (Figure 5) and for Golgi traffic (Cai et al. 2005, Sacher et al. 1998, 2001).

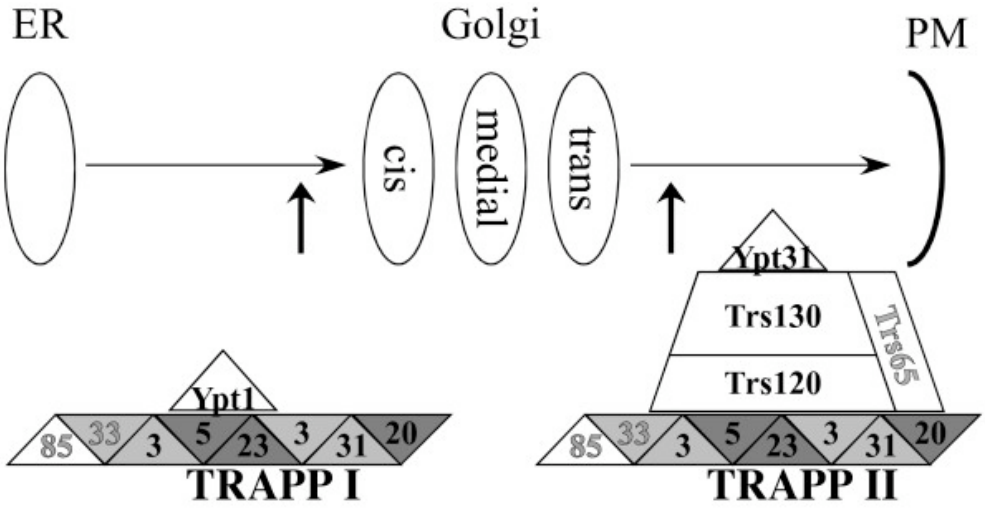

Figure 4: ***Model for the conserved structure and function of the TRAPPI and TRAPPII complexes in yeast*** (from Cox et al. 2007). TRAPP complexes mediate exocytic trafficking from the ER, trough the Golgi, to the plasma membrane. The TRAPPI complex (left) is shown as a quadrilateral with subunits indicated as triangolar sections. Subunits are 3-Bet3, 5-Bet5, 20-Trs20, 23-Trs23, 31-Trs31, 33-Trs33. The TRAPPII complex (right) includes all the TRAPPI components plus the three TRAPPII-specific subunits shown in the trapezoidal shape above TRAPPI. In both complexes, subunits essential for viability are labeled in black letters, while non-essential subunits are shown in grey letters. Functionally, TRAPPI is the GEF (Guanine exchange factor) for Ypt1 (homologue to the mammalian Rab-1), the GTPase that regulates entry into the Golgi, wherease TRAPPII is the GEF for Ypt31/32, the GTPases that regulate exit from the Golgi (Morozova et al., 2006).

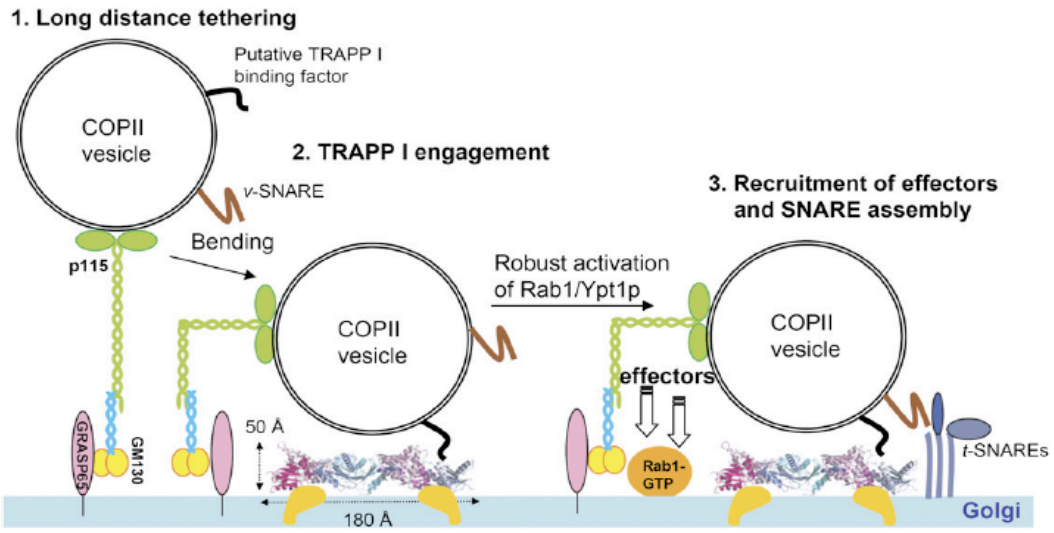

Figure 5: ***a model for the action of TRAPP I in the ER-Golgi compartment*** (from Kim et al. 2006). A transport vesicle is first captured at a long distance by long, coiled coil proteins (p115, GM130) (step 1). A bending motion in the nonhelical region of the coiled-coil protein brings the vesicle into close proximity to TRAPP I (step 2), which is anchored to the Golgi by an as yet unidentified mechanism. Upon recognition of an unidentified factor on the surface of the vesicle, the transport vesicle is more tightly tethered to the Golgi. Activation of Rab1/Ypt1p (step3) leads to recruitment of effector molecules (SNARE protein, e.g. stx5) to eventually enable fusion.

While TRAPP complexes are essential for ER-to-Golgi and intra-Golgi vesicle trafficking in yeast, TRAPP subunits participate in additional events in mammals, including post-Golgi transport. In fact, another subunit of the TRAPP complex, *Trappc4*, is found in the spines of neural dendrites in mouse. Here it is thought, with other proteins, to recruit intracellular vesicles to postsynaptic sites (Ethell et al. 2000). However a recent study has shown that mutation of some of the TRAPP subunits impair cargo retrieval from early endosomes to the TGN also in yeast (Cai et al., 2005). Together these data indicate that TRAPP subunits play a role in multiple vesicular transport events and perform specific critical functions beyond generalized ER-to-Golgi transport. In particular, the *mhyp* phenotype implicates for the first time a TRAPP subunit, *Trappc6a*, in melanosome biogenesis. There are also other complexes similar to TRAPP, like the COG complex which primary function is intra-Golgi transport. Interestingly, mutations in some subunits impair also

retrograde transport from both early and late endosomes to the TGN (Ungar et al., 2006). The yeast homolog (Sed5p) of Syntaxin-5, a t-SNARE protein important for vesicle transport and fusion between ER-Golgi, interacts with one TRAPP subunit and some COG subunits in yeast (Barrowman et al., 2000). Moreover syntaxin-5 is also required in transport events from early endosomes to the TGN (Tai et al. 2004).

1.5 Ocular Albinism Type 1 (OA1): the disease

Ocular Albinism type 1 (OA1) represents the most common form of ocular albinism, with an estimated prevalence of 1:50000. This disorder is transmitted as an X-linked recessive trait, with carrier females showing only minor signs of the disease. Affected males with OA1 exhibit optic abnormalities typical of all forms of albinism, including severe reduction of visual acuity because of fovea hypoplasia, nystagmus, strabismus, photophobia, iris translucency, hypopigmentation of the retina, and misrouting of the optic tracts, resulting in loss of stereoscopic vision (King et al.1995). Most female carriers for OA1 can be clinically identified by a typical mud splattered mosaic pattern of depigmentation in the periphery of the ocular fundus (Lang et al., 1990), suggesting that the *OA1* gene is subject to X-inactivation. Therefore diagnosis is based on the X-linked transmission and on the ophthalmologic examination of the ocular fundus in the patient's mother. As in other forms of albinism, the OA1 patients manifests an alteration of the optic tract due to a misrouting of the optic fibres at the chiasm. In the normal mature and pigmented eye the retinal ganglion cells axons originating from the nasal region of the retina cross the chiasm and are projected to the opposite (contralateral) side of the brain. Instead the fibers originated from the temporal retina do not cross the chiasm and are projected to their own

(ipsilateral) side of the brain (Figure 6). The divergence of these fibers begins early during eye development, at embryonic day E15.5. In the human adult eye the contralateral-ipsilateral fibers ratio is about 55:45. This ratio is important for the overlap of the ocular fields necessary for the stereoscopic vision. In albinism this ratio is altered: a large proportion (>90% in some forms of albinism) of optic fibers originating in temporal retina cross the midline at the chiasm and project to the contralateral hemisphere, hampering stereoscopic vision in the albino patients.

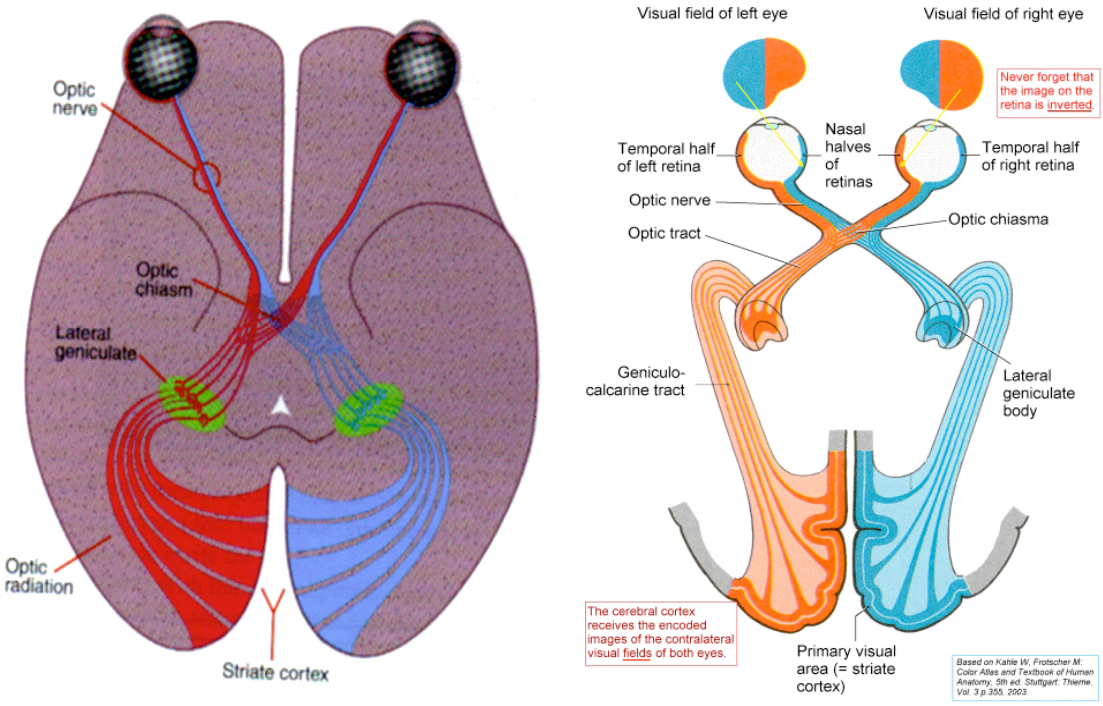

Figure 6. ***Schematic diagram of the visual field.*** The fibers from the nasal retina cross over at the optic chiasm and project to the contralateral side of the brain (lateral geniculate bodies and superior collicoli), whereas the fibers from the temporal retina, arrive at the chiasm and then do not cross, but are projected to their own side.

These features are common to all forms of albinism, including ocular albinism type 1 (OA1). Differently to the oculocutaneous albinism (OCA) in which

pigmentation is strongly affected, Oa1 patients display minimal cutaneous changes and mild hypopigmentation of skin and hair is found only in rare cases. Nevertheless, microscopic examination of melanocytes, in both retinal pigment epithelium (RPE) and in the skin, reveals the presence of large pigment granules called giant melanosomes or macromelanosomes. The macromelanosome phenotype suggest that the OA1 phenotype is not due to an impairment of melanin synthesis, but to a defect in the melanin biogenesis (Garner and Jay, 1980) (Yoshiike et al., 1985). This idea it is strongly supported by the phenotype analysis of *knock-out* mice for *Oa1*, displaying the same defects as the patients, such as misrouting of the optic fibers at the chiasm, hypopigmentation of the fundus and macromelanosomes in the RPE (Incerti et al., 2000) (Figure 7).

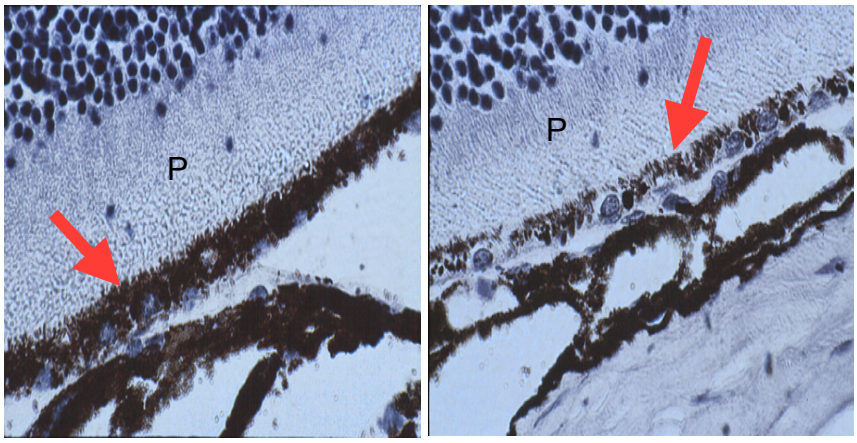

(a) (b)

Figure 7. Hystological analysis *wild-type* (a) and *Oa1 knock-out* (b) mouse RPE. Oa1 knockout RPE displays hypopigmentation and presence of giant melanosomes (red arrows). F: photoreceptors

1.6 *OA1* gene and its regulation

The gene responsible for ocular albinism was isolated by a classical positional cloning strategy from the distal short arm of the X chromosome (Bassi et al. 1995). In OA1 patients were found missense, nonsense mutations and deletions were found, suggesting that Ocular albinism type 1 is caused by "loss of function" disease. A recent study has identified a novel intronic point mutation in a family with this form of albinism. The mutation creates a new acceptor splice site in intron 7 of the *OA1* gene, leading to the formation of an aberrant spliced mRNA, unstable, that contained a premature stop codon (Vetrini et al., 2006).

OA1 transcript is expressed exclusively in pigmented cells of skin and eye, and in melanoma, consistent with the clinical phenotype of the disease. The murine *Oa1* gene starts to be transcribed in the RPE at early stages of eye development (E10.5 in mouse eyes) and continues to be expressed until adulthood in pigment cells of the eye (Surace et al., 2000) (Figure 8). *Oa1* transcript is also expressed in neural crest derived melanocytes. Similarly to other forms of oculocutaneous albinism, *Oa1* expression starts before the first melanin deposition. Indeed the albinism genes show common mechanisms of regulation at transcriptional level.

Oa1 expression is regulated similarly to that of melanogenic enzymes, such as tyrosinase (Tyr). In fact expression of *Oa1* parallels temporally and spatially that of *Tyr* during development, and is regulated by the transcription factor Mitf (Vetrini et al., 2004).

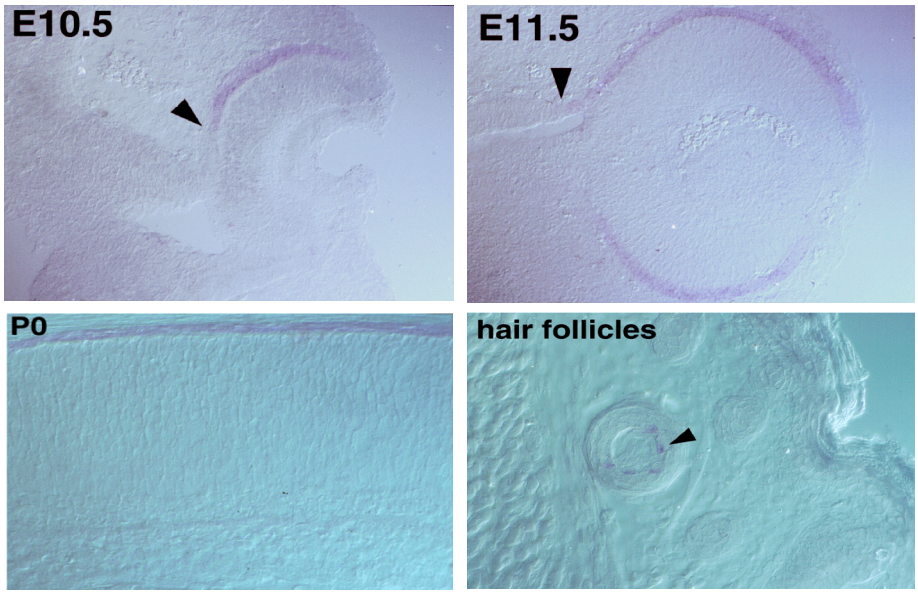

Figure 8. ***Oa1 expression in mouse RPE at different developmental stages***: at embryonic days E10.5 and E11.5), at birth (P0) and in hair follicoles. Arrow: OA1 transcript in RPE.

1.7 *OA1* protein: structure and localization

The protein product of the *OA1* gene is a pigment cell specific membrane glycoprotein of 404 aminoacids, displaying seven transmembrane domains and structural homology with G protein-coupled receptors (Innamorati et al. 2006, Schiaffino et al., 1999).

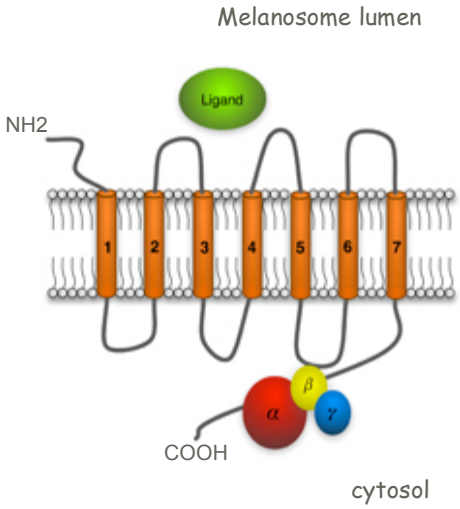

Considering that GPCRs belonging to different families do not share major primary sequence similarities, but rather a common three-dimensional structure that requires the presence of critical residues at precise positions (Gether, 2000; Pierce et al., 2002), the sequence homologies between OA1 and GPCRs viewed in the context of the seven spanning membrane topology are highly significant. Alignment between OA1 and these receptors indicates that it is equally distant from all three families, possibly defining a new GPCR subfamily (Schiaffino et al. 1999). In addiction, orthologs of OA1 have now been identified in several species. OA1 is significantly conserved in mammals, birds, amphibians and fish, particularly at the N-terminus and from the third to the seventh transmembrane domains, while the C-terminal tail displays higher divergence (Schiaffino et al. 2005).

The endogenous OA1 protein was characterized by western immunoblotting in normal human melanocytes extracts as a doublet of 45 and 48kD and a broad band of 60 kD. Studies in both melanocytes and transfected COS7 cells established that the 45 kD band corresponds to the OA1 protein backbone, the 48 kD polypeptide to a yet unknown post-translational modification, and the 60 kD band to the N-glycosylated form of both the former protein species. Glycosylation of OA1 protein initiates in the endoplasmic reticulum (ER) and is completed in the Golgi apparatus (D'Addio et al.2000). OA1 appears to be an integral membrane glycoprotein of the exocytic pathway, consistent to its homologies to GPCRs.

The endogenous OA1 was found to co-immunoprecipitate with heterotrimeric G-proteins in melanocyte extracts and in particular the third cytosolic loop and the C-terminal tail of OA1 are able to bind Gα-inhibitory proteins by *in vitro* binding assays (Schiaffino et al. 1999). These functional findings suggest that OA1 behaves as a canonical GPCR.

OA1 is localized to the membrane of an intracellular organelle, the melanosome. However some controversy exist on the precise subcellular localization of the protein. In fact studies carried out on human melanoma cell line MNT1 showed the localization of endogenous OA1 to the membrane of melanosome at early and later stages of maturation. While studies on mouse melanocytes by using the recombinant OA1-enhanced green fluorescent protein (EGFP) did not allowed for a proper localization of OA1. In these latter studies OA1 was not detected in the membrane of melanosome but only in the endo-lysosomal compartment (Samaraweera et al., 2001). This discrepancy might be due to the different techniques or cell line used. Interestingly, in contrast to previously characterized GPCRs and to other melanosome proteins (Raposo et al. 2001), OA1 does not translocate through the plasma membrane. This is a unique feature for a GPCR. In fact, OA1 represent the first example described so far of an exclusively intracellular GPCR, that mediates signal transduction from the organelle lumen to the cytosol.

1.8 The *OA1* function: an unresolved question

The exclusive intracellular localization of OA1 and its accumulation into specialized organelles such as the melanosomes are exceptional among GPCR and suggest that OA1 might transduce information from the organelle lumen to the cytosol to regulate proper melanosome biogenesis. OA1 could function as a "sensor" of melanosome maturation and control the organelle growth, triggering a signal transduction cascade mediated by inhibitory G-protein Gαi.

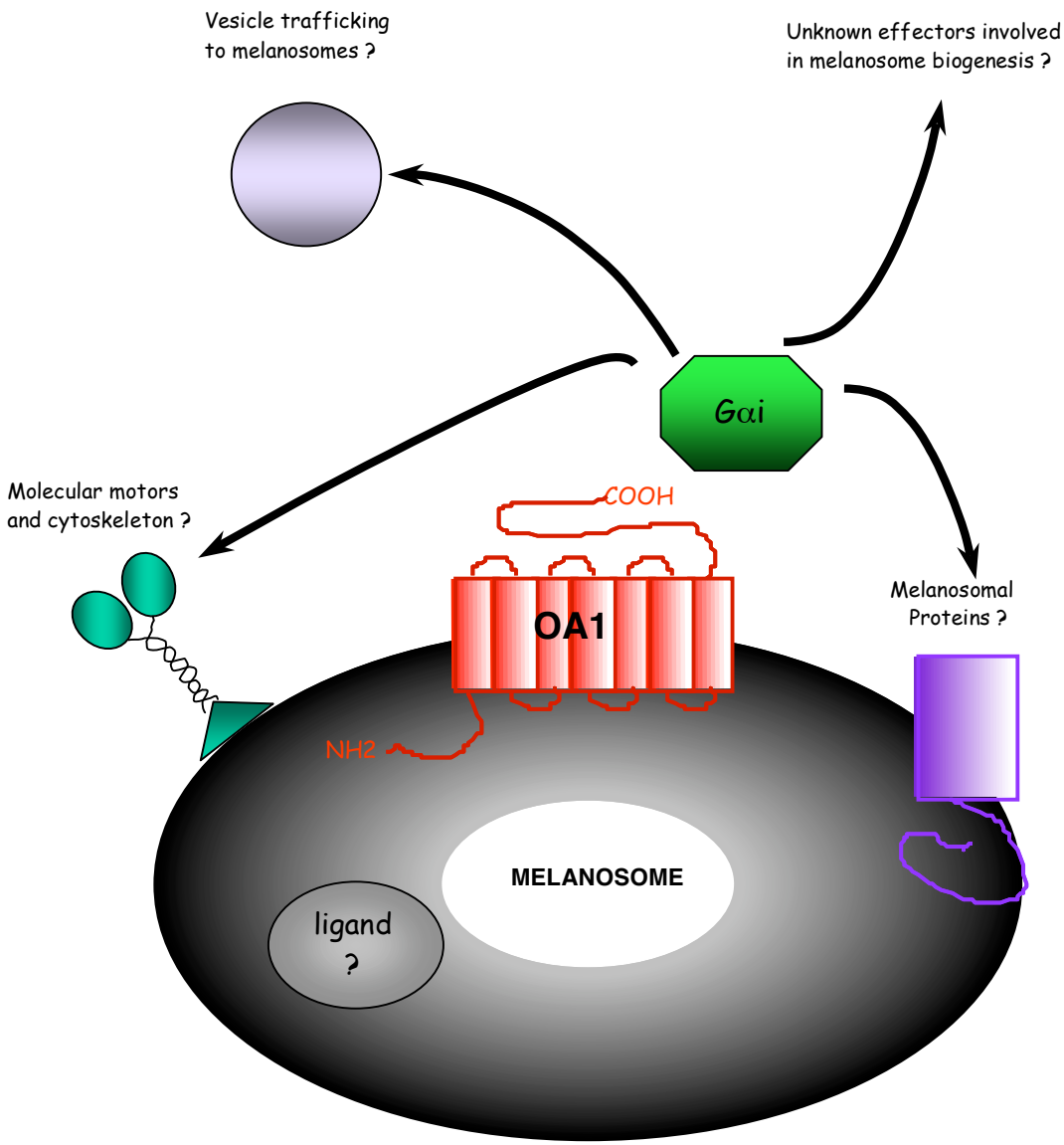

The OA1 intralumenal ligand is not known, but it may consist of melanin itself or melanin precursors and intermediate products.

Alternatively, OA1 might be activated by less conventional mechanisms, such as organelle enlargement, which in the absence of OA1 signalling could lead to macromelanosome formation. Finally, it cannot be excluded that OA1 behaves as a constitutively active receptor and, therefore, that its ligand actually acts as an inverse agonist or inhibitor.

The downstream pathway triggered by OA1 remains mysterious and at the present can only be hypothesized based on the consequence arising from the

loss-of-function of the receptor in humans and mice. The histological hallmark of OA1 loss of function is the presence of macromelanosomes in pigmented cells of eyes and skin. The Oa1 knock-out (KO) mice, showing the presence of giant melanosomes in RPE and in skin melanocytes, represent a good model for the study of the molecular consequences derived from lack of OA1. In these mice macromelanosomes are first detectable after birth and their number increases progressively until adulthood (Incerti et al., 2000). The observation of a single core melanosomes within the giant pigmented organelles and the absence of intermediates of melanosome-melanosome fusion claim against the idea that macromelanosomes derive from fusion between individual organelles. In contrast, they suggest an origin by abnormal overgrowth of apparently normal mature melanosomes, which are unable to control their final size and progressively grow by addiction of new melanin and membranes (Incerti et al., 2000). Based on these results OA1 appears to play an inhibitory role restricted to the final stages of melanosome maturation, modulating the resources (enzyme, membranes, melanin precursors) allocated to developing melanosomes via membrane traffic. Nevertheless, the function of Oa1 during melanosomes maturation is still obscure. As its downstream pathway, the role of OA1 in the development of the visual system is poorly understood. The misrouting of the optic tracts, at least in the mouse, develops much earlier in embryonic life (between E12.5-E16) than the appearance of macromelanosomes. Therefore the giant organelle might represent only an epiphenomenon of the disease and cannot be the direct cause of the optic nerve defect, which must be caused by some other alteration of the melanogenic process. In contrast to other forms of albinism, melanin is not dramatically reduced in ocular albinism, which is characterized by the unusual coexistence of the typical albino visual defects and the presence of melanin in the eyes (O'Donnell et al., 1976). The possibility that OA1 functions as a melanin receptor suggests that this protein might represent the missing link

between melanin deficiency in oculocutaneous albinisms (OCA) type 1 and 2, and the severe developmental abnormalities of the visual system observed in all types of albinism. Therefore the identification of the ligand of OA1 and unravelling of its downstream pathway could lead to crucial insight on both melanocyte biology and retinal development.

2. AIM OF THE PROJECT

OA1 is a unique G-protein coupled receptor (GPCR) that does not translocate through the plasma membrane but lays in intracellular membranes most likely melanosomes, mediating signaling transduction from the organelle lumen to the cytosol. Neither the intraluminal ligand nor the downstream pathways are known. *OA1* gene mutation causes an X-linked disease, Ocular Albinism type 1 in which the patients manifest a defect in the eye and in the skin. Among the other defects they show depigmentation of the fundus in the eye and the presence of abnormally giant melanosomes called macromelanosomes in the Retinal Pigment Epithelium (RPE) and in skin melanocytes. In our lab a knockout mouse model for this form of albinism was generated. As in OA1 patients the Oa1 null mouse shows the presence of macromelanosomes in the RPE after birth. The macromelanosome phenotype suggests that Oa1 may function as a "sensor" of melanosome maturation. Nevertheless, OA1 function in melanosome biogenesis and its downstream pathway are still elusive, hampering development of a cure for this form of albinism. Furthermore, the correlation between macromelanosome and the hypopigmentation of the RPE that causes the albinism phenotype in patients is unclear.

In order to understand why mutation of OA1 causes albinism, during the first years of my PhD work I focused my research interest in addressing OA1 function in pigment cells *in vivo*, by applying genetic approaches.

We have taken advantage of the OA1 null mouse in combination with other albinism mouse models (*Tyr* $^{c\text{-}2j}$ and *Matp*^{uw}) to study the function of OA1 in the RPE *in vivo* during development and after birth. We chose Tyr and Matp mutants because these mutant mice displayed impaired maturation of melanosomes. Tyrosinase mutant mice completely lack melanin and their

melanosomes do not develop beyond stage II (Costin et al. 2003). In Matp mutant mice melanosomes stop maturation at stage III (Sweet et al. 1998). Therefore, these two mouse models provided us with genetic tools to study OA1 function either in the absence of melanin or in impaired melanosomal maturation conditions. The phenotype of the double mutant mice compared with single mutants led us to the hypothesis that OA1 perform two functions in melanosome biogenesis. In particular, Oa1 loss of function causes a reduction in the number of melanosomes in the RPE, suggesting an OA1 control of the rate of melanosome biogenesis. In addiction, double mutant phenotype analysis unraveled a size-control function of OA1 on the final maturation stage of melanosomes. Although our finding indicated that OA1 regulates melanosome maturation and size, the trafficking events that lead to the macromelanosome phenotype were far from being elucidated. In a first attempt to elucidate these events I joined, during the last year of my PhD, Graça's Raposo "Structure and Membrane Compartments" group at the CNRS-UMR144 hosted in the Institut Curie in Paris. In this group I had the appropriate environment to study OA1 function in pigmented cells *in vitro* by applying cell biology approaches. We started with investigation of OA1 localization at ultrastructural level in melanocytic cell lines to identify the subcellular compartments at which OA1 could act. Then we have analyzed in detail the phenotype of Oa1 null melanocytes, that display macromelanosomes. In parallel we went on through a strategy of inactivation of OA1 in vitro to follow the progression of the events leading to the macromelanosome defect. Our data indicated that in the absence of OA1 there is an alteration of the trafficking of melanosomal protein and also of other proteins that normally are present in low amounts in melanosomes, suggesting a function for OA1 in maintaining melanosomal identity and composition. Although the phenotype of inactivated melanocytic cells deserves further analysis, these observations suggest that OA1 signaling ability may regulate

fusion or fission events between an intracellular compartment and melanosomes during their maturation.

An interesting aspect that we wanted also to investigate was the link between the trafficking events regulated by OA1 and its downstream pathway.

Taking advantage of a microarray analysis on murine embryonic eyes from wild type and Oa1 mutant mice we have identified interesting genes, that are involved in vesicle trafficking and are upregulated in OA1 mutant pigment cells. Our preliminary data suggested that Oa1 might function through regulation of proteins that regulate vesicle trafficking. The study of this interaction during melanosome biogenesis is a first step towards unraveling the mechanism through which Oa1 affects melanosome number and size and thus better understand the pathological condition.

3.RESULTS

3.1 Effects of Oa1 loss of function on Tyrosinase activity and the rate of melanosome biogenesis in the RPE

Differently to other forms of albinisms in which melanin is absent (e.g. TYR) or reduced (e.g. MATP), in Oa1 loss of function melanin appears to be synthesized, as suggested by pigmentation of skin and hairs in patients. However OA1 patients present hypopigmentation of the ocular fundus and this cannot simply be explained by the giant melanosomes phenotype.

To quantify this observation we measured the abundance and the activity of Tyr protein on Oa1 knock out eyes.

We started by measuring tyrosinase quantity by western blot in protein extracts from embryonic E12.5, E14.5, E16.5 and postnatal P0 and P7 Oa1

KO and wt mice eyes and we found no significant difference at all these stages (Figure 9A).

Then we measured the activity of tyrosinase in eye protein extracts from the Oa1 KO, heterozygous, and wild type mice 7 days after birth (P7) and found no significant difference among the different genotypes (Figure 9B).

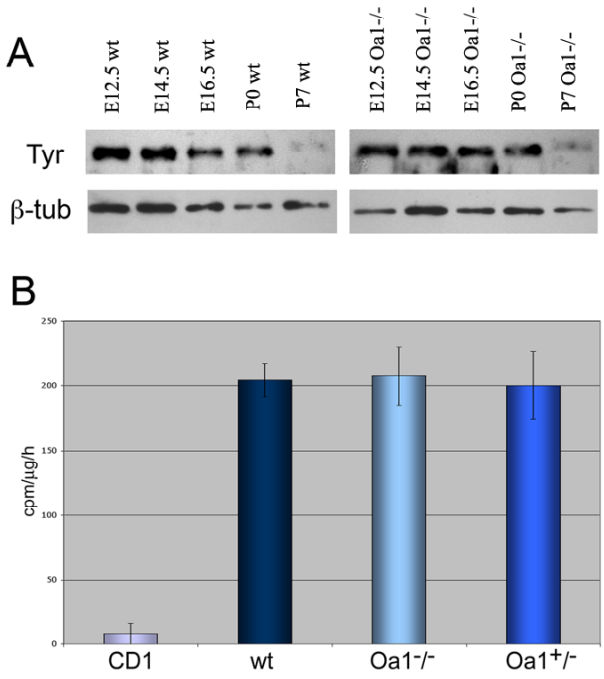

Figure 9. (A) ***Tyrosinase protein detection by western blotting*** in embryonic E12.5, E14.5, E16.5, and postnatal P0 and P7 wild type and Oa1$^{-/-}$ mutant eyes. Anti β-tubulin was used as a control to normalize protein amount. **(B)** ***Tyrosinase activity assay*** on eyes at the age of 7 days after birth. ANOVA confirmed no significant difference in the enzymatic activity among wt (n=9), Oa1 eterozygous (n=9) and homozygous (n=6) mice. Tyrosinase activity in albino control CD1 mice was significantly different from that in wt (t-test P‹0.001). Data are shown as the mean divided by the blanc (CD1 mice have a value close to 1, therefore activity equal to blanc).

Therefore, in contrast to other albinism models (LaVail et al.1978), lack of Oa1 does not impair either the quantity or activity of tyrosinase enzyme in the eye, suggesting a role of Oa1 not on melanin formation, but on melanosome biogenesis. It is possible that albinism in OA1 is due to a decreased abundance of melanosomes in the RPE.

We have performed, in collaboration with Prof. C. Tacchetti at University of Genova, ultrastuctural analysis by electron microscopy to evaluate density (number of organelles per square micrometer) and the maturation stage of

melanosomes in the RPE of wild-type and Oa1 mutant mice at different developmental and postnatal stages.

At embryonic day E15.5, newborn P0, and later postnatal stages P7 and 3 months, the melanosome population in wild-type RPE comprised mostly mature stage IV melanosomes. However, a sizable fraction of the melanosomes was still at stage II at E15.5 (31%) and at stage III at P0 (14%).

The total number of melanosomes increased progressively and reached a plateau at P7 (Table 1).

The changes in the total number of melanosomes reflected almost exclusively the modifications in the stage-IV population, probably due to the relative paucity of stages II and III at P0, P7, and 3 months.

In Oa1 KO RPE we found that the melanosome population, similar to wild-type RPE, comprises mostly stage IV melanosomes (Table 1), which included also macromelanosomes at P0, P7 and 3 months.

	Stage			
	II	III	IV	Area μm2
Wild-type				
E15.5	9	1	18	186
P0	3	13	75	186
P7	0	4	132	186
3 months	9	2	136	186
Oa1$^{-/-}$				
E15.5	2	2	17	186
P0	10	8	37	186
P7	0	4	63	186
3 months	0	5	58	186

Table 1. ***Number of melanosomes in the RPE*** of wild type and *Oa1$^{-/-}$* mice at the different developmental stages (the total area of the cell analyzed was determined by the point-intersection method and expressed in square micrometers (Rabouille et al. 1999)).

Similar to phenotype described in patients, only a fraction (20%) of melanosomes was enlarged (>1.5% μm) (Table 2).

When compared to wild type, Oa1 KO RPE shows a significant reduction of the number of melanosomes, that begins during development (25% of

reduction at E15.5) and continues after birth (40% at P0, 50% at P7 and 57% at 3 months).

This reduction was mostly attributable to the stage IV population at P0, P7 and 3 months, whereas at E15.5 it was due to changes in immature stage II melanosomes.

We didn't detect autophagosomes suggesting that the reduction of the melanosome number was probably due to a reduced rate of organelle biogenesis, rather then degradation of already formed organelles.

3.2 Effect of *Oa1*$^{-/-}$, *Tyr* $^{c\text{-}2J}$, and *Matp*^{uw} mutations on each other and cellular distribution

To define at which stage of melanosomes maturation Oa1 act, we generated double-mutant mice of Oa1 with two other albinism mouse models, Tyr (OCA1) and Matp (OCA4) in which melanosomes are unable to undergo full maturation.

In *Tyr* $^{c\text{-}2J}$ mice melanin is not synthesized and melanosomes stop their maturation at stage II (Costin et al.2003) (Figure 13), in *Matp*^{uw} mice, the mutation causes a block of maturation at stage III (Sweet et al.1998) (Figure 5).

Before generating double-mutant mice we have verified that each mutation didn't have an effect on the others. Therefore we have analyzed expression and distribution of Oa1 protein in *Tyr* $^{c\text{-}2J}$ and *Matp*^{uw} mutants.

To this end, we generated primary cultures of pigment cells dissected from wild type, *Oa1*$^{-/-}$, *Tyr* $^{c\text{-}2J}$ and *Matp*^{uw} neonatal eyes. These cultures contained both RPE and choroidal melanocytes, as defined by immunodetection of pigment cell markers (i.e.Tyr, Tyrp1, and DCT) (Figure 10).

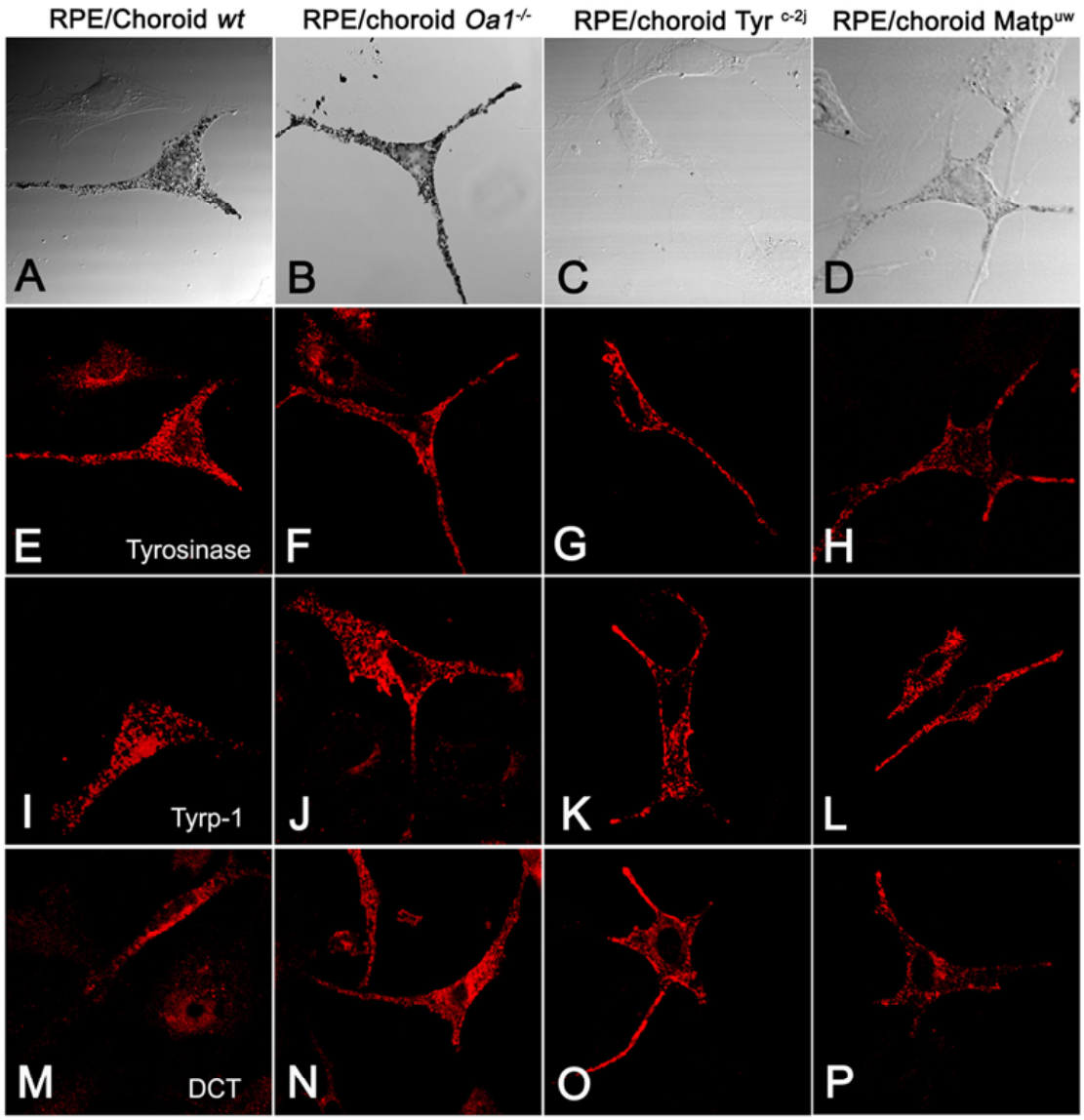

Figure 10. ***Immunofluorescence analysis of melanosomal protein (Tyrosinase, tyrp-1, DCT) distribution in pigmented cells dissociated from neonatal Oa1$^{-/-}$, Tyr^{c-2J} , Matp^{uw} and mutants eyes.*** **(A,E,I,M)** Micrographs of cell derived from wild-type; **(B,F,J,N)** from Oa1$^{-/-}$; **(C,G,K,O)** from Tyr^{c-2J} and **(D,H,L,P)** from Matp^{uw} mice. **(A,B,C,D)** Bright-field phase images of the cells in **(E),(F),(G)** and **(H)**, respectively.

To discriminate between the two cell populations, we performed immunofluorescence analysis using antibodies to Cralbp, a specific marker for RPE cells (Nawrot et al., 2004) and confirmed that cells with elliptic big pigment granules were RPE cells (Figure 3 *inset*).

Labeling with an Oa1 specific antibody shows that Oa1 was normally expressed and distributed in *Tyr $^{c-2J}$* and *Matp^{uw}* mutant RPE and choroidal melanocytes, whereas no signal was detected in *Oa1$^{-/-}$* cells (Figure 11).

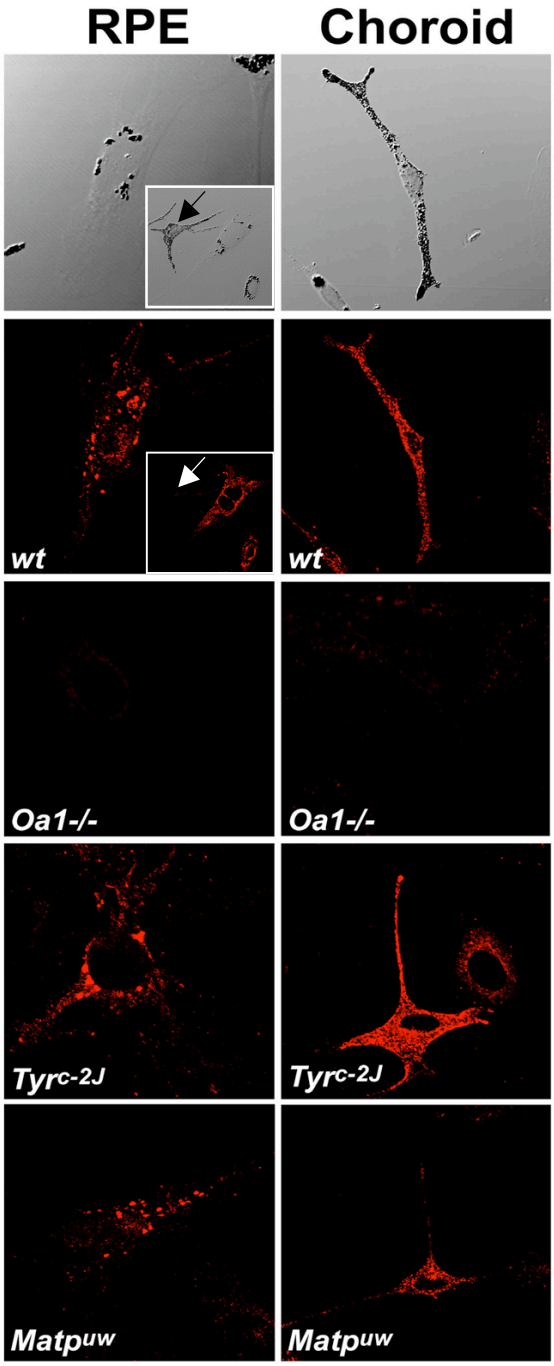

Figure 11. ***Oa1 expression and distribution in Tyr^{c-2J} and Matp^{uw} eyes.*** Pigmented cells dissociated from eyes of neonatal wild-type (*wt*), were stained with an anti-Oa1 antibody. The identity of RPE cells was assessed by staining with anti-Cralbp antibody (*inset*), which does not label choroidal pigmented cells (*arrow*). *Top*: interferential reflection micrographs of a typical RPE (*left*) and choroid (*right*) cell. *Bottom*: immunofluorescence detection of Oa1 in wild type, *Oa1*$^{-/-}$, and choroidal cells. Expression of Oa1 in *Tyr*$^{c-2J}$ and *Matp*^{uw} RPE and choroidal cells was similar to wild type, whereas Oa1 could not be detected, as expected, in *Oa1*$^{-/-}$ RPE and choroid

We then analyzed expression of *Tyr* and *Matp* mRNA in Oa1 mutant eyes at birth by quantitative real-time PCR. *Tyr* and *Matp* expression was not impaired in the *Oa1*$^{-/-}$ genotype compared with the wild type (Figure 12).

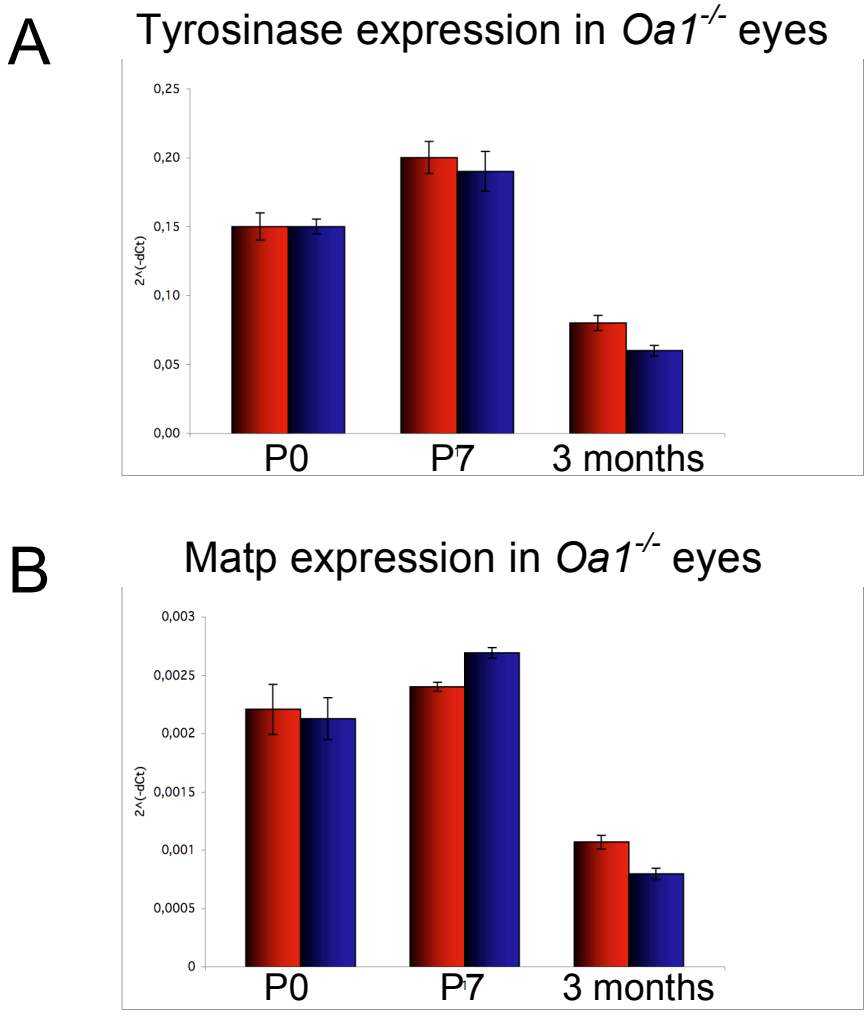

Figure 12. ***Tyrosinase and Matp expression in Oa1 mutant eyes.*** **(A)** Real-time quantitative RT-PCR of *Tyr* in neonatal (P0), 7 days after birth (P7) and 3 months wild-type (wt, *red*) and *Oa1*$^{-/-}$ (Oa1 mut, *blue*) eyes. *Y-Axis*: $2^{(-dCt)}$ value represents differences between the mean *Ct* (cycle threshold) values of tested genes and those of reference gene. **(B)** Real-time quantitative RT-PCR of *Matp* in neonatal (P0), 7 days after birth (P7) and 3 months wild-type (wt, *red*) and *Oa1*$^{-/-}$(Oa1 mut, *blue*) eyes.

Moreover, we have analyzed by immunofluorescence Tyr distribution in RPE and choroidal melanocyte primary cultures derived from *Oa1*$^{-/-}$ neonatal eyes.

Also in this case we found no significant differences of Tyr localization as compared to wt (Figure 10A, 10B, 10E, 10F), showing that Oa1 loss of function does not interfere with the distribution of Tyr.

Therefore, the absence of Oa1 does not influence the expression of tyr and Matp. Altogether, these results suggest that Oa1, Tyr and Matp do not reciprocally influence each other expression and subcellular distribution.

3.3 Effect of Oa1 on the rate of melanosome biogenesis and organelle size.

We generated *Oa1*$^{-/-}$*; Tyr* $^{c\text{-}2J}$*/Tyr* $^{c\text{-}2J}$ double mutant mice and analyzed the melanosome phenotype in RPE at P7. We chose this stage because at this time point both the reduced number of melanosomes and the giant melanosome phenotype are easily detectable in Oa1-null mice. At P7, no melanin was deposited in the melanosomes of *Tyr* $^{c\text{-}2J}$*/Tyr* $^{c\text{-}2J}$ single mutant or *Oa1*$^{-/-}$*; Tyr* $^{c\text{-}2J}$*/Tyr* $^{c\text{-}2J}$ double mutant RPE, and melanosomes stopped their maturation at stage II (Figure 13).

The number of stage II melanosomes was reduced in the *Oa1-/-; Tyr* $^{c\text{-}2J}$*/Tyr* $^{c\text{-}2J}$ double mutant compared with the Tyr $^{c\text{-}2j}$/Tyr $^{c\text{-}2j}$ single mutant RPE (Table 3).

We then evaluated whether the size of melanosomes was affected by the combination of the two mutations. To this purpose, we compared the diameter at P7 of the most mature stages in each genotype (stage II in *Tyr* $^{c\text{-}2J}$*/Tyr* $^{c\text{-}2J}$ and *Oa1*$^{-/-}$*; Tyr* $^{c\text{-}2J}$*/Tyr* $^{c\text{-}2J}$ and stage IV in *Oa1*$^{-/-}$*)*.

Stage II melanosomes had an average diameter of 0.56 μm in Tyr $^{c\text{-}2j}$/Tyr $^{c\text{-}2j}$ single mutant RPE and 0.67 μm in the double mutant RPE (Table 2). These values were similar to those obtained from wild type stage IV melanosomes (0.51 μm), but smaller compared with *Oa1*$^{-/-}$ macromelanosomes (0.9 μm).

The reduced number of stage-II melanosomes in double mutant RPE demonstrates that Oa1 contributes to the rate of melanosome maturation at early stages and independently of melanin synthesis.

However, we could not define yet whether melanin synthesis and/or melanosome maturation are necessary for the regulation of melanosomal size by Oa1.

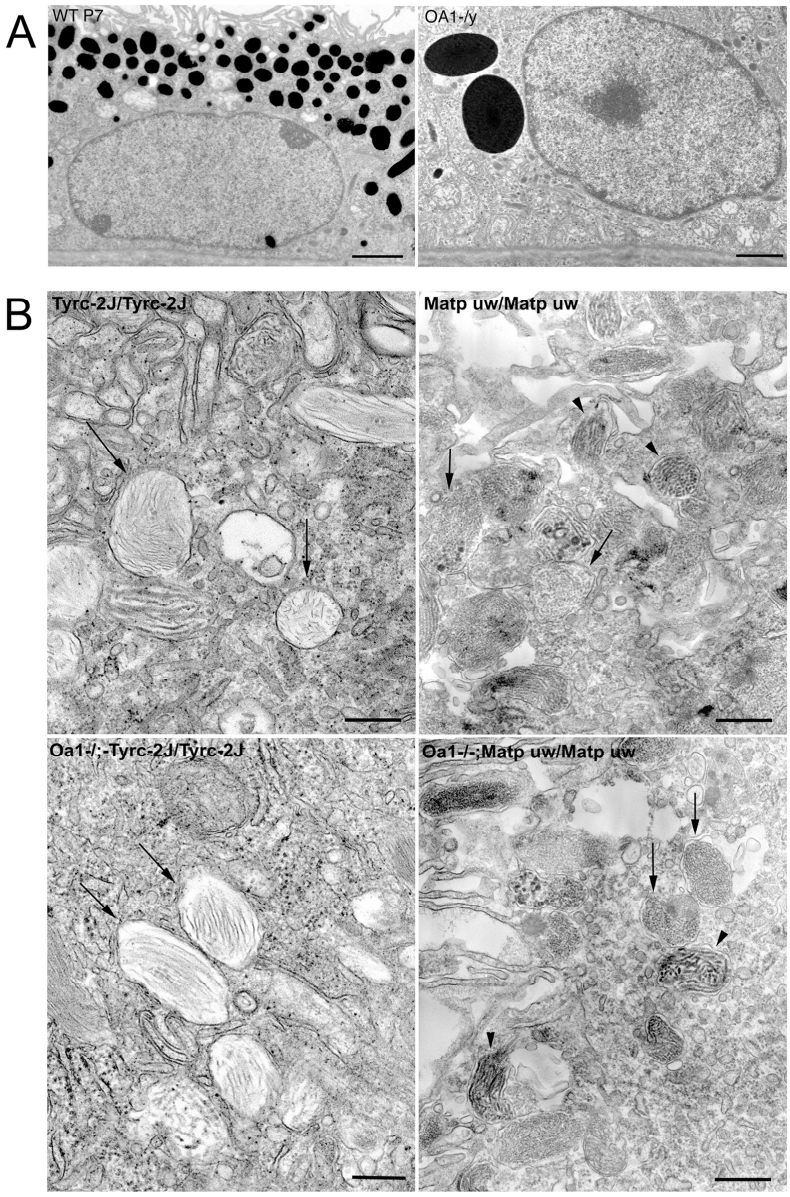

Figure 13. ***Ultrastructural analysis of RPE melanosomes in different genotypes.*** **(A)** Micrographs of RPE cells from wild type and *Oa1-/-* mice at P7. Photographs are at the same magnification and show the difference in size of the melanosomes in the two animals. *Bar*: 2.5μm. **(B)** Micrographs of RPE melanosomes from $Tyr^{c\text{-}2J}/Tyrc^{\text{-}2J}$ and $Oa1^{-/-}$; $Tyr^{c\text{-}2J}/Tyrc^{\text{-}2J}$ and $Matp^{uw}/Matp^{uw}$ and $Oa1^{-/-}$; $Matp^{uw}/Matp^{uw}$ mutant mice. *Arrows*: representative stage-II melanosomes. Different stages of melanosomes were found in RPE of $Matp^{uw}/Matp^{uw}$ single and $Oa1^{-/-}$; $Matp^{uw}/Matp^{uw}$ double-mutant mice. *Arrowheads*: stage-III melanosomes. *Bar*: 0.47 μm.

Table 2. ***Size distribution of melanosomes in the RPE of different genotypes***

	Diameter			Mean diameter (μm)
	<1 μm	1-1.5 μm	>1.5 μm	
Stage IV				
Wild-type				
P7				
%	90	10	0	0.51
n	106	11	0	
3 months				
%	92	8	0	0.61
n	98	9	0	
Oa1$^{-/-}$				
P7				
%	63	14	23	0.90
n	30	7	11	
3 months				
%	44	40	16	1.00
n	21	19	8	
Stage II				
Tyr$^{c\text{-}2J}$/*Tyr*$^{c\text{-}2J}$				
P7				
%	100	0	0	0.56
n	118	0	0	
Oa1$^{-/-}$;*Tyr*$^{c\text{-}2J}$/*Tyr*$^{c\text{-}2J}$				
P7				
%	95	5	0	0.67
n	41	2	0	
Stage III				
Matp^{uw}/*Matp*^{uw}				
3 months				
%	87	13	0	0.54
n	14	2	0	
Oa1$^{-/-}$;*Matp*^{uw}/*Matp*^{uw}				
3 months				
%	97	3	0	0.56
n	40	1	0	

Data report the number (*n*) and the percentage (%) of melanosomes counted in each condition and falling in each of the three ranges of diameter shown.

Table 3. Number of melanosomes in RPE of *Tyr*$^{c\text{-}2J}$/*Tyr*$^{c\text{-}2J}$and *Oa1*$^{-/-}$;*Tyr*$^{c\text{-}2J}$/*Tyr*$^{c\text{-}2J}$ mutant mice, and *Matp*^{uw}/*Matp*^{uw} and *Oa1*$^{-/-}$;*Matp*^{uw}/*Matp*^{uw} mutant mice.

	Stage			Area (μm^2)
	II	III	IV	
Stage IV				
Tyr$^{c\text{-}2J}$/*Tyr*$^{c\text{-}2J}$				
P7	97	0	0	355
Oa1$^{-/-}$;*Tyr*$^{c\text{-}2J}$/*Tyr*$^{c\text{-}2J}$				
P7	62	0	0	355
Matp^{uw}/*Matp*^{uw}				
3 months	31	20	0	186
Oa1$^{-/-}$;*Matp*^{uw}/*Matp*^{uw}				
3 months	17	50	0	186

The total area of the cell analyzed (area) was determined by the point-intersection method and expressed in square micrometers.

3.4 Effect of Oa1 in melanosome maturation

To address whether melanin deposition and/or melanosome maturation are involved in the macromelanosome phenotype, we analyzed the RPE in P7 and 3 month old *Oa1*$^{-/-}$*;Matp*^{uw}*/Matp*^{uw} double-mutant mice. In fact *Matp*^{uw}*/Matp*^{uw} adult RPE display smaller but pigmented melanosomes (Sweet et al.1998).

At P7 we did not detect any melanosome in both single and double mutant mice. At 3 months of age, in both genotypes RPE melanosomes did not proceed beyond stage III (Figure 13).

The number of stage II melanosomes was reduced in the *Oa1*$^{-/-}$*;Matp*^{uw}*/Matp*^{uw} double mutant compared with the *Matp*^{uw}*/Matp*^{uw} single mutant RPE (Table 3).

By morphometry, we measured similar diameters in the *Matp*^{uw}*/Matp*^{uw} single mutant (0.54 μm) and in the *Oa1*$^{-/-}$*;Matp*^{uw}*/Matp*^{uw} double mutant (0.56 μm) RPE (Table 2).

Altogether these results suggested that Oa1 exerts a size control function only on fully developed stage IV melanosomes, independent of melanin synthesis.

Therefore, melanosome maturation and not melanin deposition has a direct influence on the formation of macromelanosomes.

Our findings indicate that Oa1 is involved in the regulation of melanosome maturation at two steps. Acting at early maturation stages, Oa1 controls the abundance of melanosomes in RPE cells. At later stages, Oa1 has a function in the maintenance of a correct melanosomal size.

3.5 OA1 protein localization in pigmented cells *in vitro*

Given the limitation to further explore the function of Oa1 in RPE cells using genetic approaches we decided to go further onto the role of Oa1 in melanosome maturation in pigmented cells *in vitro* taking advantage of cell biology methods.

In contrast to canonical GPCRs, OA1 does not translocate to the plasma membrane, but is exclusively detectable on the membrane of intracellular organelles in pigmented cells (Schiaffino et al. 1999). Moreover, some controversy exists on the precise subcellular localization of the protein. Our aim was to identify the subcellular compartments "sensitive" to Oa1 activity analyzing the intracellular localization of OA1 in HeLa cells and in human and mouse melanocytes.

To this purpose we generated two different OA1 tagged constructs (humanOA1-EGFP and humanOA1-Flag) in which the full length OA1 cDNA was cloned at the N-terminal of the tag sequences in the pEGFPN1 and pcDNA3-Flag vectors.

First we tested their expression in HeLa cells, in which OA1 normally is not expressed. Given the high efficiency of transfection in HeLa (85%), we used this cell line to find the best condition to express this integral membrane protein spanning the membrane 7 times and to validate the constructs by IF and western blot analysis. Immunofluorescence analysis on HeLa transfected cells with both constructs revealed an intracellular localization of OA1 in punctate structures (Figure 14A, 14B).

Interestingly, only cells expressing OA1-Flag shows the presence of all the maturation forms of OA1 (48kDa unglycosilated and 60kDa glycosilated forms) as detected by Western blot analysis of HeLa transfected cells (Figure 14D). In fact, the OA1-EGFP fusion protein (48kD of OA1+27kDa of EGFP) lacks the glycosilated mature form of 87kDa (60kDa+27kDa) and shows only the unglycosilated doublet of 75kDa (48kDa+27kDa), suggesting that the protein doesn't mature properly (Figure 14C).

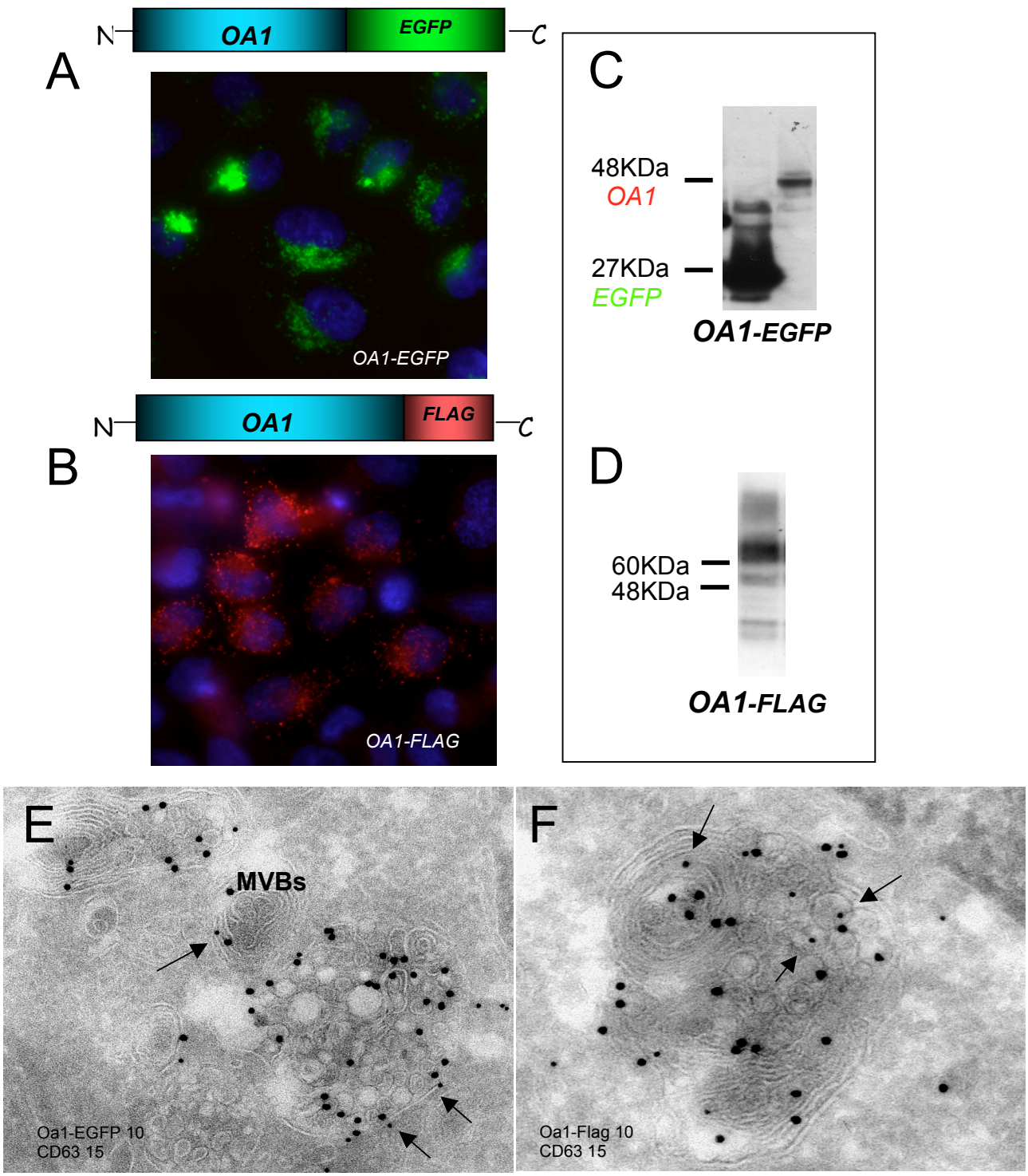

Figure 14. ***Localization of OA1 in late endosome (MVBs) and lysosome in HeLa transfected cells.*** **(A, B)** Immunofluorescence analysis of OA1 localization in HeLa transfected cells, using OA1-EGFP and OA1-Flag tagged constructs. **(C, D)** Western blotting analysis of HeLa cells transfected with the two OA1-tagged constructs shows the presence of all the maturation forms of OA1 only in the OA1-flag cells 48kDa, 60kDa and 90 kDa). **(E, F)** Ultrathin cryosections from OA1-EGFP and OA1-flag transfected Hela cells were double immunogold labeled with anti-EGFP or anti-flag (10 nm gold) and anti-CD63 (15 nm gold), a tetraspanin protein present on the MVBs. The bulk of OA1 localizes to late endosomes (MVBs) and lysosomes. Note the distribution of OA1-flag in the limiting membrane and in the internal vesicles of MVBs, whereas the OA1-EGFP, that is not fully mature (see western blotting) is mostly retained in the limiting membrane.

To investigate the nature of the intracellular compartments to which OA1 localizes we have carried immunocytochemistry at EM level.

Ultrathin cryosections from OA1-EGFP and OA1-Flag transfected HeLa cells were double immunogold labeled with antiEGFP or antiFlag (10nm gold) and antiCD63 (15 nm gold), a tetraspanin protein present in late endocytic MVBs, or Lamp1(15 nm gold), a transmembrane protein localized in MVBs and lysosomes. As shown by the OA1 co-localization with CD63 and Lamp1 the bulk of OA1 localizes to the multivesicular-multilamellar late endosomes (MVBs) and lysosomes. Interestingly, OA1-EGFP that is not fully mature (as shown in WB) is mostly retained in the limiting membrane of MVBs, whereas the OA1-Flag is distributed also in the internal vesicles, like CD63 (Figures 14E, 14F) and Lamp1 (data not shown).

The incomplete maturation of OA1-EGFP protein may explain why previous studies using GFP tagged OA1 reported OA1 protein localization only in late endosomes and not in melanosomes (Samaraweera et al., 2001). For this reason we have used only the OA1-flag construct to study OA1 localization in pigmented cells.

IF experiments performed in melanocytic cell lines revealed that OA1 localizes in pigmented melanosomes but also in not pigmented compartments (Figures 15A-C). Indeed, OA1 almost totally overlaps with Lamp1, and partially overlaps with Tyrp-1, a melanosomal enzyme involved in melanin synthesis and localized mostly to mature melanosomes. In contrast we did not observed overlay with the premelanosomal protein Pmel17, a major component of the stage II premelanosomes (Figures 15D-J).

Further on, we have analyzed the OA1 subcellular distribution at ultrastructural level by Electron Microscopy in human melanoma cells (MNT1) and mouse melanocytes (melan-A).

Immunogold labeling on ultrathin cryosections of transfected MNT1 and melan-A cells revealed that OA1 is present in mature melanosomes (stage III

and IV). In those, OA1 was often observed at the limiting membrane but also in small intraluminal vesicles that are labeled by Tyrp-1.

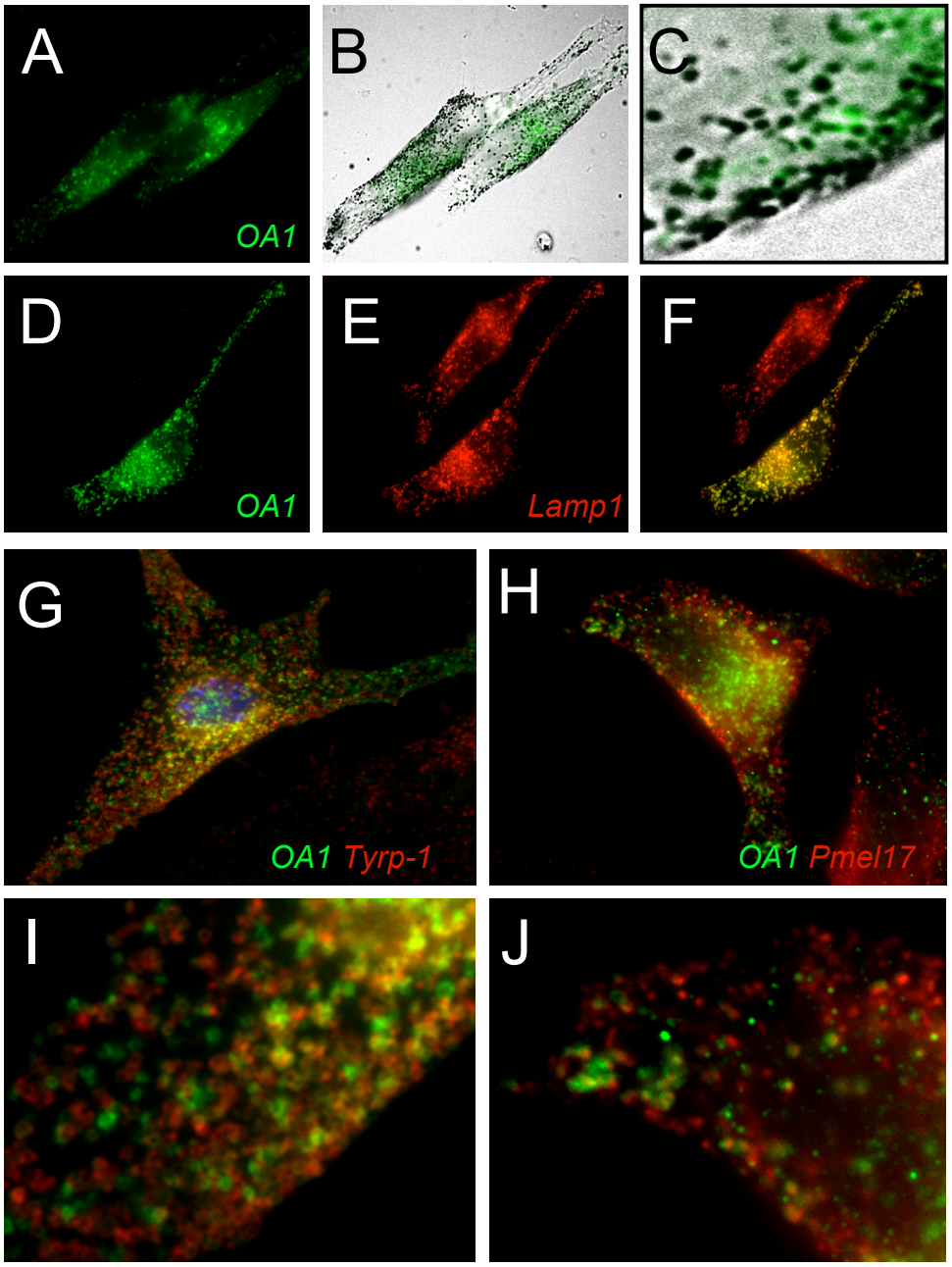

Figure 15. ***OA1 subcellular distribution in melanocytic pigmented cells***. Melanocytes were transiently transfected with OA1-flag and subsequently analyzed by immunofluorescence. **(A, B)** Oa1 (*green*) localizes in pigmented melanosomes but also in not pigmented compartments **(A, B, C).** OA1 (*green*) almost totally overlaps with Lamp-1 (*red*) **(D, E, F)**, only partially co-localizes with Tyrp-1 (*red*) **(G, I)** but not with Pmel17 (*red*) **(H, J).**

Interestingly, OA1 was also present in membrane vesicles "endosome-like" that are electron lucent and are very often close to melanosomes in both MNT1 and melan-A cells (Figure 16). These vesicles contained also Tyrp-1. Despite the observations by IF that OA1 partially overlaps with Tyrp1, the detailed analysis at the ultrastructural level demonstrates that at "steady state" OA1 localizes to mature melanosomes and to closely apposed vesicles, both labeled also for Tyrp-1, suggesting an involvement of OA1 in controlling at some step the biosynthetic or endocytic trafficking of Tyrp-1^{+} vesicles.

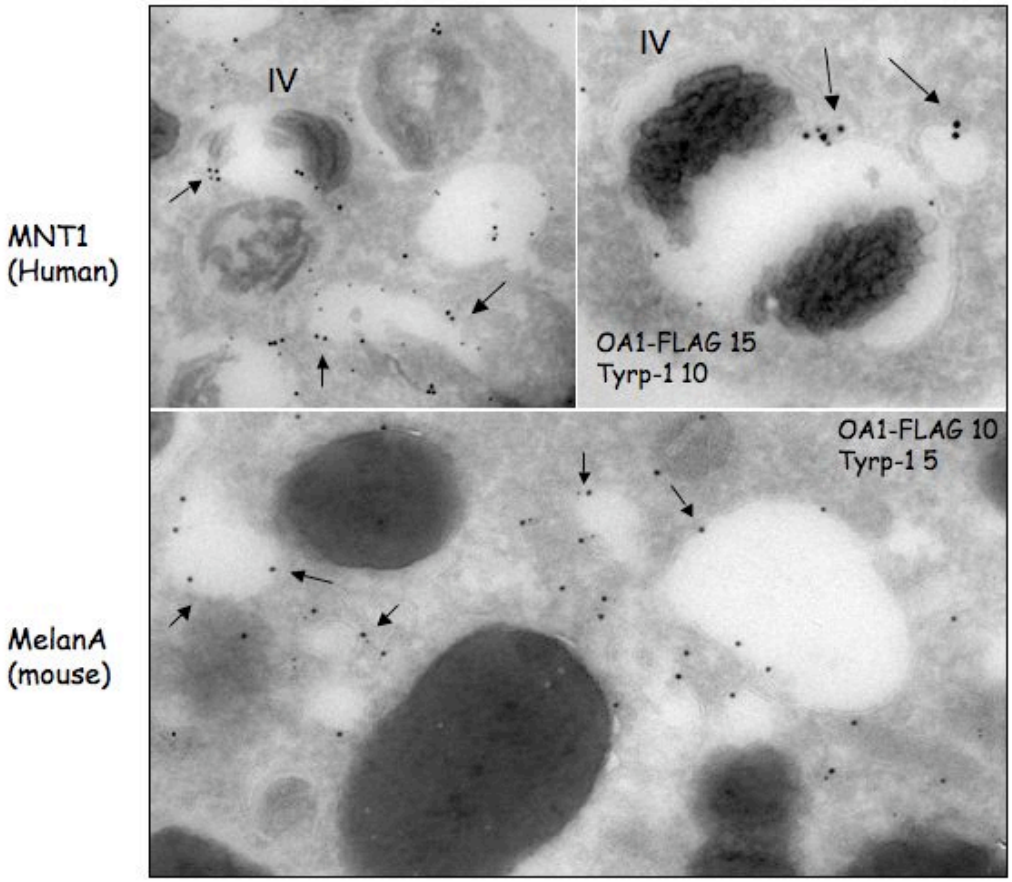

Figure 16. ***OA1-Flag localizes to melanosomes and vesicles.*** Ultrathin cryosections of human (MNT1) and mouse (melanA) melanocytic cells transfected with OA1-flag were immunogold labeled with anti-Flag (15 nm gold) and anti-tyrp-1 (10 nm gold) antibodies. Labelling for OA1 is indicated by arrows.

3.6 *In vitro* analysis of the melanosomal phenotype in *Oa1* null melanocytes

In order to understand the trafficking steps affected by the absence of Oa1 protein, we performed a detailed analysis of the macromelanosome phenotype of Oa1 null skin murine melanocytes. By light microscopy we observed that the Oa1 KO melanocytes cultured *in vitro* contain less melanosomes of different sizes mixed with giant macromelanosome, as we have previously seen in the RPE *in vivo*. Of note, the giant melanosomes were retained in perinuclear region and appear to be less motile than the normal melanosomes (Figure 10B). It's possible that these macromelanosomes are not properly mature organelle and/or their composition in melanin proteins is altered, leading to a failure in the recruitment of effector proteins necessary to delivery them to periphery.

We performed IF experiments to verify the distribution of melanosomal proteins involved in melanin synthesis (Tyrosinase, Tyrp-1, DCT) or constituents of the striations of premelanosomes (Pmel17) and also of one late endosome/lysosome protein (Lamp1). We didn't find evident differences in their distribution as compared to wild type melanocytes (Figure 17).

We then performed ultrastructural analysis by Electron Microscopy in these cells and we found the presence of abnormal melanosomes with a heterogeneous content. Sometimes they appeared as a mixture of immature striated melanosomes with an electron-dense pigmented content (Figure 18C-18F).

The immunocytochemistry experiments performed at EM level to localize melanosomal protein in Oa1 KO melanocytes did not allow identifying a clear defect in trafficking of melanosomal proteins.

However, we found that the fibrillar structures apposed to these abnormal melanosomes were mostly labeled for Pmel17, a major component of the typical stage II striations (Figure 18G).

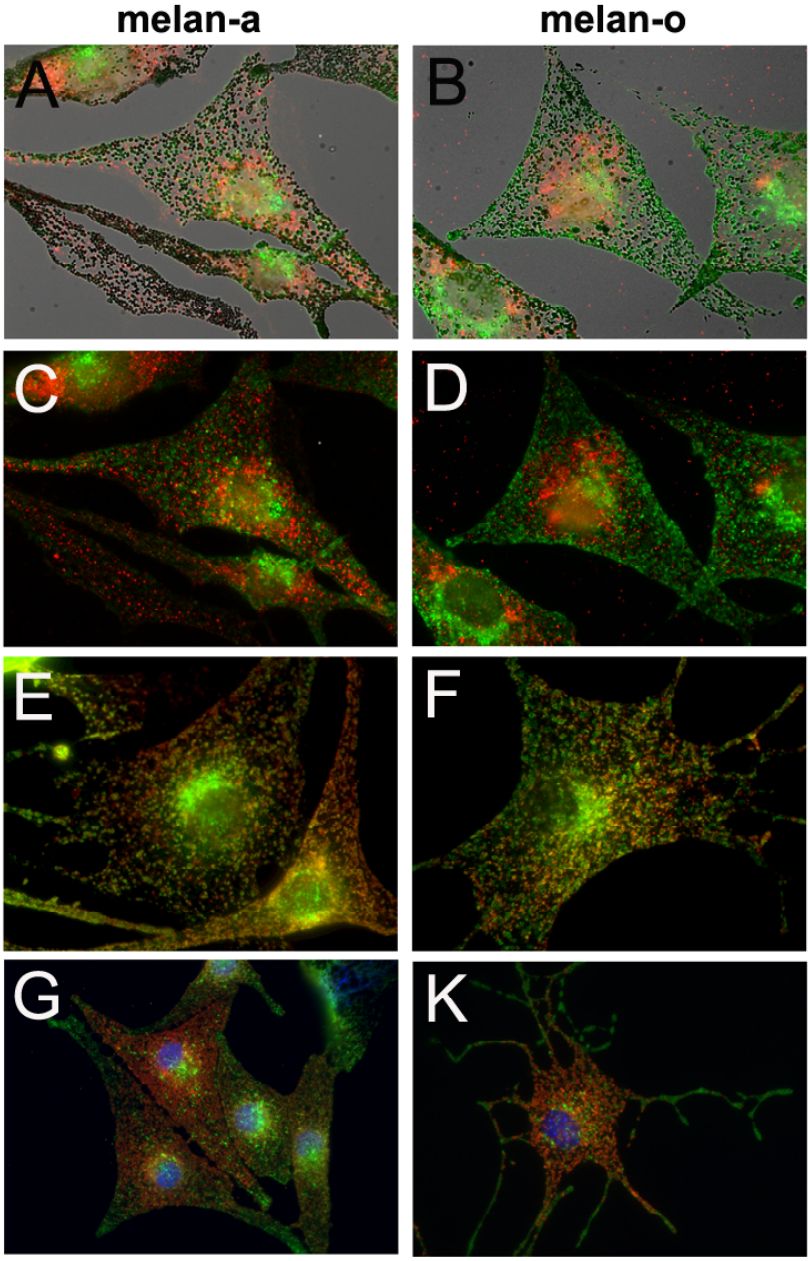

Figure 17: ***Expression and distribution of melanosomal proteins in Oa1$^{-/-}$ (melan-o) skin melanocytes.*** We analyzed the localization of melanosomal (tyrosinase, tyrp-1, pmel17) and lysosomial (lamp-1) proteins in *Oa1*$^{-/-}$ (melan-O) (**B, D, F, K**) compared with wild-type melanocytes (melan-a) (**A, C, E, G**). **A** and **B** are interferential reflection micrographs of wild-type (melan-a) and *Oa1*$^{-/-}$ (melan-O) melanocytes shown in C and D; immunofluorescence detection of Tyrosinase (*green*)/Pmel17 (*red*) (**C,D**); Tyrosinase (*green*)/ Tyrp-1(*red*) (**E,F**); Tyrp-1(*red*)/Lamp-1(*green*)(**G,K**). All these proteins did not display evident differences in their expression and distribution when compared in the two genotypes. Note the astrocyte-like shape of the majority of *Oa1*$^{-/-}$ melanocytes (**K**).

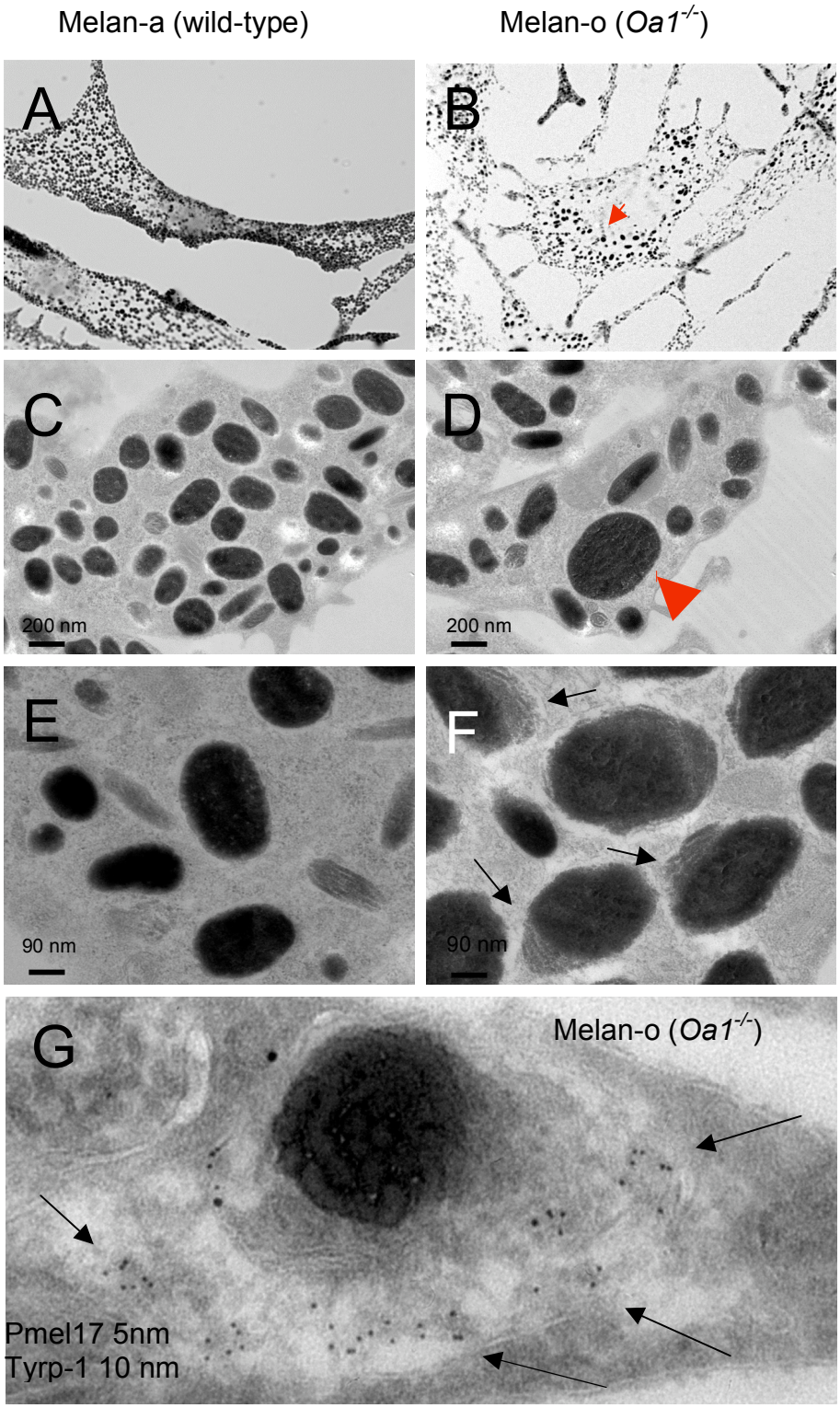

Figure 18: ***Oa1$^{-/-}$ mouse skin melanocytes (melan-o) show a reduction of the number of melanosomes and the presence of macromelanosomes*** as observed by light **(B)** and elecron microscopy **(D).** wild-type melanocytes are shown in **A, C, E.** *Red arrowhead*: macromelanosome. ***A subset of melanosomes in Oa1$^{-/-}$ displays an irregular shape and a not homogeneous melanin content.*** They appear as a mixture of immature striated melanosomes (*arrows*) with an electron dense pigment content **(F)**. The striation at the periphery is Pmel17 positive (5 nm gold), as indicated by the *arrows* in **(G)**.

The Oa1 KO phenotype analysis in skin melanocytes suggests that the absence of Oa1 affects melanosome maturation *in vitro*, but did not allow a clearly understanding of the trafficking step that is affected by loss of Oa1.
In fact, in these cells we were observing an "end-point" situation, with primarily mature organelles and it may represent the consequence of many sequential events. We are therefore interested in developing a method that allows us to looking at the progression of the events that really leads to the macromelanosome phenotype.

3.7 OA1 inactivation in human melanoma MNT1 cells *in vitro*

In order to analyze the progression of the events that lead to the macromelanosome phenotype we performed RNA interference of OA1 using siRNA in MNT1 cells *in vitro* and then analyzed the phenotype by performing immunocytochemistry at ultrastructural level. This methodology will allow following melanosomal maturation right after the loss of OA1 activity and, therefore, unraveling the sequential steps leading to the macromelanosome.
We have tested 3 different sequences of oligonucleotides targeting 3 different regions of the human OA1 mRNA. As a control we have used a double strand siRNA targeting a transcript expressed exclusively in plants. After 1 week of inactivation we performed qPCR to verify the reduction of mRNA levels on interfered cells. Among the 3 sequences one was confirmed to be very efficient in reducing the expression of OA1 mRNA levels (about 85-90%) (Figure 19A).
We have also tested the ability of this sequence to downregulate OA1 protein. Because an antibody anti-human OA1 was not available, we performed this analysis on OA1-EGFP transfected MNT1 cells and we found that the OA1-EGFP protein was strongly reduced in the MNT1 interfered cells *in vitro* as shown by western blot (Figure 19B).

After 1 week of inactivation melanin assay shows that the melanin content in siOA1 MNT1 cells was reduced as much as 50% compared to cells treated with the control siRNA (Figure 19C). Ultrastructural analysis on siOA1 MNT1 cells showed a reduction of the total number of melanosomes in siOA1 MNT1 cells as compared with the control cells (Figure 19E, 19F).

These observations indicated that OA1 interference in MNT1 cells leads to a significant reduction of pigmentation and of the number of melanosomes, reproducing the phenotype characterized in the Oa1 KO mouse and in patients.

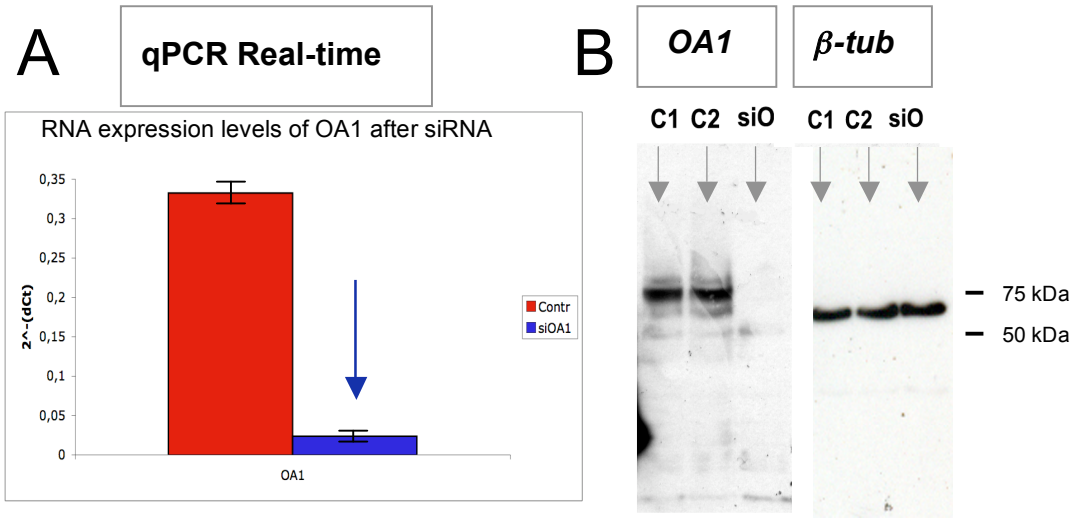

Figure 19 (A, B): ***1 week interference (siRNA) of OA1 leads to a significant reduction of its mRNA and protein levels in MNT1 cells*** as quantified by qPCR **(A)** and western blotting **(B)**, respectively. Quantitative PCR was performed on siOA1 MNT1 to detect the mRNA levels of endogenous OA1. Western blotting was performed on MNT1 cells transfected with OA1-EGFP and then interfered using siOA1 oligos. After 1 week we detected the protein levels of OA1-EGFP. We used as control MNT1 cells transfected with pEGFP vector and then interfered with a non-targeting sequence.

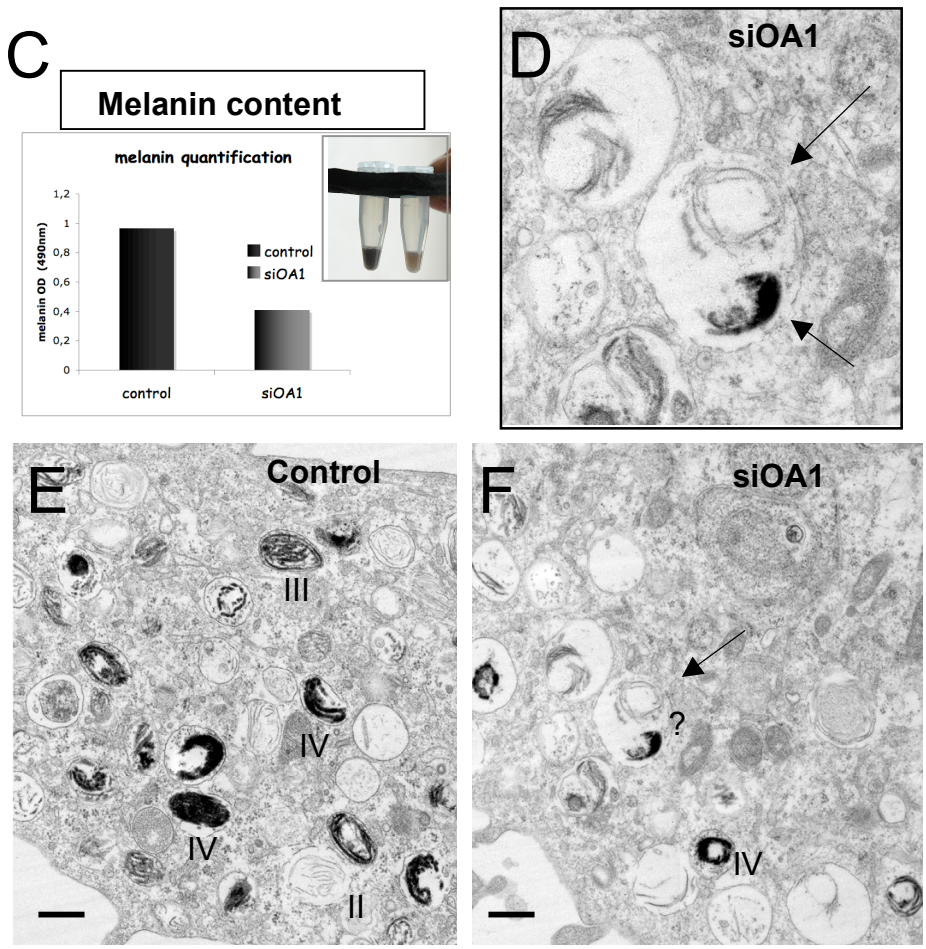

Figure 19 (C, D, E, F): ***Inactivation of OA1 in MNT1 cells by siRNA leads to a decrease in melanin content*** as analyzed by quantification of melanin **(C)** ***and to a decrease number of melanosomes*** as analyzed by Electron Microscopy **(E, F). (D)**: siOA1 cells display abnormal pigmented structures (*arrow*) that are bigger then melanosomes in wild type. *Bar*: 250 nm

We did not detect macromelanosomes (certainly, the macromelanosome phenotype requires more then 1 week to develop *in vitro*), but, interestingly, we have observed an accumulation of Tyrp-1 in large vacuolar compartments, often very close or even in continuity with the melanin containing membrane structures. Although the melanin content was reduced in siOA1 MNT1 cells, Western blot experiments performed in these cells display an increase in the amount of Tyrp-1, suggesting a defect in its trafficking and/or degradation (Figure 20).

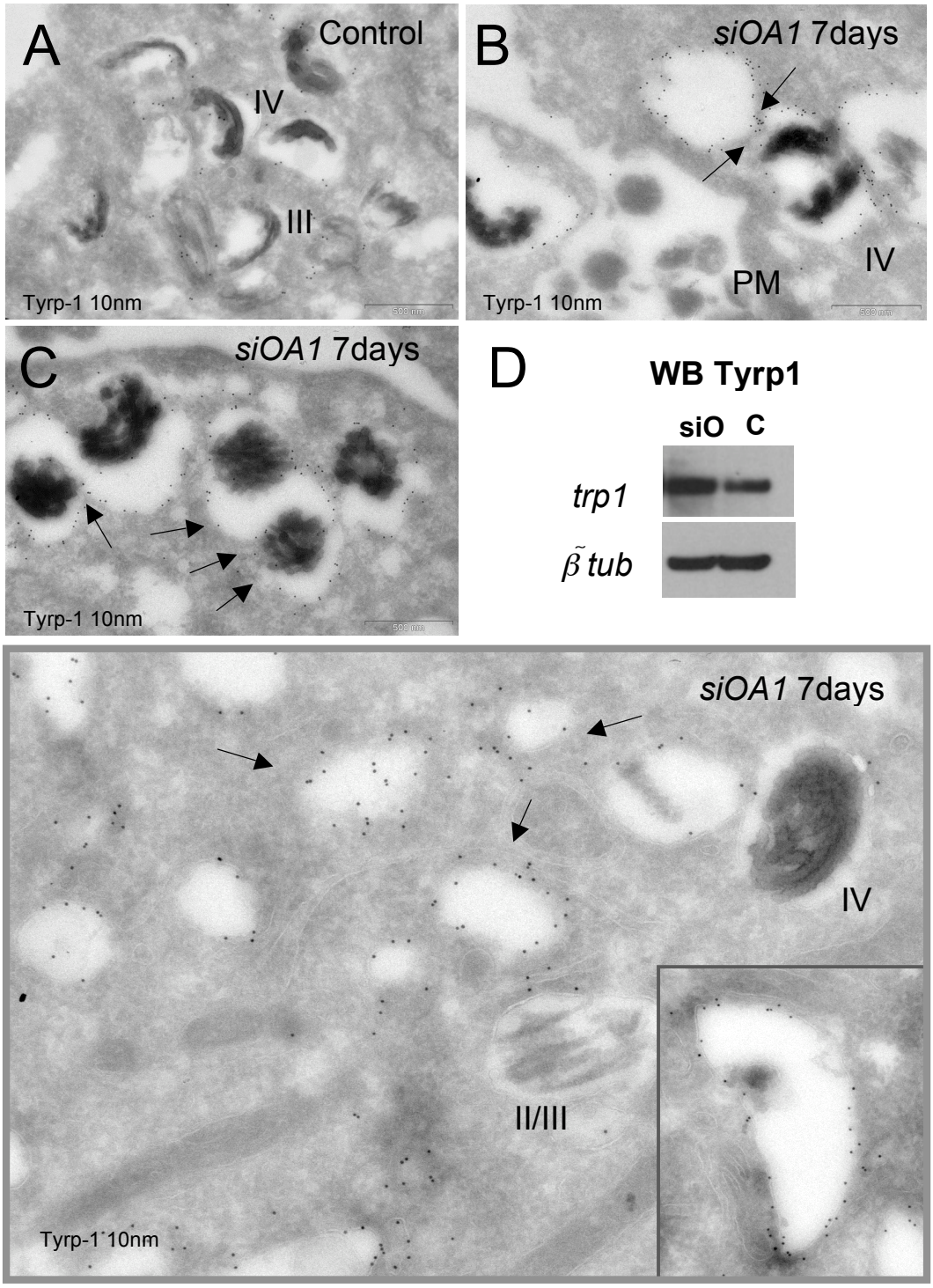

Figure 20. ***Accumulation of Tyrp-1 in large vacuolar compartments in siOA1 MNT1 interfered cells.*** *Top:* After 1 week of OA1 inactivation macromelansomes are not detectable, but there is an accumulation of large vacuolar structures in siOA1 MNT1 cells **(B)** compared with the control cells **(A)**. These vacuoles contain a big amount Tyrp-1, a melanosome enzyme normally present in mature melanosomes (stage III, IV), and are very close to the melanin containing compartments (arrows). Western blotting analysis confirmed the up-regulation of Tyrp-1 protein in siOA1 MNT1 cells **(D)**. Note the presence of pigmented melanosomes with increased membrane and Tyrp-1 quantity **(C)**. *Bottom*: typical field of siOA1 MNT1 cells displaying Tyrp-1 positive vacuoles accumulation.

To better characterize Tyrp-1 labelled vacuoles and in particular their possible endosomal nature we allowed the siMNT1 and control cells to internalize transferrin (Tf-biotin) for 45 min (a kinetics necessary to load the early endosomal system). The Tyrp-1 vacuoles in siOA1 MNT cells did not appear to be easily accessed by transferrin when compared to the control cells (Figure 21A-D). These findings suggested that these compartments are not part of the early endocytic system and they may represent a subdomain not accessible to the transferrin receptor.

Of note, these vacuoles contain Pmel17, a component of immature melanosomes (Figure 21E). Surprisingly, Tyrp-1/Pmel17 containing vacuoles accumulated also Lamp1, a late endosomal and lysosomal protein (figure 22). These studies revealed an increased amount of Lamp1 also at the membrane of the pigmented structures. In some cases the vacuolar compartment is labeled also for TGN46, a protein that localizes mostly to TGN (Figure 21F).

On the whole, the ultrastructural analysis of the OA1 inactivated cells showed that in the absence of OA1 the decrease of the number of melanosomes is accompanied by an increase of enlarged compartments containing melanosomal proteins (Tyrp-1 and Pmel17) but also other proteins that are not normally present in high amounts in pigmented structures (Lamp1 and TGN46). Further studies are needed to further characterize this intracellular compartment and to understand how the absence of OA1 leads to the reduction of melanosome number and the giant melanosome phenotype. However, these results all together indicate a function for OA1 in the maintenance of melanosome identity and composition. Moreover, we speculate that OA1 signaling activity may control fusion or fission events between an intracellular compartment and melanosomes during their maturation.

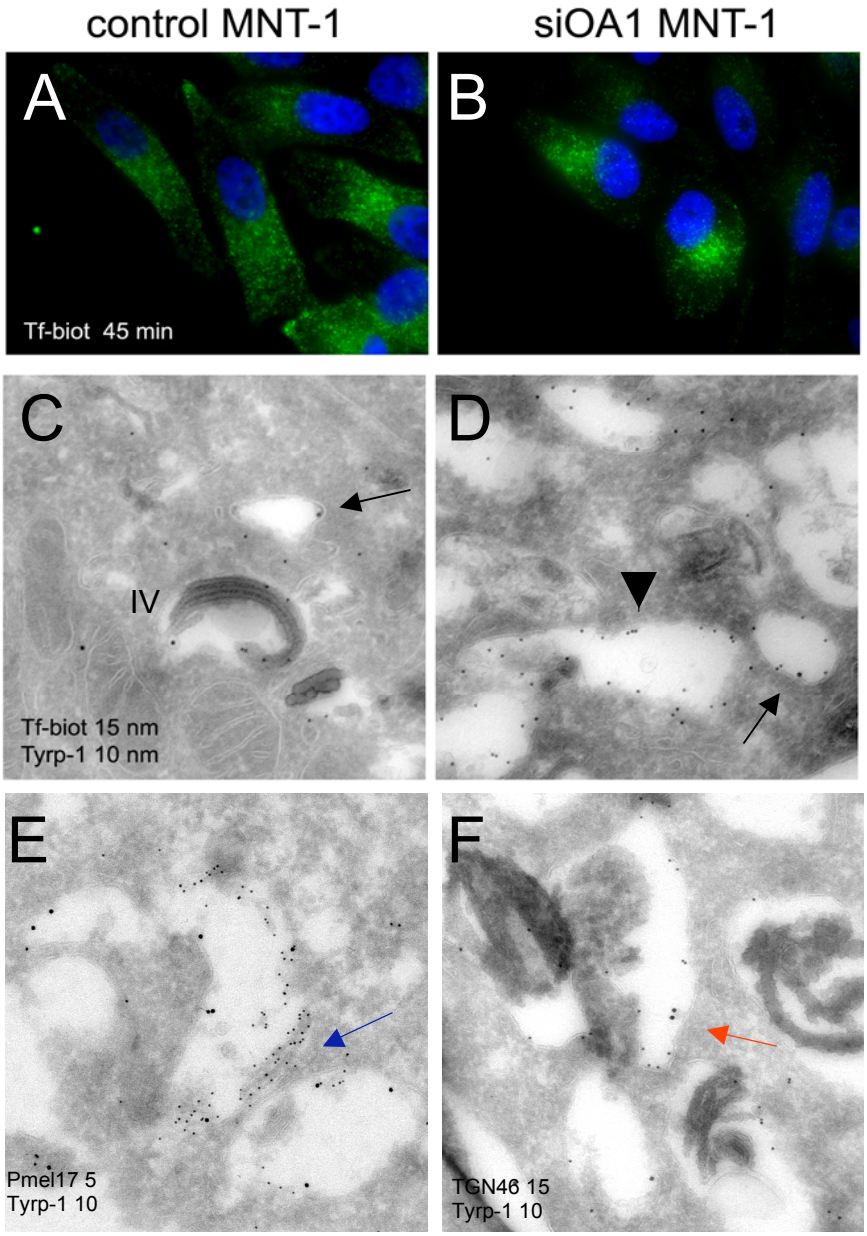

Figure 21: (A,B,C,D): ***Tyrp-1 containing vacuoles are not easily accessed by transferrin.*** Transferrin (early-recycling endosome tracer) conjugated with biotin was internalized for 45 min in siOA1 MNT1 **(B,D)** and control **(A,C)** cells. Internalization was controlled by immunofluorescence **(A,B)** and electron microscopy **(C,D)** by using anti-biotin antibody. Transferrin (Tf-biot 15 nm) was present in early endosomes (arrows) in both siOA1 and control cells, but preferentially not in the large vacuoles Tyrp-1 (10 nm) positive (*arrowhead* in D). **(E,F):** ***Tyrp-1 vacuolar compartments contain Pmel17*** (5 nm; *blue arrow* in E), ***a component of immature melanosomes, and in some cases, TGN46*** (15 nm; *red arrow* in F) **,** ***a TGN protein.*** Tyrp-1 (10 nm).

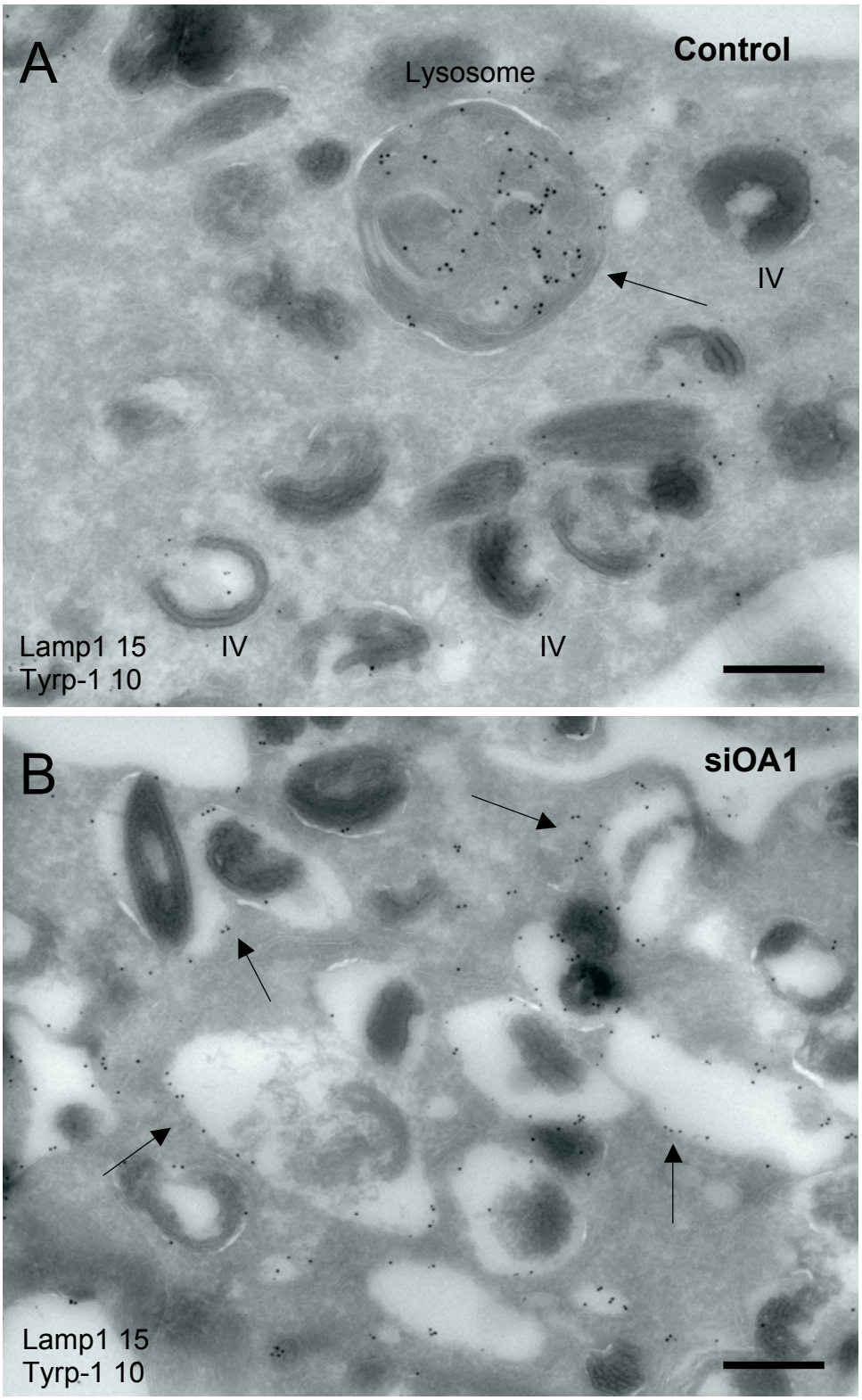

Figure 22: ***Tyrp-1 positive vacuoles contain also Lamp1, a late endosome-lysosome protein***. Note the increased amount of Lamp1 at the membrane of the melanosomes (*arrows* in **B**) in siOA1 MNT1 cells, compared to the normal levels in the control MNT1, in which Lamp1 is predominantly present in lysosome (*arrow* in **A**).

3.8 Microarray expression analysis on *Oa1*$^{-/-}$ embryonic RPE to elucidate OA1 downstream pathway

In order to identify factors affected by the Oa1 loss of function we compared the transcriptome of wild type and Oa1 null pigment cells. As previously described, Oa1 null skin melanocyte are not a good system to identify genes involved in the sequential events leading to the OA1 phenotype. For this reason we chose to perform a microarray analysis on embryonic tissue. Melanocytes cannot be easily purified from embryos while RPE is more easily accessible due to its anatomical location. We therefore collected murine embryonic eyes from E14.5 wt and Oa1 mutant mice, derived from the same litter to limit differences derived from gestation, to be compared by microarray analysis (Affimetrix mouse whole genome chip). Microarray experiments have been repeated with three biological samples to allow statistical analysis. We chose E14.5 developmental age because at this stage RPE is pigmented and the number of melanosomes is already reduced in the *Oa1* null mouse. The gene with the highest difference was OA1 (GPR143) itself, confirming the quality of this analysis.

Among the several genes either up or down regulated in *Oa1* null eyes (Table 4), genes involved in vesicle trafficking caught our attention. The most interesting genes among these were Trappc4 (Ethell et al. 2000, Kim et al. 2006, Miller et al, 2007), Cog-4 (Ungar et al. 2002, 2006) and Syntaxin-5a (Barrowman et al., 2000; Tai et al. 2004), all involved in vesicle transport in the biosynthetic pathway (ER-Golgi-TGN). In fact the reduced number of melanosomes and their increased size in Oa1 null mice may be related to defective trafficking from the biosynthetic pathway to the melanosomes.

Table 4. ***Genes up or down regulated in Oa1 null (Oa1$^{-/-}$) eyes.***

genes	description	*Oa1*$^{-/-}$
Ttn (Titin)	Structural constituent of cytoskeleton	–
Kifc1 (Kinesin family member C1)	Microtubule motor	–
Gpr126 (GPCR126)	G protein coupled receptor	–
Synpo2l (Synaptopodin-2-like)	Actin binding protein	–
Cart1 (Cartilagine homoprotein-1)	Transcription factor	–
Trappc4 (Transport protein particle subunit 4)	TRAPP multiproteic complex subunit, ER-Golgi vesicles trafficking	++
COG4 (Component of oligomeric golgi complex 4)	COG multiproteic complex subunit, intra-Golgi vesicles trafficking	++
Mcoln1 (Mucolipin-1)	Cation ion channel in late endosomes and lysosomes	+
Sytx-5a (syntaxin-5a)	SNARE protein, ER-Golgi-TGN vesicle transport and fusion	++
Golga1 (Golgi autoantigen-1)	Golgi apparatus protein	+
Gpaa1 (GPI anchor attachment protein-1)	GPI anchor protein	+
Gas5 (Growth arrest specific 5)	Non-protein-coding small nucleolar RNA	+
Dolpp1 (Dolichyl pyrophosphate phosphatase 1)	Endoplasmic Reticulum protein	+
Tmem23 (Transmembrane protein 23)	Golgi transmembrane protein	+

In order to confirm the variation of expression of these genes, we performed qPCR on the same RNA used for the microarray (Figure 23A), and on wt and *Oa1*$^{-/-}$ embryonic (Figure 23D), neonatal (Figure 23B) and 7 days postnatal (Figure 23C) RPE dissected and separated from the neural retina. We confirmed the upregulation of these genes in Oa1 mutant embryonic and neonatal RPE, but not at P7, when the macromelanosomes were completely formed, suggesting that Oa1 regulate these genes before macromelanosome formation. Interestingly, when we dissected RPE from neural retina we confirmed the specificity of the effect in the pigmented cells because no change of expression was detected in mRNA derived from *Oa1*$^{-/-}$ neural retina.

In order to understand whether changes in Trappc-4, Cog-4 and Stx5-a could be reproduced *in vitro* we analyzed the expression of these genes after 7 days of OA1 inactivation in MNT1 cells *in vitro* by qPCR and western blot. As expected, we confirmed an upregulation of these genes in the Oa1 defective cells and also of the proteins they encode (Figure 23E, 23F).

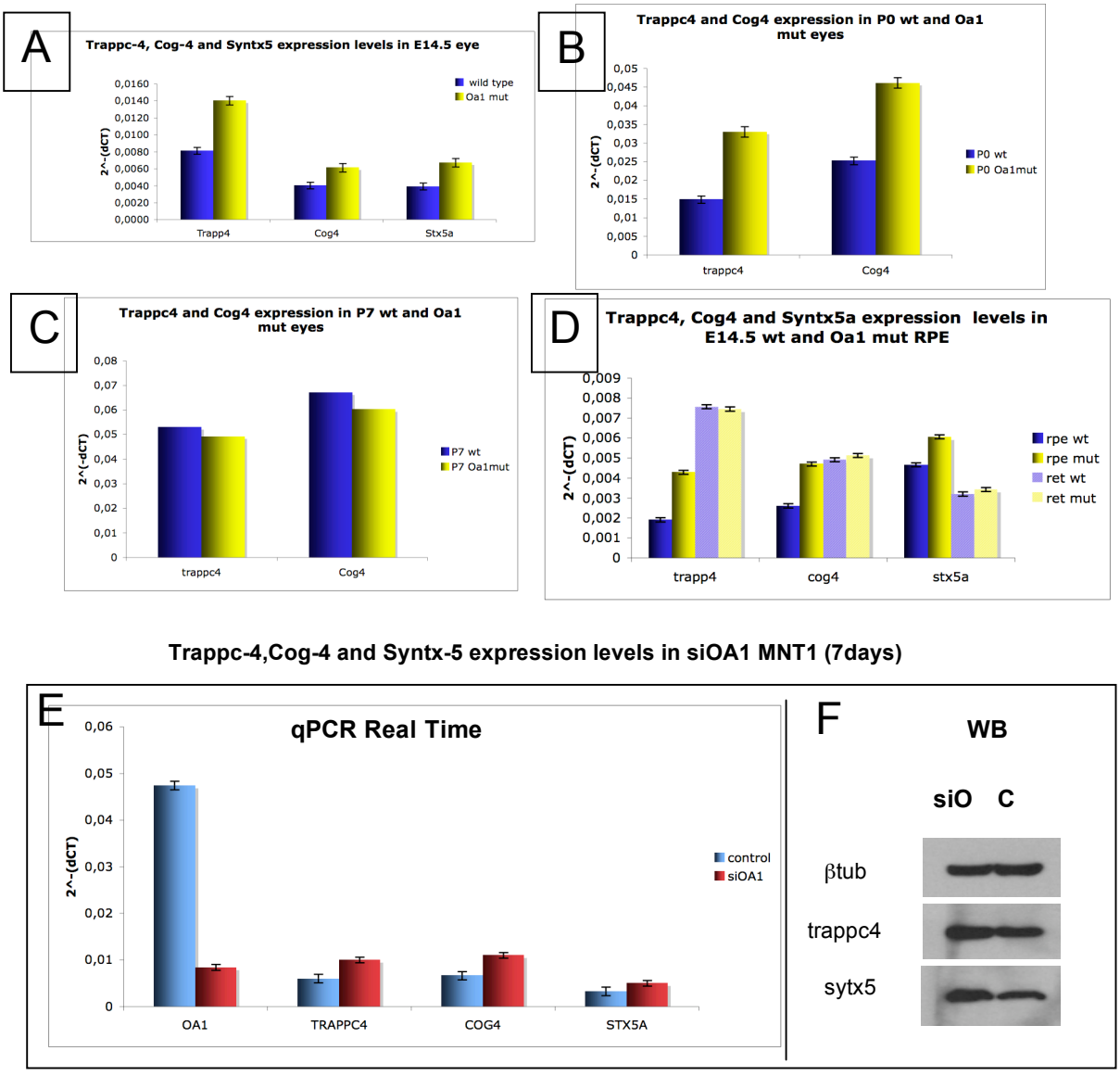

Figure 23. ***Upregulation of ER-Golgi vesicle trafficking genes (Trappc-4, Cog-4 and Syntaxin-5) in OA1 mutant eyes and in siOA1 interfered MNT1 cells.*** **(A,B,C,D):** Real time quantitative PCR shows upregulation of ER-Golgi vesicle trafficking genes (Trappc-4, Cog-4 and Syntaxin-5) in OA1 mutant embryonic (E14.5) eyes **(A),** embryonic (E14.5) dissected RPE **(D)** and neonatal (P0) **(B)** eyes compared to wild-type. We did not detect any difference of the expression levels of these genes at P7 postnatal day. **(E,F):** Real time quantitative PCR **(E)** and Western blotting **(F)** confirmed upregulation of ER-Golgi vesicle trafficking genes also in siOA1 MNT1 after 1 week of inactivation *in vitro*: RNA (Trappc-4, Cog-4 and Syntaxin-5) and protein (Trappc-4, Sytx-5) quantification.

Oa1 null skin melanocytes did not show differences in the expression of these genes when compared to the wild type melanocytes. Interestingly, they displayed an expansion of the ER and the Golgi as showed by the broader intracellular distribution of GM130, a coiled coil protein involved in tethering of vesicles coming from ER to the cis-Golgi (Moyer et al., 2001; Alvarez et al., 2001; Appenzeller-Herzog et al. 2006) and of Rab-1 (Allan et al., 2000; Cao et al., 1998; Moyer et al., 2001; Appenzeller-Herzog et al. 2006), a small GTP-ase involved in the events that precede the fusion of this vesicles with the cis-Golgi surface (Figure 24). We should point out that also OA1 inactivated melanocytic cells displayed the same phenotype. Our preliminary data showed a putative link between OA1 defect and proteins that regulate biosynthetic trafficking during melanosome biogenesis.

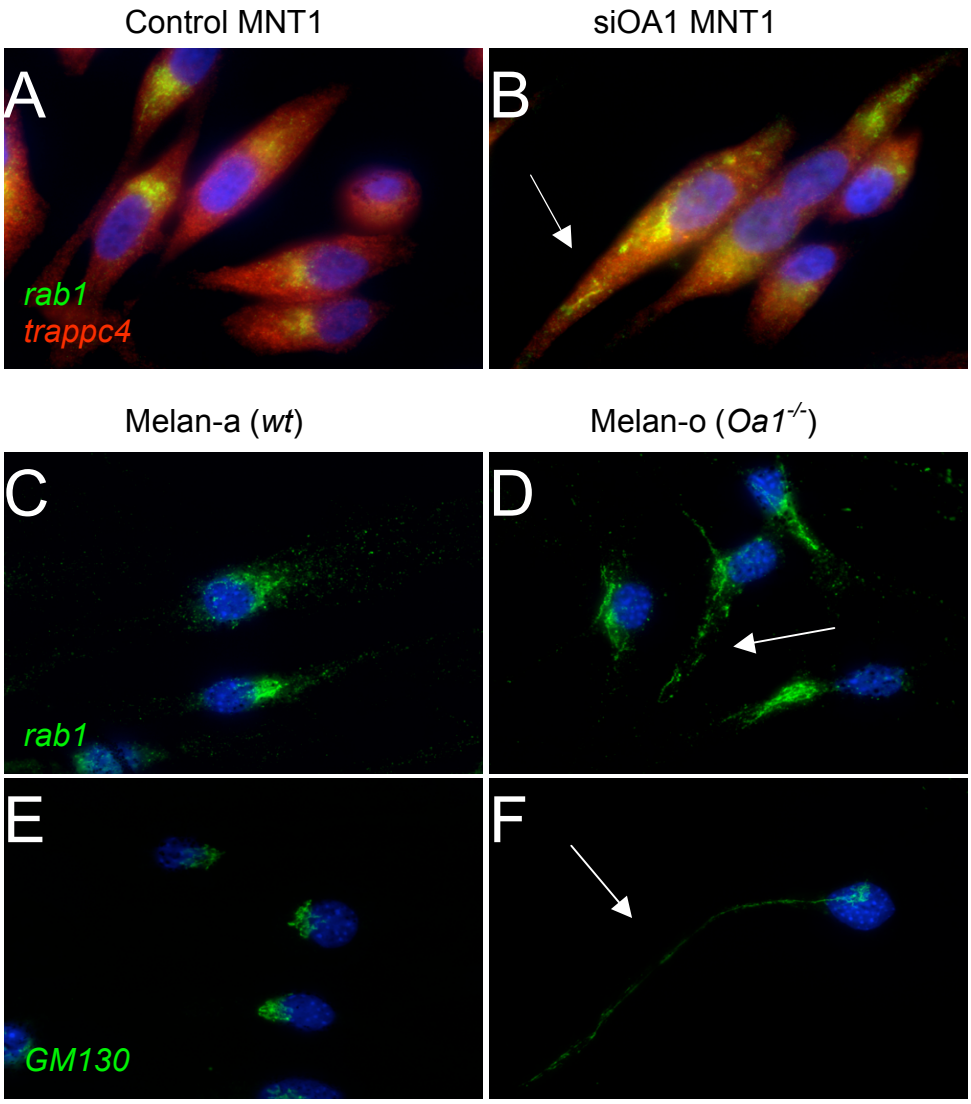

Figure 24. ***Subcellular distribution of proteins involved in ER-Golgi vesicle transport in siOA1 MNT1 cells*** **(A,B)** ***and mouse Oa1$^{-/-}$ melanocytes*** **(C,D,E,F).** Immunofluorescence detection of Rab 1 (green) and Trappc4 (red) proteins displays an expansion (*arrow*) of the Rab1 compartment in siOA1 MNT1 cells **(B)** compared with the control cells **(A)**. The expansion of Rab1 compartment, **(C,D)** as well as of GM130 **(E,F)** , was present also in *Oa1$^{-/-}$* (melan-o) compared to wt (melan-a) melanocytes..

4. FUTURE PRESPECTIVES

Further studies are needed to better understand OA1 function in melanosome biogenesis. We will focus on three different aspects:

1) we are planning to go deeper in the analysis of the phenotype of the siOA1 melanocytic cells *in vitro i)* measuring the pH in the intracellular compartments including melanosomes, *ii)* analysing the activity of tyrosinase, *iii)* performing BSA-gold internalization). Another aspect that we are going to investigate is the link between trafficking and Oa1 downstream signalling pathways. Our first aim is to unravel Oa1 signaling mechanism (via cAMP and/or Calcium increase) by measuring the intracellular levels of cAMP and Calcium in Oa1 inactivated cells.

2) we are going to better characterize the genetic interaction between OA1 and the newly identified genes involved in vesicle trafficking. We are preparing constructs to either downregulate Trappc-4, Cog-4 and Stx5-a by RNAi or upregulate them by transfection. These approaches are aimed to define the involvement of these proteins in melanosome biogenesis. We expect that if trafficking proteins are actively acting in melanosome biogenesis a melanosomal phenotype similar to the Oa1 null phenotype will be detectable in the over-expression experiments.

We are also planning to knock-down these proteins in Oa1 mutant murine skin melanocytes in vitro to define whether their up-regulation detected in Oa1 null cells is causative of the Oa1 phenotype. For all these experiments we will perform ultrastructural analysis at the EM level.

These studies will be a first step towards a characterization of the Oa1 signaling pathway, and they will open new perspectives to design specific therapeutic approaches for this disease.

5. DISCUSSION

Two main classes of albinism that affect pigmentation in the eye have been described: oculocutaneous albinism (OCA) and ocular albinism (OA). In OCA hypopigmentation is caused by inadequate melanization of an apparently normal number of melanosomes, whereas OA1 was suggested to result from reduced number of melanosomes (O'Donnell et al., 1976). Patients with OA1 have a severe reduction of visual acuity, horizontal and rotatory nistagmus, photophobia, and lack of stereoscopic vision due to misrouting of the optic tract. A peculiar melanosome phenotype in these patients is characterized by the presence of pigmented melanosomes with a giant size (Wong et al., 1983; O'Donnell et al., 1976), suggesting that the absence of OA1 could interfere with the normal melanosome biogenesis. However, we still lack a comprehensive view of how this phenotype is acquired and how it relates to the hypopigmentation observed in the RPE.

The focus of the studies reported in this thesis have been to address the following questions: i) how the presence of pigmented melanosomes reconciled with the observed albino phenotype in the RPE; ii) at which stage(s) of melanosome maturation OA1 exerted its function; iii) whether an impaired control of melanin synthesis and/or of rate of melanosome biogenesis was involved in giant melanosome formation. The first 2 questions were addressed during the first two years of PhD studies during which we defined the differences between OA (albinism isolated to the eye) and OCA. For these studies we took advantage of murine models of OCA and OA1. We focused our attention on two aspects of melanogenesis in the RPE: rate of melanosome formation and size control. Through a deep ultrastructural analysis of melanosomes in Oa1 mutant RPE we found that these events are both affected by lack of Oa1 activity.

We first characterized Oa1 interaction with Tyr in Oa1 mutant mice and showed that there is no impairment of Tyr activity and expression. This aspect of the phenotype differentiates Oa1 from other albino mice in which melanin production is affected (LaVail et al., 1978). However, the number of mature melanosomes in Oa1 mutant eyes was reduced by 50% in the RPE after birth explaining the depigmented ocular fundus. This reduction was in the number of stage IV melanosomes. It is possible that the effect on others melanosomal stages is masked by the lower number of stage-II and stage-III melanosomes. In fact, a reduction in the number of stage-II melanosomes was detected in mutants when melanosome maturation is stopped previous to stage IV (*Oa1*$^{-/-}$*;Tyr*$^{c\text{-}2J}$*/Tyr*$^{c\text{-}2J}$ and *Oa1*$^{-/-}$*;Matp*^{uw}*/Matp*^{uw} double mutants) and at embryonic stages. These results demonstrate, for the first time, that the reduced pigmentation of the RPE observed in patients with ocular albinism type 1 is caused by reduced number of pigmented melanosomes.

Another relevant aspect of Oa1 function highlighted by our studies in the Oa1 mutant mouse is the size control activity of Oa1 specifically on stage-IV melanosomes. This conclusion is based on the absence of melanosome enlargement in the RPE of *Oa1*$^{-/-}$*;Tyr*$^{c\text{-}2J}$*/Tyr*$^{c\text{-}2J}$ and *Oa1*$^{-/-}$*;Matp*^{uw}*/Matp*^{uw} double mutant mice which lack stage-IV melanosomes and display either stage-II or stage-III, respectively. Therefore, in the absence of fully mature melanosomes Oa1 is dispensable for size control.

Whereas the Oa1 size control activity is specific for the most mature melanosomes, an additional Oa1 function appears to be exerted at earlier stages of maturation. In particular, in *Oa1*$^{-/-}$ single and double mutants, the number of stage-II was reduced at the earliest stages of maturation analyzed: E15.5 for *Oa1*$^{-/-}$, and P7 or 3-month postnatal stages for *Oa1*$^{-/-}$*;Tyr*$^{c\text{-}2J}$*/Tyr*$^{c\text{-}2J}$ and *Oa1*$^{-/-}$*;Matp*^{uw}*/Matp*^{uw} double mutants. In contrast stage-III were more abundant in *Oa1*$^{-/-}$*;Matp*^{uw}*/Matp*^{uw} double mutants compared with *Matp*^{uw}*/Matp*^{uw} single mutant mice. This suggests that Oa1 may at the same

time control the maturation rate of melanosomes and inhibit the overgrowth of the most mature ones. We cannot exclude, however, that the phenotype observed in double mutant mice could also be due to a specific interaction between the two genes. Although our findings indicated that Oa1 regulates melanosome maturation and size, by using the double mutant approach we have not defined yet the mechanisms by which Oa1 may perform its double function. Heterotrimeric G-proteins associated with intracellular organelles have been described to participate in various steps of secretion and vesicular fusion and organelle maturation, even though no specific intracellular GPCR has yet been described for these functions. One hypothesis is that OA1 may act as a melanosome GPCR, either constitutively active, or activated by melanin or by a product of melanin synthesis, that control membrane delivery to the melanosomes. OA1 represents the first example identified so far of an exclusively intracellular GPCR (Schiaffino et al., 1999). Discrepant data have been published on OA1 subcellular localization (Schiaffino et al., 1996; Samaraweera et al. 2001) leaving an open controversy.

The studies performed in the last period of my phD, making profit of cell biological methods, allowed us to solve this controversy and to better understand Oa1 function in melanosome biogenesis elucidating some of the trafficking events leading to the two *Oa1*$^{-/-}$ defects, the reduction of early stage melanosomes and the presence of macromelanosomes.

We addressed the issue of OA1 localization by immunofluorescence and immunogold analysis of the OA1 distribution primarily in pigmented cells (mouse and human melanocytes) and also in not pigmented cells. This strategy made use of OA1-tagged constructs, in particular OA1-flag that allowed a complete maturation of the OA1 protein when transfected in melanocytes. Of notice is that studies, suggesting OA1 protein localization only in late endosomes and not in melanosomes, were performed using a GFP tagged OA1 that in our hands did not allow post-translational modifications

(Samaraweera et al., 2001). We found that OA1 is similarly distributed along both the late endosomal-lysosomal (as shown by the co-localization with Lamp-1, a late endosome protein) and the melanosomal compartments in melanocytic cells (as shown by the colocalization with Tyrp-1, a melanosome specific protein). In particular, electron microscopy showed that OA1 is present in the limiting membrane and also in internal vesicles of late stage melanosomes, mostly associated with Tyrp-1. Correlation of OA1 expression with Tyrp1 suggests that OA1 may be involved in controlling some steps of the biosynthetic or endocytic trafficking of this protein at later stages of melanosome maturation.

A detailed analysis of the melanosomal phenotype in mouse *Oa1*$^{-/-}$ melanocytes revealed that macromelanosomes are intermixed with normal size melanosomes as also seen in the RPE of mutant mice (Cortese et al., 2005). Furthermore, macromelanosomes, that are three times bigger than the normal melanosomes, were retained in the perinuclear region of melanocytes and appeared to be less motile than normal melanosomes. This phenotype opens the hypothesis that these giant melanosomes are not properly mature organelle and/or their composition in proteins is altered, leading to a failure in the recruitment of effectors proteins necessary to delivery them to the periphery. EM analysis showed the presence of melanosomes with irregular shape and not homogeneous melanin content in *Oa1*$^{-/-}$ melanocytes. They appear as a mixture of immature striated melanosomes, pmel17 positive, with a central core similar to pigmented mature melanosomes.

Many studies using mouse models of other pigmentary disorders (e.g. Hermansky Pudlack Syndrome, HSP) have helped to understand the steps affected by mutations in the HSP genes in vesicle trafficking controlling melanosome biogenesis. The analysis of the phenotype generated by Oa1 loss of function in skin melanocytes suggests that the absence of Oa1 affects melanosome maturation and their protein composition, but did not allow to

clearly understand the trafficking step involved in the generation of the OA1 defect. In fact, in these cells we were observing an "end-point" situation that is the consequence of many events that have produced the Oa1 defect.

To overcome this limit we chose to follow the morphological and molecular events starting as soon as OA1 is inactivated. To this purpose we have downregulated OA1 mRNA by siRNA in human MNT1 melanocytic cells. This approach has revealed very helpful to follow melanosomal maturation right after the loss of OA1 activity and, therefore, unravel the sequential steps leading to the formation of macromelanosomes.

We confirmed that this technique was very efficient in reducing the expression of OA1 mRNA and protein as analyzed by real-time RT-PCR and western blotting. After 1 week of inactivation of OA1, MNT1 cells did not contain the typical macromelanosomes, but they showed a significative reduction of melanin content and of the number of melanosomes, as in *Oa1*$^{-/-}$ RPE *in vivo*. This was the first evidence that siRNA can reproduce the OA1 phenotype in vitro. The ultrastructural analysis of OA1 inactivated cells showed that in the absence of OA1 the reduction in the number of melanosomes is accompanied by an increase of enlarged compartments containing melanosomal proteins (Tyrp-1 and Pmel17) but also proteins that are not normally present in high amounts in pigmented structures (Lamp1 and TGN46). These enlarged compartments cannot be labeled by transferring in endocytosis experiments, suggesting that they are not part of the early endocytic pathway, but they may represent a subdomain not accessible to the transferrin receptor. Our studies revealed an increased amount of Lamp1 also at the membrane of the pigmented structures. Although further studies are needed to better characterize this intracellular compartment and to understand how the absence of OA1 leads to the reduction of melanosome number and the giant melanosome phenotype, all together our results indicate OA1 may be a key factor controlling the maintenance of melanosome identity and

composition. In fact in aberrant vesicles forming as a consequence of OA1 knockdown we detected melanosomal and lysososmal and TGN proteins.

We can also speculate that OA1 signalling activity may influence fusion or fission events between intracellular compartments and melanosomes, but also in between different melanosomal stages, during their maturation. This hypothesis was forwarded based on the evidence that absence of OA1 caused reduction of early stage melanosomes, presence of aberrant pigmented structures that appears as a mixture of early stage (stage-II) with pigmented late stage (stage-IV) melanosomes.

Detailed ultrastructural analysis defined morphological alterations that are possibly due to vesicle trafficking defects. In order to identify molecules, important for these cellular events, that are affected by lack of OA1 we undertook a systematic analysis of the transcriptome of Oa1 wild type and mutant RPE. We chose to use tissue from the mouse model because we wanted to identify factors that are causative of the albino phenotype. RNA was purified from murine E14.5 embryonic eyes from wild type and Oa1 mutant mice. We preferred to use embryonic tissue because at this stage melanosomes are already less abundant but macromelanosomes are not evident yet suggesting that melanogenesis is still active and molecular defects can be revealed. With these samples we probed whole murine genome microarrays and identified interesting genes, involved in vesicle trafficking, that are upregulated in *Oa1* mutant RPE. The most interesting genes among them were *Trappc-4* (Cai et al. 2005; Sacher et al. 1998, 2001), *Cog-4* (Ungar et al., 2006) that are two subunits of two large multiprotein complex called TRAPP and COG Also *Syntaxin-5* (Barrowman et al., 2000; Guihua et al. 2004), a SNARE protein, was upregulated in Oa1 null eyes. Interestingly, the yeast homologue of Syntaxin-5 interacts with one subunit of TRAPP and some subunits of COG complexes (Barrowman et al. 2000). These three complexes are all involved in vesicle transport during the biosynthetic

pathway (ER-Golgi-TGN). Based on several recent evidences the different subunits of the tethering complex, like the TRAPP complex, may participate in additional events in mammals, playing a role in multiple vesicular transport events and performing specific critical function beyond generalized ER-to-Golgi transport (Ethell et al. 2000) (Cai et al., 2005) (Ungar et al., 2006). We wanted to confirm the link between the tethering complex with Oa1 and define the time window during which it happens. To this purpose we collected RNA from embryonic neonatal and adult murine eyes. These experiments highlighted that up-regulation of TRAPP, COG and Syntaxin can be observed in the mutant RPE up to the neonatal stage, but not at P7, when melanosome biogenesis is completed in the murine eye. From this information we deduce that Oa1 exerts its function in controlling melanosome targeted vesicle trafficking during melanosome formation and we do not know whether it acquires a different function after melanosome maturation.

We further confirmed the reliability of the in vitro model in MNT1 cells by detecting upregulation of these same genes after siRNA treatment.

Overall, these results suggest that Oa1 functions through regulation of proteins involved in vesicle trafficking events. The importance of the tethering complex in melanosome biogenesis is confirmed by a recent study in which a new mouse model for mosaic hypopigmentation (*mhyp)* is caused by mutations of another TRAPP subunit, *Trappc6*. The analysis of the phenotype in this albinism model showed that *Trappc6* mutant RPE had patchy areas of depigmentation and smaller melanosomes (Gwynn B. et al., 2006).

In summary, our in vivo studies on Oa1 null mouse and double mutant mice with Tyr and Matp together with molecular and morphological approaches *in vivo* and *in vitro* indicate that Oa1 is an intracellular GPCR lying on intracellular membranes (mature melanosomes and late endosomes) with a specific function fundamental for the identity of the melanosome. Malfunction of OA1 lead to two phenotypes, abundance of melanosomes

detectable at early stages of maturation and melanosomal size, detectable only in highly pigmented organelles. These two phenomena up to now were seen as two separated roles of OA1, however our results suggest that are probably based on a common defect. This hypothesis is based on the evidence that, in the absence of Oa1, vesicles containing markers of different membranous compartments can be detected. In fact, its signalling activity may control fusion or fission events between an intracellular compartment and melanosomes during their maturation, but also in between different melanosomal stages (Figure 25). In support of this idea come our molecular data showing a link between Oa1 and proteins that regulate vesicle tethering. OA1 probably functions by regulating proteins involved in vesicle trafficking events. The study of this interaction during melanosome biogenesis is a first step towards unraveling the mechanism through which Oa1 affects melanosome number and size and thus better understand the pathogenetic events underlying Ocular albinism type 1.

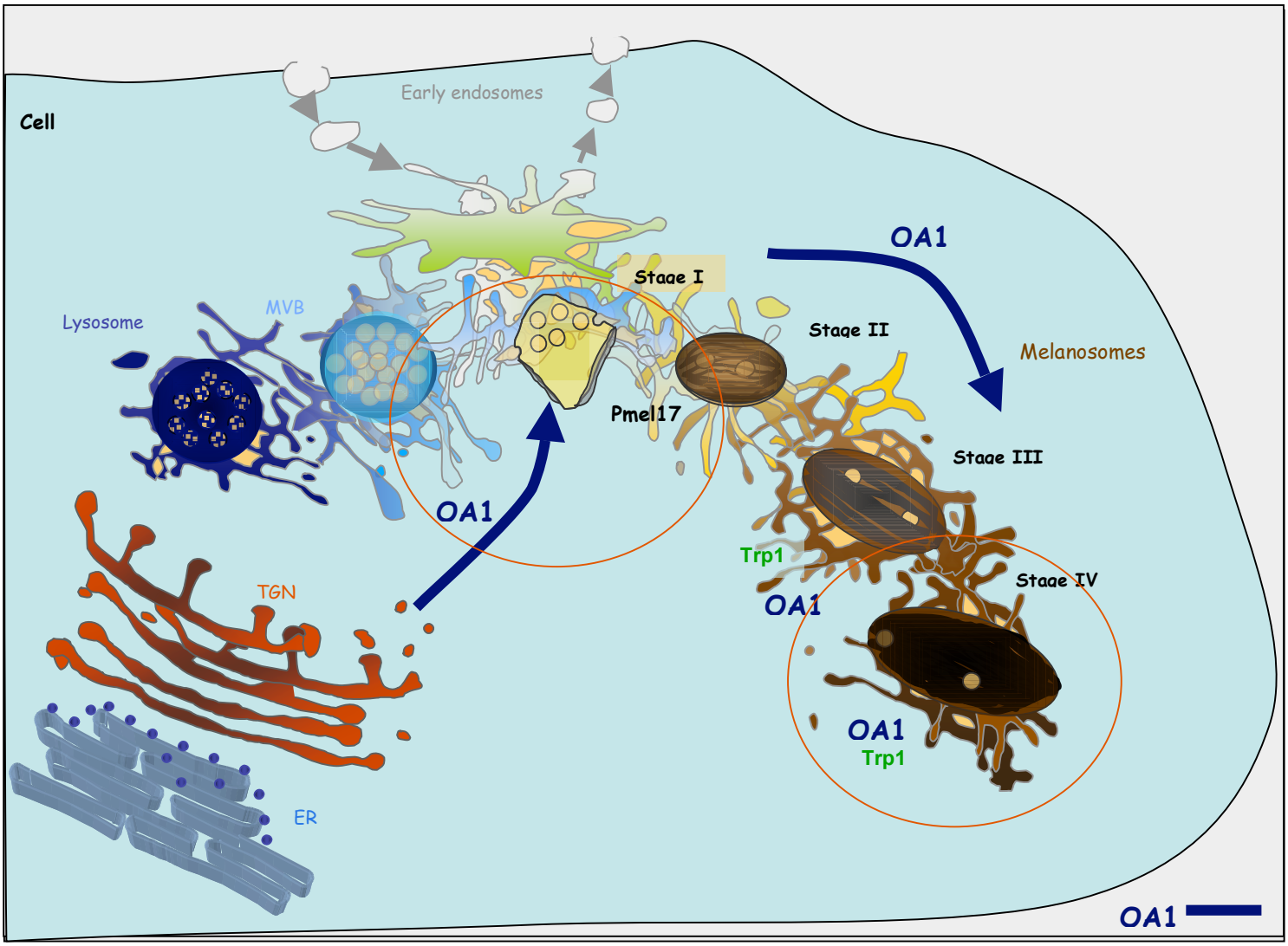

Figure 25. ***OA1 function model.*** Oa1 controls the abundance of melanosomes at early maturation stages (stage I), and melanosomal size, at later stages (stage IV). We speculate that OA1 exerts its role by regulating fusion or fission events between an intracellular compartment and melanosomes during their maturation, but also in between different melanosomal stages.

6.MATERIALS AND METHODS

6.1 Mouse Breeding

All the procedures on mice (including their euthanasia) were performed in accordance with ARVO Statement for Use of Animals in Ophthalmic and Vision Research and with institutional guidelines for animal research. Mice in this study were bred and maintained in a 12-hour light–dark cycle. *Oa1*$^{-/-}$ mice were bred on a C57BL/6 genetic background. In these mice, the first exon of the *Oa1* gene is replaced by an Hprt cassette, eliminating the start codon and inactivating Oa1 protein formation (Incerti et al. 2000). *Tyr* $^{c\text{-}2j}$ and *Matp*^{uw} mice, both on a C57BL/6 background, were purchased from the Jackson Laboratory (Bar Harbor, ME) and maintained inbred in the animal house. The *Tyr* $^{c\text{-}2j}$ allele is a recessive mutation due to a G-to-T base change at nucleotide 291 resulting in an amino acid change from arginine to leucine at residue 77. No tyrosinase activity was found in hair bulb extracts from *Tyr* $^{c\text{-}2j}$ homozygous mice (Kwon et al. 1987). The Matp^{uw} allele is due to a 7-bp deletion in exon 3 resulting in a 43 amino acid frameshift and premature stop codon, which predicts that the Matp protein lacks the C-terminal six-transmembrane domains (Du et al. 2002).

To generate *Oa1*$^{-/-}$*;Tyr* $^{c\text{-}2j}$*/Tyr* $^{c\text{-}2j}$ and *Oa1*$^{-/-}$*;Matp*^{uw}*/Matp*^{uw} double-mutant mice, single homozygous mutant mice were crossed, and the resultant F_1 double-heterozigous progenies were intercrossed. F_2 progeny was scored for coat color (*Tyr* $^{c\text{-}2j}$*/Tyr* $^{c\text{-}2j}$*, Matp*^{uw}*/Matp*^{uw}) and by diagnostic PCR on genomic DNA obtained from the tail for Oa1$^{-/-}$. The primers used to genotype the *Oa1* null allele were the following: OA1f (ACA TGA CGC CCA ATC TCC CTC), OA1r (TAG ACT ACC CTC TGA GTC CAG), HPRTf (TAA GTT CTT TGC TGA CCT GCT), HPRTr (GGC TTT GTA TTT GCC TTT TCC).

6.2 Tyrosinase Activity Assay

Eyes were dissected from killed littermates (P7) of different genotypes and frozen at -70°C. Each mouse was genotyped and at least four eyes for each genotype were used for the assay. Each pair of eyes was homogenized on ice in 10% glucose in PBS with 50 μg/ml leupeptin, 20 μg/ml aprotinin, and 5 mM benzamide. Protein concentration was determined using the Bradford method (Bio-Rad, Hercules, CA). Equal quantities of protein were used in each reaction. After the addiction of tritiated tyrosine (GE Healtcare, Arlington Heights, IL) to the reaction, Tyr activity was assayed radiometrically by meseauring production of tritiated water from hydrolysis of tyrosine, as reported in a published protocol (Chiu et al. 1993). Activity was expressed as counts per million per microgram per hour of total protein.

6.3 Quantitative RT-PCR

Total RNA was extracted from wild type and Oa1-null either whole eyes or dissected RPE and retina at embryonic stage E14.5; wildtype and Oa1-null postnatal whole eyes at birth (P0) and 7 days after birth (P7); wild type and Oa1-null skin melanocytes (melanA, melanO); siOA1 (at 7 days of OA1 interference *in vitro, see below*) human melanoma MNT-1 and control cells using RNeasy MiniKit (Quiagen, Milan, Italy) according to the manufacturer's instructions. The same amount of cDNA for each genotype or treatment was synthesized using Superscript II (Invitrogen) and random primers. Real time PCR was carried out with the GeneAmp 7000 Sequence Detection System (Applied Biosystem). The RT-PCR reaction was performed using cDNA, 12.5 μl SYBR green master mix (Applied Biosystem) and 400 nM primers for each gene (*see list below*).

Water was added to a final reaction volume of 25 μl. the PCR conditions were as follows: preheating at 50°C for 2 min and 95°C for 10 min; 40 cycles of 15 s at 95°C and 1 min at 60°C.

Quantification results were expressed in terms of the cycle threshold (Ct). All real-time quantitative PCR reactions were run in triplicate and the Ct values were averaged from three independent samples. Data were normalized to the internal control, the reference genes (S26 for human samples and GAPDH for murine samples). Differences between the mean Ct values of each gene and those of the reference gene were calculated as $\Delta Ct = Ct_{gene} - Ct_{reference}$ and represented as $2^{-\Delta Ct}$.

Table 5. *Sequences of the forward (f) and reverse (r) intron-spanning primers used for Real-time quantitative PCRs:*

mouseGAPDHf	GTA TGA CTC CAG TCA CGG CAA A
mouseGAPDHr	TTC CCA TTC TCG GCC TTG
mouseTYRf	CAA GGA TCT GGG ATA TGA CTA CAG C
mouseTYRr	GCT CAA TAT AAT TTC TGT AAA AGC CTG G
mouseMATPf	CCT CCA CTA CCA TGC CCT CCT
mouseMATPr	CCC AGT CTA TGG CAC CCA AA
mouseOA1f	GCT ATG CAG TTG ATG TAT ACT TGG TGA
mouseOA1r	GAT GTG GTA CAG CAG GAT GGT G
mouseTRAPPC4f	AGC TTA TGC TGG CCT CGA TG
mouseTRAPPC4r	ACT GCC CTG TTC CGG AGA TA
mouseCOG4f	CGC CTC TCT CAG ATG GCT ACA
mouseCOG4r	GGC CAG AGT TAG CAC CCA
mouseSYTX5f	CAG CAA TTG GCA CAC ATG GT
mouseSYTX5r	GGC TCC AAG CAC ATT CTC GT
humanS26f	CCG TGC CTC CAA GAT GAC AA
humanS26r	GCA ATG ACG AAT TTC TTA ATG GCC T
humanOA1f	CGG AGA TCG GCA GGA CTG AGC AC
humanOA1r	ATA GTG GGG GAT GGC GTG GT
humanTRAPPC4f	AGA CTT TGC CCT CAA GAA TCC A
humanTRAPPC4r	GGT TCT GGT CAA AGA GCT CAC AC
humanCOG4f	ACA AGT TTG CCC GGC TCT C
humanCOG4r	CCC CAG TAA TCG AGG ATC TCG
humanSYTX5f	CAG CTC ATT GAC GAG CAG GAT T
humanSYTX5r	CCT AGC ACG TTC TCG TCG ATC CTC

6.4 Antibodies

We used the following primary antibodies: αPEP7, αPEP1, αPEP8, affinity-purified rabbit antiserum to the carboxyl termini of murine melanogenic proteins respectively Tyrosinase, Tyrp-1 and Dct (Jimenez et al., 1991); polyclonal anti-Oa1, raised against the C-terminus (last 14 amino acids) of murine Oa1 (Cortese K., **Giordano F.** et al., 2005); rabbit polyclonal anti-CRALBP (Nawrot et al., 2004); FITC- conjugated rat anti mouse Lamp1 (BD Bioscience); polyclonal anti EGFP (Molecular Probes); monoclonal anti flag M2 antibody (Sigma-Aldrich); polyclonal anti flag (Sigma Aldrich); monoclonal anti β-tubulin antibody (SIGMA, Milan, Italy); TA99 mouse anti-TRP1 mAb (American Type Culture Collection; Thompson et al., 1985) for immunofluoscence and immunogold labelling and monoclonal anti-TRP1 75KD (Abcam) for western blotting; anti-Lamp1 mouse mAb (BD PharMingen); monoclonal anti-CD63 (Caltag Laboratories); melanoma Ab-2 anti-Pmel17 (clone HMB50) (Lab Vision Corporation); mouse monoclonal anti-Pmel17 (clone HMB45) (Novocasta); rabbit anti-GM130 (Calbiochem); polyclonal anti-Rab1 (from Jaakko Saraste); monoclonal anti-Trappc-4 and anti Syntaxin-5 (Abnova Corporation); sheep anti-human TGN46 (AbD Serotec); rabbit anti mouse IgG was from Dakopatt; polyclonal anti biotin (Polysciences Biovalley).

6.5 Western Blotting

Eyes were dissected from either wild type or Oa1-null mice at different embryonic stages (E12.5, E14.5, E16.5) and postnatal ages (P0, P7, 3 months), and proteins were extracted using the TRIzol reagent (Life Technologies), according to the manufacturer's instructions and dissolved in 1% SDS in PBS containing a protease inhibitor cocktail (Roche Diagnostic, Monza, Italy). Proteins were extracted from the Hela or melanocyte cultures with lysis buffer (1% Triton-X100, 1mM EDTA pH 8,0, 150mM NaCl,

20mM Tris pH 7,5) in the presence of protease inhibitor cocktail (Roche Diagnostic, Monza, Italy) on ice for 30 min. The lysed cells were then centrifuged at 21,000g for 20 min at 4°C. Protein concentrations were determined by Micro BCA^{TM} Protein Assay Reagent Kit (Pierce). The protein samples were mixed with an equal volume of loading buffer containing 2% SDS and 5% β-mercaptoethanol and then boiled for 2 min. To detect OA1-tagged protein, protein samples were mixed with an equal volume of 14% SDS and warmed at 37°C for 5 min. In fact, lower SDS concentration or boiling were avoided due to the precipitations of the OA1 protein under these conditions. Equal amount of proteins were loaded and separated in an 8% SDS-PAGE gel. The separated proteins were then transfered to polyvinylidene difluoride membrane (Millipore) and the membreanes were blocked in PBS/0.1%Tween-20 (PBS/T) with 5% nonfat dried milk, incubated with primary antibody in PBS/T, washed four times in blocking solution, and incubated with horseradish peroxidase-conjugated secondary antibody (anti-rabbit or anti-mouse; 1:10000; Jackson ImmunoResearch Laboratories) followed by washing in PBS/T. Visualization of the antibody binding was carried out with ECL Plus Western blotting detection system (GE Healthcare) according to the manufacturer's instruction.

6.6 Cells and culture conditions

Melanocytes, MNT-1 and Hela cells:

The immortal Oa1 null and wild type melanocytes cell lines were derived from wild type or Oa1$^{-/-}$ C57Bl/6 mouse skin (obtained from E.Sviderskaya). Cells were maintained in RPMI-1640 supplemented with 10%FCS and 200nM phorbol 12-myristate 13-acetate at 37°C with 10% CO_2.

MNT-1 human melanoma cells were maintained in DMEM supplemented with 10% AIM-V medium (Life Technologies), 20% FCS, non-essential

aminoacids, and sodium pyruvate. Hela cells were cultured in DMEM with 10% FCS.

Primary RPE cell culture:

Primary retinal pigment epithelium cells (RPE) and choroidal melanocytes were isolated from P1 eyes of wild-type, *Oa1*$^{-/-}$, *Tyr* $^{c\text{-}2j}$ and *Matp*^{uw} mice.

After a brief (30 sec-1 min) treatment with 2 mg/ml Dispase II (Roche , Indianapolis, IN) in Hanks' balanced salt solution (Invitrogen) choroids and RPE were gently separated from neural retina, lens, and vitreous and incubated in 2 ml of 0.5 mg/ml trypsin (Sigma-Aldrich, St.Louis, MO) in Hanks' at 37C for 30 minutes.

After adding 1 volume of 0.2 mg/ml trypsin inhibitor (Roche) in DMEM (Invitrogen), the tissue was triturated 50 times with a borehole glass pipette. The single-cell suspension was resuspended in 1 ml/eye DMEM-Ham's F12 1:1 (Invitrogen) containing 5% FBS and N2 hormone mix (Invitrogen) and plated on extracellular matrix (ECM) gel (SIGMA) at 37°C in a 5% CO2 atmosphere. Cells were cultured for 4 to 5 days and not propagated in culture. Cell identity was defined by pigmentation and by expression of Tyr, Tyrp-1 and Tyrp-2 for RPE and choroidal melanocytes and by CRALBP for RPE cells.

6.7 Immunofluorescence (IF)

Cells were grown on glass coverslips (coated with ECM for RPE primary cells) and transfected with plasmid constructs or siRNA. Cells on coverslips were rinsed in PBS, fixed for 15min with 4% paraformaldehyde/PBS, rinsed again and permeabilized with 0.1% saponin in PBS. After 30 min of blocking the cells were incubated with primary antibodies for 1,5 h, washed several times and incubated with Alexa 488- or Alexa 568-conjugated anti-rabbit or anti-mouse secondary antibodies (1:200; Molecular probes) and washed again. All incubations and wash steps were performed with PBS/BSA/0.01%

saponin. Coverslips were mounted in mowiol mounting medium, viewed on a Microscope Leica DM 6000 and the images were obtained with the Metamorphe software.

Immunofluorescences on RPE primary cells were visualized with a laser confocal microscope system (Leica, Heidelberg, Germany) and the images were processed with Photoshop 7 (Adobe).

6.8 Electron Microscopy (EM)

Ultrastructural Analysis of Retina Pigment Epithelium (in collaboration with Prof. C. Tacchetti , University of Genova):

P7 and 3 month-old mice of different genotypes were anesthetized and perfused with 4% paraformaldehyde and 2% glutaraldehyde in PBS. Eyes were removed and placed in 0.1 cacodylate buffer, containing 2.5% glutaraldehyde, for 3 hours at room temperature. Eyes were postfixed in OsO_4 for 1 hour and uranyl acetate for another hour. Subsequently, samples were dehydrated through a graded ethanol series and propylene oxide and embedded in resin (Poly-Bed; Polysciences, Inc., Warrington, PA) overnight at 42°C and 2 days at 60°C. A dorsoventral orientation was maintained during embedding. Semithin sectioning (0.5 μm) was started at the frontal pole of the embedded eye (corresponding to the cornea) and ultrathin sections (50 nm) were collected, starting when the RPE was observed. Ultrathin sections were stained with uranyl acetate and lead citrate and observed with an electron microscope (model CM10 or model G2 Tecnai; Philips, Eindhoven, The Netherlands). Comparable regions of the different genotypes were analyzed.

The number of melanosomes and their maturation stages in the RPE of single- and double-mutant mice were counted on 10 random micrographs at X21.000, either at the apical zone or the basal zone of the epithelium. The basal zone was defined by the presence of basal lamina, the apical zone by the presence of microvilli, and the limit between the two regions was drawn at half

distance between the apical and basal surfaces. Diameters were measured on melanosomes at different stages of maturation (stage II, III and IV) in each micrograph (Photoshop 7.0 software; Adobe System, Mountain View, CA). For statistical analysis we applied unpaired *t-test* assuming equal variances.

Ultrastructural analysis and immunogold labeling of cultured cells:

For conventional EM, cells grown on coverslips were fixed with 2.5% glutaraldehyde in 0.1M cacodylate buffer for 24 h. After several washes with 0.1M cacodylate buffer, the cells were postfixed with 2% OsO4, dehydrated in ethanol, and embedded in Epon while on the coverslips. Ultrathin sections were prepared and counterstained with uranil acetate and lead citrate before the observation.

For immunogold labelling, cells were fixed with a mixture of 2%PFA and 0.2% glutaraldehyde in 0.1M phosphate buffer, pH 7.4. Cells were scraped in 0.1M phosphate buffer containing 1% gelatin and pelleted in 10% gelatin. The cell pellets were solidified on ice and cut into small blocks, which were infused in 2.3M sucrose overnight at 4°C for cryoprotection. Afterwards, the blocks were mounted on aluminium pins and frozen in liquid nitrogen. Ultrathin cryosectioning and immunogold labelling were done as described (Raposo et al. 1997). Briefly, ultrathin (~65 nm) cryosections were prepared with an Ultracut FCS ultracryotome (Leica), and single- or double-immunogold labelled with antibodies and protein A coupled to 5 or 10 or 15-nm gold, as indicated in the legends to the figures. Ultrathin cryosections were retrieved with a mixture of methylcellulose and uranyl acetate (Liou et al. 1996) for better preservation of membranes. Sections were analyzed on Philips CM120 electron microscope, equipped for cryo-EM and with a 1Kx1K GATAN SSC camera.

6.9 Cloning of OA1-tagged constructs

The human OA1 coding sequence was amplified by polymerase chain reaction (PCR) by using *Pfu* DNA polymerase (Promega) and the following primers containing EcoRI and XhoI restriction sites: OA1f: CG*GAATTC*ATGACCCAGGCAGGCCGG;OA1r:CCG*CTCGAG*TCACACC TGGACACGGAAG. The PCR product was digested by EcoRI and XhoI and subsequently cloned into EcoRI/XhoI-digested pcDNA3 vector (pRIZZO-flag) to express OA1 with a Flag-tag at the C-terminal. The same PCR product was also cloned into pEGFP-N1 vector (Invitrogen) to express OA1with an EGFP-tag at the C-terminal.

6.10 Transfection and siRNA interference

NMT1 and HeLa cells were grown on glass coverslips and transfected with plasmid constructs using Lipofectamine 2000 (Invitrogen) following manufacturer's recommendations. Cells were analyzed after 48 h.

Three synthetic siRNA duplex oligomers (21-mers) targeting human OA1 (first: GGA UAU GAA CCA CAC GGA A; second: GGC UGU AAA GUA AGU GUA A; third: GGU UGU CGA AUA UCA UCA A) were designed and then ordered from QIAGEN. As control, a non-targeting control siRNA was used. Cells were transfected using Oligofectamine (Invitrogen) according to the manifacturer's instructions. The final concentration of siRNA oligos was 1 μM. Cells were subjected to two rounds of transfection on day 0 and 4, were passaged as required, and were analyzed on day 7.

6.11 Transferrin incorporation

OA1 interfered and control MNT-1 cells were washed with serum-free medium seven days after transfection and starved for 45 min before incubation with biotin-conjugated transferrin (60 μg/ml) (Sigma-Aldrich) continuously for 45 min at 37°C. After washing with ice-cold medium, cells were fixed and processed for ultracryotomy.

6.12 Melanin content assay

OA1 interfered and control MNT-1 cells were disrupted by sonication in 50 mM Tris-HCl, pH 7.4, 2 mM EDTA, 150 mM NaCl, 1 mM dithiothreitol and protease inhibitors seven days after transfection. Pigment was pelleted at 20,000g for 15 min at 4°C, rinsed once in ethanol/ether (1:1), and dissolved in 2M NaOH/ 20% dimethylsulfoxide at 60°C. Melanin content was measured as optical density at 492 nm.

6.13 Microarrays *(in collaboration with Dr. Stefano Volinia, University of Ferrara)*

The detailed procedure used for DNA microarray analysis is available at: http://biotecnologie.unife.it/microarrays/. Briefly, 3μg of total RNA, isolated using an RNeasy Mini Kit (Qiagen) from wild type and OA1 null E14.5 embryonic eyes derived from the same litter, were used to derive fluorescently labelled cDNAs, which were hybridized on Affimetrix mouse whole genome chip (GeneChip® Mouse Genome 430 2.0). The experiments of microarray were repeated with three different biological samples.

REFERENCES

Allan, B. B., Moyer, B. D., and Balch, W. E. (2000). Rab1 recruitment of p115 into a cis-SNARE complex: programming budding COPII vesicles for fusion. Science *289*, 444-448.

Alvarez, C., Garcia-Mata, R., Hauri, H. P., and Sztul, E. (2001). The p115-interactive proteins GM130 and giantin participate in endoplasmic reticulum-Golgi traffic. J Biol Chem *276*, 2693-2700.

Appenzeller-Herzog, C., and Hauri, H. P. (2006). The ER-Golgi intermediate compartment (ERGIC): in search of its identity and function. J Cell Sci *119*, 2173-2183.

Aroca, P., Urabe, K., Kobayashi, T., Tsukamoto, K., and Hearing, V. J. (1993). Melanin biosynthesis patterns following hormonal stimulation. J Biol Chem *268*, 25650-25655.

Bassi, M. T., Schiaffino, M. V., Renieri, A., De Nigris, F., Galli, L., Bruttini, M., Gebbia, M., Bergen, A. A., Lewis, R. A., and Ballabio, A. (1995). Cloning of the gene for ocular albinism type 1 from the distal short arm of the X chromosome. Nat Genet *10*, 13-19.

Barrowman, J., Sacher, M., and Ferro-Novick, S. (2000). TRAPP stably associates with the Golgi and is required for vesicle docking. Embo J *19*, 862-869.

Bennett, D. C., and Lamoreux, M. L. (2003). The color loci of mice-a genetic century. Pigment Cell Res *16*, 333-344.

Berson, J. F., Harper, D., Tenza, D., Raposo, G., and Marks, M. S. (2001). Pmel17 initiates premelanosome morphogenesis within multivesicular bodies. Mol Biol Cell *12*, 3451-3464.

Berson, J. F., Theos, A. C., Harper, D. C., Tenza, D., Raposo, G., and Marks, M. S. (2003). Proprotein convertase cleavage liberates a fibrillogenic fragment of a resident glycoprotein to initiate melanosome biogenesis. J Cell Biol *161*, 521-533.

Bonifacino, J. S., and Glick, B. S. (2004). The mechanisms of vesicle budding and fusion. Cell *116*, 153-166.

Cai, H., Zhang, Y., Pypaert, M., Walker, L., and Ferro-Novick, S. (2005). Mutants in trs120 disrupt traffic from the early endosome to the late Golgi. J Cell Biol *171*, 823-833.

Cao, X., Ballew, N., and Barlowe, C. (1998). Initial docking of ER-derived vesicles requires Uso1p and Ypt1p but is independent of SNARE proteins. Embo J *17*, 2156-2165.

Chi, A., Valencia, J. C., Hu, Z. Z., Watabe, H., Yamaguchi, H., Mangini, N. J., Huang, H., Canfield, V. A., Cheng, K. C., Yang, F.*, et al.* (2006). Proteomic and bioinformatic characterization of the biogenesis and function of melanosomes. J Proteome Res *5*, 3135-3144.

Chiu, E., Lamoreux, M. L., and Orlow, S. J. (1993). Postnatal ocular expression of tyrosinase and related proteins: disruption by the pink-eyed unstable (p(un)) mutation. Exp Eye Res *57*, 301-305.

Cortese, K., **F. Giordano**, E.M. Surace, C. Venturi, A. Ballabio, C. Tacchetti, and V. Marigo. 2005. The ocular albinism type 1 (OA1) gene controls melanosome maturation and size. *Invest Ophthalmol Vis Sci*. 46:4358-64.

Costin, G. E., Valencia, J. C., Vieira, W. D., Lamoreux, M. L., and Hearing, V. J. (2003). Tyrosinase processing and intracellular trafficking is disrupted in mouse primary melanocytes carrying the underwhite (uw) mutation. A model for oculocutaneous albinism (OCA) type 4. J Cell Sci *116*, 3203-3212.

Cox, R., Chen, S. H., Yoo, E., and Segev, N. (2007). Conservation of the TRAPPII-specific subunits of a Ypt/Rab exchanger complex. BMC Evol Biol *7*, 12.

d'Addio, M., Pizzigoni, A., Bassi, M. T., Baschirotto, C., Valetti, C., Incerti, B., Clementi, M., De Luca, M., Ballabio, A., and Schiaffino, M. V. (2000). Defective intracellular transport and processing of OA1 is a major cause of ocular albinism type 1. Hum Mol Genet *9*, 3011-3018.

Di Pietro, S. M., and Dell'Angelica, E. C. (2005). The cell biology of Hermansky-Pudlak syndrome: recent advances. Traffic *6*, 525-533.

Du, J., and Fisher, D. E. (2002). Identification of Aim-1 as the underwhite mouse mutant and its transcriptional regulation by MITF. J Biol Chem *277*, 402-406.

Ethell, I. M., Hagihara, K., Miura, Y., Irie, F., and Yamaguchi, Y. (2000). Synbindin, A novel syndecan-2-binding protein in neuronal dendritic spines. J Cell Biol *151*, 53-68.

Futter, C. E. (2006). The molecular regulation of organelle transport in mammalian retinal pigment epithelial cells. Pigment Cell Res *19*, 104-111.

Garner, A., and Jay, B. S. (1980). Macromelanosomes in X-linked ocular albinism. Histopathology *4*, 243-254.

Gerst, J. E. (1999). SNAREs and SNARE regulators in membrane fusion and exocytosis. Cell Mol Life Sci *55*, 707-734.

Gether, U. (2000). Uncovering molecular mechanisms involved in activation of G protein-coupled receptors. Endocr Rev *21*, 90-113.

Griffiths, G., and Simons, K. (1986). The trans Golgi network: sorting at the exit site of the Golgi complex. Science *234*, 438-443.

Gwynn, B., Smith, R. S., Rowe, L. B., Taylor, B. A., and Peters, L. L. (2006). A mouse TRAPP-related protein is involved in pigmentation. Genomics *88*, 196-203.

Hearing, V. J., and Tsukamoto, K. (1991). Enzymatic control of pigmentation in mammals. Faseb J *5*, 2902-2909.

Hearing, V. J., Tsukamoto, K., Urabe, K., Kameyama, K., Montague, P. M., and Jackson, I. J. (1992). Functional properties of cloned melanogenic proteins. Pigment Cell Res *5*, 264-270.

Hearing, V. J. (1999). Biochemical control of melanogenesis and melanosomal organization. J Investig Dermatol Symp Proc *4*, 24-28.

Incerti, B., Cortese, K., Pizzigoni, A., Surace, E. M., Varani, S., Coppola, M., Jeffery, G., Seeliger, M., Jaissle, G., Bennett, D. C.*, et al.* (2000). Oa1 knock-out: new insights on the pathogenesis of ocular albinism type 1. Hum Mol Genet *9*, 2781-2788.

Innamorati, G., Piccirillo, R., Bagnato, P., Palmisano, I., and Schiaffino, M. V. (2006). The melanosomal/lysosomal protein OA1 has properties of a G protein-coupled receptor. Pigment Cell Res *19*, 125-135.

Jackson, I. J., Chambers, D. M., Tsukamoto, K., Copeland, N. G., Gilbert, D. J., Jenkins, N. A., and Hearing, V. (1992). A second tyrosinase-related protein, TRP-2, maps to and is mutated at the mouse slaty locus. Embo J *11*, 527-535.

Jimenez, M., Tsukamoto, K., and Hearing, V. J. (1991). Tyrosinases from two different loci are expressed by normal and by transformed melanocytes. J Biol Chem *266*, 1147-1156.

Kim, Y. G., Raunser, S., Munger, C., Wagner, J., Song, Y. L., Cygler, M., Walz, T., Oh, B. H., and Sacher, M. (2006). The architecture of the multisubunit TRAPP I complex suggests a model for vesicle tethering. Cell *127*, 817-830.

King, R.A., Hearing, V.J., Creel, D.J., and Oetting, W.S: (1995). Albinism. In the metabolic and molecular bases of inherited disease. D. Valle, ed. (New York: McGraw-Hill, Inc.), pp. 4353-4392.

Kwon, B. S., Haq, A. K., Pomerantz, S. H., and Halaban, R. (1987). Isolation and sequence of a cDNA clone for human tyrosinase that maps at the mouse c-albino locus. Proc Natl Acad Sci U S A *84*, 7473-7477.

Lang, G. E., Rott, H. D., and Pfeiffer, R. A. (1990). X-linked ocular albinism. Characteristic pattern of affection in female carriers. Ophthalmic Paediatr Genet *11*, 265-271.

Liou, W., Geuze, H. J., and Slot, J. W. (1996). Improving structural integrity of cryosections for immunogold labeling. Histochem Cell Biol *106*, 41-58.

Lowe, M. (2000). Membrane transport: tethers and TRAPPs. Curr Biol *10*, R407-409.

Marks, M. S., and Seabra, M. C. (2001). The melanosome: membrane dynamics in black and white. Nat Rev Mol Cell Biol *2*, 738-748.

Miller, E. A. (2007). Vesicle tethering: TRAPPing transport carriers. Curr Biol *17*, R211-213.

Moyer, B. D., Allan, B. B., and Balch, W. E. (2001). Rab1 interaction with a GM130 effector complex regulates COPII vesicle cis-Golgi tethering. Traffic *2*, 268-276.

Morozova, N., Liang, Y., Tokarev, A. A., Chen, S. H., Cox, R., Andrejic, J., Lipatova, Z., Sciorra, V. A., Emr, S. D., and Segev, N. (2006). TRAPPII subunits are required for the specificity switch of a Ypt-Rab GEF. Nat Cell Biol *8*, 1263-1269.

Nawrot, M., West, K., Huang, J., Possin, D. E., Bretscher, A., Crabb, J. W., and Saari, J. C. (2004). Cellular retinaldehyde-binding protein interacts with ERM-binding phosphoprotein 50 in retinal pigment epithelium. Invest Ophthalmol Vis Sci *45*, 393-401.

O'Donnell, F. E., Jr., Hambrick, G. W., Jr., Green, W. R., Iliff, W. J., and Stone, D. L. (1976). X-linked ocular albinism. An oculocutaneous macromelanosomal disorder. Arch Ophthalmol *94*, 1883-1892.

Orlow, S. J. (1995). Melanosomes are specialized members of the lysosomal lineage of organelles. J Invest Dermatol *105*, 3-7.

Pierce, K. L., Premont, R. T., and Lefkowitz, R. J. (2002). Seven-transmembrane receptors. Nat Rev Mol Cell Biol *3*, 639-650.

Pfeffer, S. R. (1996). Transport vesicle docking: SNAREs and associates. Annu Rev Cell Dev Biol *12*, 441-461.

Piper, R. C., and Luzio, J. P. (2001). Late endosomes: sorting and partitioning in multivesicular bodies. Traffic *2*, 612-621.

Rabouille, C. 1999. Quantitative aspects of immunogold labeling in embedded and nonembedded sections. *Methods Mol Biol*. 117:125-44.

Raposo, G., Kleijmeer M., Posthuma G., Slot J.V., and Geuze H.J (1997). Immunogold labeling of ultrathin cryosections: application in immunology. Chapter 208. In Handbook of experimental immunologo. *Vol 4*. L.A. Herzenberg, D. Weir, L.A. Herzenberg, and C. Blackwell, editors. Blackwell Sciente, Inc., Cambridge, MA. 1-11.

Raposo, G., Tenza, D., Murphy, D. M., Berson, J. F., and Marks, M. S. (2001). Distinct protein sorting and localization to premelanosomes, melanosomes, and lysosomes in pigmented melanocytic cells. J Cell Biol *152*, 809-824.

Raposo, G., and Marks, M. S. (2002). The dark side of lysosome-related organelles: specialization of the endocytic pathway for melanosome biogenesis. Traffic *3*, 237-248.

Raposo, G., and Marks, M. S. (2007). Melanosomes--dark organelles enlighten endosomal membrane transport. Nat Rev Mol Cell Biol *8*, 786-797.

Rohn, W. M., Rouille, Y., Waguri, S., and Hoflack, B. (2000). Bi-directional trafficking between the trans-Golgi network and the endosomal/lysosomal system. J Cell Sci *113 (Pt 12)*, 2093-2101.

Sacher, M., Jiang, Y., Barrowman, J., Scarpa, A., Burston, J., Zhang, L., Schieltz, D., Yates, J. R., 3rd, Abeliovich, H., and Ferro-Novick, S. (1998). TRAPP, a highly conserved novel complex on the cis-Golgi that mediates vesicle docking and fusion. Embo J *17*, 2494-2503.

Sacher, M., Barrowman, J., Wang, W., Horecka, J., Zhang, Y., Pypaert, M., and Ferro-Novick, S. (2001). TRAPP I implicated in the specificity of tethering in ER-to-Golgi transport. Mol Cell *7*, 433-442.

Samaraweera, P., Shen, B., Newton, J. M., Barsh, G. S., and Orlow, S. J. (2001). The mouse ocular albinism 1 gene product is an endolysosomal protein. Exp Eye Res *72*, 319-329.

Schiaffino, M. V., d'Addio, M., Alloni, A., Baschirotto, C., Valetti, C., Cortese, K., Puri, C., Bassi, M. T., Colla, C., De Luca, M., *et al.* (1999). Ocular albinism: evidence for a defect in an intracellular signal transduction system. Nat Genet *23*, 108-112.

Schiaffino, M. V., and Tacchetti, C. (2005). The ocular albinism type 1 (OA1) protein and the evidence for an intracellular signal transduction system involved in melanosome biogenesis. Pigment Cell Res *18*, 227-233.

Seabra, M. C., and Coudrier, E. (2004). Rab GTPases and myosin motors in organelle motility. Traffic *5*, 393-399.

Seiji, M., Fitzpatrick, T. B., Simpson, R. T., and Birbeck, M. S. (1963). Chemical composition and terminology of specialized organelles (melanosomes and melanin granules) in mammalian melanocytes. Nature *197*, 1082-1084.

Sober, A. J., Lew, R. A., Koh, H. K., and Barnhill, R. L. (1991). Epidemiology of cutaneous melanoma. An update. Dermatol Clin *9*, 617-629.

Surace, E. M., Angeletti, B., Ballabio, A., and Marigo, V. (2000). Expression pattern of the ocular albinism type 1 (Oa1) gene in the murine retinal pigment epithelium. Invest Ophthalmol Vis Sci *41*, 4333-4337.

Tai, G., Lu, L., Wang, T. L., Tang, B. L., Goud, B., Johannes, L., and Hong, W. (2004). Participation of the syntaxin 5/Ykt6/GS28/GS15 SNARE complex in transport from the early/recycling endosome to the trans-Golgi network. Mol Biol Cell *15*, 4011-4022.

Theos, A. C., Tenza, D., Martina, J. A., Hurbain, I., Peden, A. A., Sviderskaya, E. V., Stewart, A., Robinson, M. S., Bennett, D. C., Cutler, D. F., *et al.* (2005). Functions of adaptor protein (AP)-3 and AP-1 in tyrosinase sorting from endosomes to melanosomes. Mol Biol Cell *16*, 5356-5372.

Theos, A. C., Truschel, S. T., Tenza, D., Hurbain, I., Harper, D. C., Berson, J. F., Thomas, P. C., Raposo, G., and Marks, M. S. (2006). A lumenal domain-dependent pathway for sorting to intralumenal vesicles of multivesicular endosomes involved in organelle morphogenesis. Dev Cell *10*, 343-354.

Ungar, D., Oka, T., Brittle, E. E., Vasile, E., Lupashin, V. V., Chatterton, J. E., Heuser, J. E., Krieger, M., and Waters, M. G. (2002). Characterization of a mammalian Golgi-localized protein complex, COG, that is required for normal Golgi morphology and function. J Cell Biol *157*, 405-415.

Ungar, D., Oka, T., Krieger, M., and Hughson, F. M. (2006). Retrograde transport on the COG railway. Trends Cell Biol *16*, 113-120.

Van Den Bossche, K., Naeyaert, J. M., and Lambert, J. (2006). The quest for the mechanism of melanin transfer. Traffic *7*, 769-778.

Vetrini, F., Tammaro, R., Bondanza, S., Surace, E. M., Auricchio, A., De Luca, M., Ballabio, A., and Marigo, V. (2006). Aberrant splicing in the ocular albinism type 1 gene (OA1/GPR143) is corrected in vitro by morpholino antisense oligonucleotides. Hum Mutat *27*, 420-426.

Wei, M. L. (2006). Hermansky-Pudlak syndrome: a disease of protein trafficking and organelle function. Pigment Cell Res *19*, 19-42.

Whyte, J. R., and Munro, S. (2002). Vesicle tethering complexes in membrane traffic. J Cell Sci *115*, 2627-2637.

Williams, R. L., and Urbe, S. (2007). The emerging shape of the ESCRT machinery. Nat Rev Mol Cell Biol *8*, 355-368.

Winder, A. J. (1994). A stopped spectrophotometric assay for the dopa oxidase activity of tyrosinase. J Biochem Biophys Methods *28*, 173-183.

Yoshiike, T., Manabe, M., Hayakawa, M., and Ogawa, H. (1985). Macromelanosomes in X-linked ocular albinism (XLOA). Acta Derm Venereol *65*, 66-69.

ACKNOWLEDGEMENTS

I would like to thank my supervisor Dr.Valeria Marigo for giving me the opportunity to work in this project, as well as for her thoughtful guidance and encouragement throughout all my research study. I'm grateful to Dr. Graça Raposo for accepting me in her group during my last year of PhD course and I express my gratitude to her for sharing her knowledge with me, and for her generous support.

I would also like to thank my recent and previous colleagues Francesco, Roberta, Carmine, Mara, Donatella, Alberto, Daniela, Antonella, Sabrina, Cedric, and Guillaume for creating such a wonderful atmosphere at the lab, their suggestions and support during the period we spent working together. I especially wish to thank Roberta for her help at the beginning of my thesis project, and Daniele, Ilse and Maryse for their precious advice.

Lastly, I would like to express my gratitude to all my friends, to Natascia, Paolo and my father. Although far away from me, they have always been present in my heart and in my life.

ARTICLES

1. Katia Cortese[(1)], **Francesca Giordano[(1)],** E.M.Surace, Consuelo Venturi, Andrea Ballabio, Carlo Tacchetti, Valeria Marigo.
   The Ocular Albinism Type 1 (OA1) gene controls melanosome maturation and size (2005). IOVS Dec; 46 (12):4358-4364

   (1) Katia Cortese and Francesca Giordano contributed equally to the work therefore should be considered equivalent authors

2. **Francesca Giordano,** Anna De Marzo, Francesco Vetrini, Valeria Marigo
   Fibroblast growth factor and epidermal growth factor differently affect differentiation of murine retinal stem cells *in vitro* (2007). Molecular Vision; 13:1842-1850

The Ocular Albinism Type 1 (*OA1*) Gene Controls Melanosome Maturation and Size

Katia Cortese,[1,2] *Francesca Giordano,*[2,3] *Enrico M. Surace,*[3] *Consuelo Venturi,*[1] *Andrea Ballabio,*[1,4] *Carlo Tacchetti,*[1] *and Valeria Marigo*[3]

Purpose. The authors took advantage of the *Oa1* mutant mouse in combination with other albinism mouse models (i.e., Tyrosinase and membrane-associated transporter protein [*Matp*]) to study the function of *Oa1*, the gene mutated in ocular albinism type 1, in the RPE during development and after birth.

Methods. Enzyme activity and protein localization were analyzed by immunohistochemistry of tyrosinase (Tyr) in Oa1-null mice. Ultrastructural analysis and morphometry were performed by electron microscopy, of the RPE in Oa1-knockout mouse and double-mutant mice of Oa1 with either Tyr or Matp.

Results. Differently from other albinism models, Tyr activity was not impaired in $Oa1^{-/-}$ eyes. Hypopigmentation of the RPE in $Oa1^{-/-}$ mice is due to a reduced number of melanosomes. Analysis of $Oa1^{-/-}$;$Tyr^{c\text{-}2J}$/$Tyr^{c\text{-}2J}$ and $Oa1^{-/-}$;$Matp^{uw}$/$Matp^{uw}$ double-knockout mice, which display a block at stages II and III of melanosome maturation, respectively, revealed that Oa1 controls the rate of melanosome biogenesis at early stages of the organellogenesis, whereas the control on the organelle size is exerted at the final stage of melanosome development (stage IV).

Conclusions. The findings indicate that Oa1 is involved in the regulation of melanosome maturation at two steps. Acting at early maturation stages, Oa1 controls the abundance of melanosomes in RPE cells. At later stages, Oa1 has a function in the maintenance of a correct melanosomal size. This study helps to define ocular albinism type 1 as a defect in melanosome organellogenesis and not in melanin production. (*Invest Ophthalmol Vis Sci.* 2005;46:4358–4364) DOI: 10.1167/iovs.05-0834

From the [3]Telethon Institute of Genetics and Medicine (TIGEM), Naples, Italy; [1]MicroSCoBiO Research Center and IFOM Center of Cell Oncology and Ultrastructure, Department of Experimental Medicine, University of Genoa, Genoa, Italy; and [4]Medical Genetics, Department of Pediatrics, Federico II University, Naples, Italy.

[2]Contributed equally to the work and therefore should be consider equivalent authors.

Supported in part by Grant 1-FY01-117 from the March of Dimes Birth Defects Foundation, grants from Fondazione Telethon and the Vision of Children Foundation (VM), National Eye Institute Grant 1R01EY015136-01 (AB), and Fondazione Telethon (GTF03001) and MIUR (CT).

Submitted for publication June 29, 2005; revised August 23, 2005; accepted October 20, 2005.

Disclosure: **K. Cortese**, None; **F. Giordano**, None; **E.M. Surace**, None; **C. Venturi**, None; **A. Ballabio**, None; **C. Tacchetti**, None; **V. Marigo**, None

The publication costs of this article were defrayed in part by page charge payment. This article must therefore be marked "*advertisement*" in accordance with 18 U.S.C. §1734 solely to indicate this fact.

Corresponding author: Valeria Marigo, Telethon Institute of Genetics and Medicine (TIGEM) via P. Castellino, 111 80131 Naples, Italy; marigo@tigem.it.

The X-linked form of albinism (ocular albinism type 1) in humans is due to mutations in the ocular albinism type 1 (*OA1*, recently renamed *GPR143*) gene.[1] Although skin pigmentation appears normal, patients manifest the characteristic defects of albinism in the eye, such as translucent iris, photophobia, foveal hypoplasia, nystagmus, and miswiring of the optic tract. Studies conducted in the mouse showed that *Oa1* is specifically expressed in pigment cells of skin and eye.[2] OA1 protein localizes on the membrane of mature melanosomes[3] and in the endolysosome–premelanosome compartment.[4] The protein has homology with members of the G protein-coupled receptor (GPCR) superfamily and binds heterotrimeric G proteins ($G\alpha_i$)[5]; however, a ligand has not been identified yet. The Oa1-null mouse was generated by knocking out the first exon of the mouse gene.[6] As observed in humans, Oa1 loss of function causes the formation of abnormally giant melanosomes (macromelanosomes). Macromelanosomes were detected in the retinal pigment epithelium (RPE) of these mice after birth. Electron microscopy demonstrated that macromelanosomes contain a central core region within the electron-dense melanin, which closely resembled the structure of a normal membrane-free melanosome.[6] This result suggested a mechanism of macromelanosome formation based on overgrowth of a single melanosome rather than fusion of several melanosomes. Nevertheless, the function of Oa1 during melanosome maturation is still obscure. Furthermore, the correlation between macromelanosome and the hypopigmentation of the RPE that causes the albinism phenotype in patients is unclear.

Melanosomes are organelles specialized in the biosynthesis and storage of melanin,[7] in melanocytes of skin and ear, and in RPE cells. Melanosome maturation occurs through sequential maturation stages (I–IV) that can be defined based on morphology.[8] Stage I premelanosomes lack pigment and contain internal membranous vesicles. Stage II melanosomes are elongated in shape, lack pigmentation and contain intraluminal matrix fibers organized in a striated array. Deposition of black melanin along the matrix fibers begins in stage III melanosomes. Finally, stage IV melanosomes are characterized by a dense homogeneous deposit of melanin that covers all the internal structures of the matrix.[8] Melanin is synthesized from the amino acid tyrosine. In the initial step, tyrosine is hydroxylated to L-DOPA, which is in turn oxidized to dopaquinone. Both steps are catalyzed by the enzyme tyrosinase (Tyr). Then dopaquinone is converted into melanin.

There is no evidence of differences in melanosome organellogenesis between RPE and skin melanocytes. However, in contrast to skin melanocytes that transfer their melanosomes to surrounding keratinocytes in the epidermis,[9] ocular melanosomes are retained.[10] Melanization in RPE cells apparently occurs only for a limited period after initial differentiation, and then they permanently halt melanin synthesis.[11]

Mouse mutants have been of great value for the elucidation of the pigmentation process. The albino (*c*) mouse is a spon-

Investigative Ophthalmology & Visual Science, December 2005, Vol. 46, No. 12

taneous mutant with a mutation in the *Tyr* gene, causing loss of tyrosinase enzyme activity and lack of pigmentation. Recently, the molecular basis of the *underwhite* (*uw*) mouse has been defined.[12] The affected gene encodes the membrane-associated transporter protein (Matp). An in vitro study on $Matp^{uw}$ mutant melanocytes suggested that this mutation causes abnormal processing and intracellular trafficking of Tyr to the melanosome.[13] These two spontaneous albino mutants show different phenotypes in the RPE. The Tyr^{c} mouse completely lacks melanin, and melanosomes do not develop beyond stage II. Ultrastructural studies of different *Matp* alleles suggested that the defect was at the level of the melanosome showing irregular shape, reduced size, and maturation impairment.[14] Therefore, these two mouse models provided us with genetic tools to study Oa1 function, either in the absence of melanin production or in impaired melanosomal maturation conditions.

In this study, we addressed the function of Oa1 in pigment cells in vivo, to define better why mutations in *OA1* cause albinism. We generated double-mutant mice of *Oa1* and either $Tyr^{c\text{-}2J}$ or $Matp^{uw}$ and analyzed melanosome phenotype in the absence of melanin synthesis and impaired melanosome maturation. The phenotype of the double-mutant mice compared with single mutants led us to the hypothesis that Oa1 performs two functions in melanogenesis. In particular, Oa1 loss of function causes a reduction in the number of melanosomes in the RPE, suggesting an Oa1 control on the rate of melanosome biogenesis. In addition, double mutant phenotype analysis unraveled a size-control function of Oa1 on the final maturation stage of melanosomes (stage IV).

Material and Methods

Mouse Breeding

The use of animals in this work was in accordance with the ARVO Statement for the Use of Animals in Ophthalmic and Vision Research. Mice were bred and maintained in a 12-hour light–dark cycle. $Oa1^{-/-}$ mice were bred on a C57BL/6 genetic background. $Tyr^{c\text{-}2J}$ and $Matp^{uw}$ mice, both on a C57BL/6 background, were purchased from the Jackson Laboratory (Bar Harbor, ME) and maintained inbred in the animal house. The $Tyr^{c\text{-}2J}$ allele is a recessive mutation due to a G-to-T base change at nucleotide 291 resulting in an amino acid change from arginine to leucine at residue 77. No tyrosinase activity was found in hair bulb extracts from $Tyr^{c\text{-}2J}$ homozygous mice.[15] The $Matp^{uw}$ allele is due to a 7-bp deletion in exon 3 resulting in a 43 amino acid frameshift and premature stop codon, which predicts that the Matp protein lacks the C-terminal six-transmembrane domains.[16]

To generate $Oa1^{-/-}$;$Tyr^{c\text{-}2J}$/$Tyr^{c\text{-}2J}$ and $Oa1^{-/-}$;$Matp^{uw}$/$Matp^{uw}$ mice, single homozygous mutant mice were crossed, and the resultant F_1 double-heterozygous progenies were intercrossed. F_2 progeny was scored for coat color ($Tyr^{c\text{-}2J}$/$Tyr^{c\text{-}2J}$, $Matp^{uw}$/$Matp^{uw}$) and by diagnostic PCR on genomic DNA obtained from the tail for $Oa1^{-/-}$.

Tyrosinase Activity Assay

Eyes were dissected from killed littermates (P7) of different genotypes and frozen at −70°C. Each mouse was genotyped and at least four eyes for each genotype were used for the assay. Each pair of eyes was homogenized on ice in 10% glucose in PBS with 50 μg/mL leupeptin, 20 μg/mL aprotinin, and 5 mM benzamide. Protein concentration was determined using the Bradford method (Bio-Rad, Hercules, CA). Equal quantities of protein were used in each reaction. After the addition of tritiated tyrosine (GE Healthcare, Arlington Heights, IL) to the reaction, Tyr activity was assayed radiometrically by measuring production of tritiated water from hydrolysis of tyrosine, as reported in a published protocol.[17] Activity was expressed as counts per million per microgram per hour of total protein.

Quantitative RT-PCR

Eyes were dissected from either wild-type or *Oa1*-null mice at birth (P0), and total RNA was extracted (TRIzol reagent; Invitrogen-Life Technologies, Gaithersburg, MD), according to the manufacturer's instructions. cDNAs were synthesized (Superscript II; Invitrogen, Carlsbad, CA) and random primers and then amplified (SYBRR Green PCR Master Mix; Applied Biosystems, Inc. [ABI], Foster City, CA) with the forward (f) and reverse (r) intron-spanning primers: GAPDHf (GTATGACTCCAGTCACGGCAAA) and GAPDHr (TTCCCATTCTCGGCCTTG) for glyceraldehyde-3-phosphate; TYRf (CAAGGATCTGGGATATGACTACAGC) and TYRr (GCTCAATAT AATTTCTGTAAAAGCCTGG) for *Tyr*; and MATPf (CCTCCACTACCATGCCCTCCT) and MATPr (CCCAGTCTATGGCACCCAAA) for *Matp*. Quantitative PCR reactions were run in triplicate for each gene (model 7000; ABI). Cyclical reaction values were recorded and preprocessed with the accompanying software (ABI). Data were then normalized to the internal control and statistically analyzed (*t*-test).

RPE Cell Culture

Primary retinal pigment epithelium cells (RPE) and choroidal melanocytes were isolated from P1 eyes of wild-type, $Oa1^{-/-}$, $Tyr^{c\text{-}2J}$ and $Matp^{uw}$ mice.

After a brief (30-minute) treatment with 2 mg/mL Dispase II (Roche, Indianapolis, IN) in Hanks' balanced salt solution (Invitrogen) choroid and RPE were gently separated from neural retina, lens, and vitreous and incubated in 2 mL of 0.5 mg/mL trypsin (Sigma-Aldrich, St. Louis, MO) in Hanks' at 37°C for 30 minutes.

After adding 1 volume of 0.2 mg/mL trypsin inhibitor (Roche) in DMEM (Invitrogen), the tissue was triturated 50 times with a borehole glass pipette. The single-cell suspension was resuspended in 1 mL/eye DMEM-Ham's F-12 1:1 (Invitrogen) containing 5% FBS and N2 hormone mix (Invitrogen) and plated on extracellular matrix (ECM) gel (Sigma) at 37°C in a 5% CO_2 atmosphere. Cells were cultured for 4 to 5 days and not propagated in culture. Cell identity was defined by pigmentation and by expression of Tyr, Trp1, and Trp2[18–20] for RPE and choroidal melanocytes and by Cralbp for RPE cells.[21]

Immunofluorescence

Cells were fixed in 4% paraformaldehyde/PBS, permeabilized with 0.1% saponin in 10%FBS/PBS and incubated with polyclonal antibodies anti-Oa1, raised against the C terminus (last 14 amino acids) of murine Oa1, anti-Tyr,[19] anti-Cralbp[21] in 0.01% saponin, 1% FBS/PBS. Alexa Fluor goat anti-rabbit was used as the secondary antibody (Molecular Probes, Eugene, OR). Immunofluorescence was visualized with a laser confocal microscope system (Leica, Heidelberg, Germany).

Ultrastructural Analysis

P7 and 3-month-old mice of different genotypes were anesthetized and perfused with 4% paraformaldehyde and 2% glutaraldehyde in PBS. Eyes were removed and placed in 0.1 M cacodylate buffer, containing 2.5% glutaraldehyde, for 3 hours at room temperature. Eyes were postfixed in osmium tetroxide for 1 hour and uranyl acetate another hour. Subsequently, samples were dehydrated through a graded ethanol series and propylene oxide and embedded in resin (Poly-Bed; Polysciences, Inc., Warrington, PA) overnight at 42°C and 2 days at 60°C. A dorsoventral orientation was maintained during embedding. Semithin sectioning (0.5 μm) was started at the frontal pole of the embedded eye (corresponding to the cornea) and ultrathin sections (50 nm) were collected, starting when the RPE was observed. Ultrathin sections were stained with uranyl acetate and lead citrate and observed with an electron microscope (model CM10 or Model G2 Tecnai; Philips, Eindhoven, The Netherlands). We analyzed comparable regions of the different genotypes.

The number of melanosomes and their maturation stages in the RPE of single- and double-mutant mice were analyzed on 10 random micrographs at ×21,000, either at the apical zone or the basal zone of the

epithelium. The basal zone was defined by the presence of basal lamina, the apical zone by the presence of microvilli, and the limit between the two regions was drawn at half distance between the apical and basal surfaces. Diameters were measured on melanosomes at different stages of maturation (II, III and IV) in each micrograph (Photoshop 7.0 software; Adobe Systems, Mountain View, CA). For statistical analysis, we applied unpaired *t*-test assuming equal variances.

RESULTS

Effect of Oa1 Loss of Function on Tyr activity and the Rate of Melanosome Biogenesis in the RPE

The albino phenotype in patients with ocular albinism type 1 is often correlated with macromelanosome formation; however hypopigmentation of the ocular fundus could not simply be explained by giant melanosomes. In fact, melanin appears to be synthesized in the absence of OA1, as suggested by pigmentation of skin and hair in patients. To quantify this observation, we measured activity of Tyr in eye protein extracts from the Oa1 mutant, heterozygous, and wild-type mice 7 days after birth (P7) and found no significant difference among the different genotypes (Fig. 1). Therefore, in contrast to other albinism models,[22] lack of Oa1 does not impair Tyr activity in the eye. It is otherwise possible that albinism in OA1 is due to a decreased abundance of melanosomes in the RPE. In one of our previous studies, based on light microscopy analysis, we failed to detect differences in pigment granule number in the RPE of Oa1-knockout mice.[6] We therefore chose a more sensitive technique, such as morphometric studies by electron microscopy. We evaluated density (number of organelles per square micrometer) and distribution of melanosomes in the RPE of wild-type and Oa1 mutant mice at different developmental and postnatal stages. At embryonic day (E)15.5, newborn (P0), and later postnatal stages (P7 and 3 months), the melanosome population in wild-type RPE comprised mostly mature stage-IV melanosomes (Table 1). However, a sizable fraction of the melanosomes was still at stage II at E15.5 (31%), and at stage III at P0 (14%). The total number of melanosomes increased progressively and reached a plateau at P7 (Table 1). The changes in the total number of melanosomes reflected almost exclusively the modifications in the stage-IV population, probably due to the relative paucity of stages II and III at P0, P7, and 3 months (Table 1).

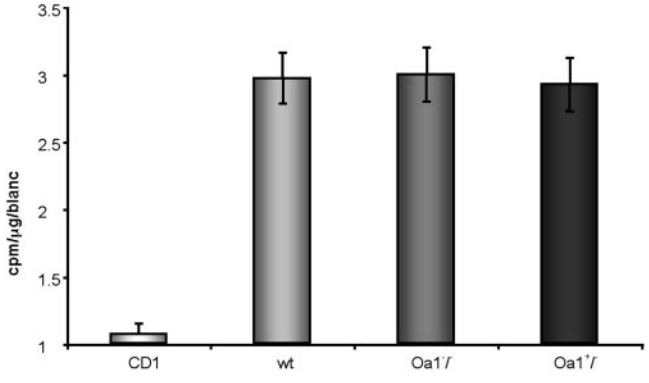

FIGURE 1. Tyrosinase activity assay on eyes at the age of 7 days after birth. ANOVA confirmed no significant difference in the enzymatic activity among wild-type (wt, $n = 9$), Oa1 heterozygous ($Oa1^{+/-}$, $n = 9$), and homozygous ($Oa1^{-/-}$, $n = 6$) mice. Tyrosinase activity in albino control CD1 mice was significantly different from that in wild-type (*t*-test $P < 0.001$). Data are shown as the mean divided by the blanc (CD1 mice that have no Tyr activity have a value close to 1, therefore activity equal to blanc).

TABLE 1. Number of Melanosomes in the RPE of Wild-Type and $Oa1^{-/-}$ Mice at the Different Developmental Stages

	Stage			
	II	III	IV	Area μm^2
Wild-type				
E15.5	9	1	18	186
P0	3	13	75	186
P7	0	4	132	186
3 months	9	2	136	186
$Oa1^{-/-}$				
E15.5	2	2	17	186
P0	10	8	37	186
P7	0	4	63	186
3 months	0	5	58	186

The total area of the cell analyzed (area) was determined by the point-intersection method and expressed in square micrometers.[29]

In Oa1 mutant RPE we found that the melanosome population, similar to wild-type RPE, comprised mostly stage IV melanosomes (Table 1), which included also macromelanosomes at P0, P7, and 3 months. Similar to the phenotype described in patients,[23] only a fraction of melanosomes was enlarged, and we calculated that approximately 20% of melanosomes in the RPE displayed the macromelanosome phenotype (>1.5 μm; Table 2). Of note, when compared with wild-type RPE, the total number of melanosomes was lower, showing 25% reduction at E15.5 ($P < 0.05$), 40% at P0, 50% at P7, and 57% at 3 months ($P = 0.01$, Table 1). A more detailed analysis of the relative changes among different stages of melanosomes revealed that the reduction was mostly attributable to the stage-IV population at P0, P7, and 3 months, whereas at E15.5, it was due to changes in immature stage II melanosomes (Table 1). With respect to the cellular distribution of melanosomes, Oa1 mutants did not show differences when compared with wild-type RPE (data not shown).

The reduced number of stage-IV melanosomes was not accompanied by the appearance of autophagosomes, suggesting that the event was probably due to a reduced rate of melanosome biogenesis, rather than degradation of already formed organelles.

Effect of $Oa1^{-/-}$, $Tyr^{c\text{-}2J}$, and $Matp^{uw}$ Mutations on Each Other and Cellular Distribution

Our analysis of the Oa1 mutant RPE suggested that Oa1 is involved in controlling both the rate of melanosome biogenesis and the size of stage-IV melanosomes. To define which stage of melanosome maturation was the target of Oa1 activity, we generated double-mutant mice of Oa1 with two other albinism mouse models (i.e., $Tyr^{c\text{-}2J}$ and $Matp^{uw}$) in which melanosomes are unable to undergo full maturation. Although in $Tyr^{c\text{-}2J}$ mice melanin is not synthesized and melanosomes stop their maturation at stage II (Fig. 4B), in $Matp^{uw}$ mice, the mutation causes a block of maturation at stage III (Ref. 24 and Fig. 4B). The double mutant strategy would have only been successful if each pair of selected gene mutations did not interfere with their reciprocal expression and/or distribution. Therefore, before generating double-mutant mice we analyzed expression and distribution of Oa1 protein in $Tyr^{c\text{-}2J}$ and $Matp^{uw}$ mutants. To this end, we generated primary cultures of pigment cells dissected from wild-type, $Oa1^{-/-}$, $Tyr^{c\text{-}2J}$, and $Matp^{uw}$ neonatal eyes. These cultures contained both RPE and choroidal cells as defined by immunodetection of pigment cell markers (i.e., Tyr, Tyrp1, and Tyrp2, data not shown). To discriminate between the two cell populations, we performed

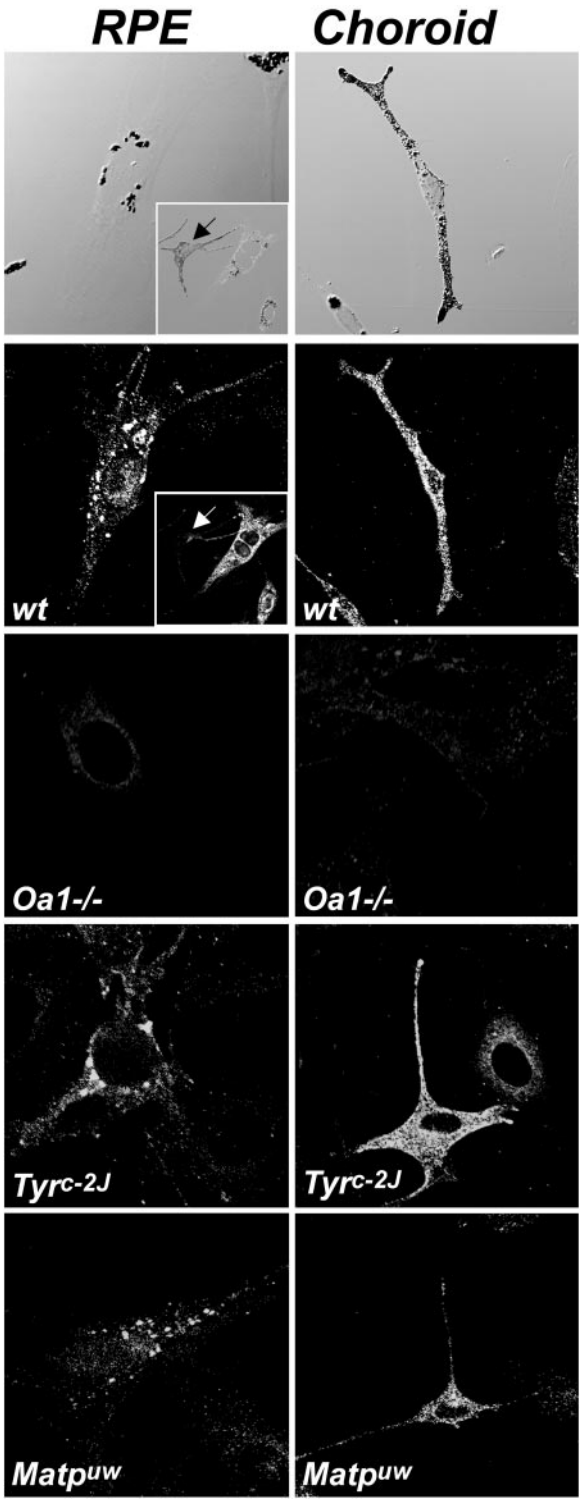

FIGURE 2. Oa1 expression and distribution in $Tyr^{c\text{-}2J}$ and $Matp^{uw}$ eyes. Pigmented cells dissociated from eyes of neonatal wild-type (wt), $Oa1^{-/-}$, $Tyr^{c\text{-}2J}$, and $Matp^{uw}$ mice were stained with an anti-Oa1 antibody. The identity of RPE cells was assessed by staining with anti-Cralbp antibody (*inset*), which does not label choroidal pigmented cells (*arrow*). *Top*: interferential reflection micrographs of a typical RPE (*left*) and choroid (*right*) cell. *Bottom*: immunofluorescence detection of Oa1 in wild type, $Oa1^{-/-}$; $Tyr^{c\text{-}2J}$, and $Matp^{uw}$ in RPE and choroidal cells. Expression of Oa1 in $Tyr^{c\text{-}2J}$ and $Matp^{uw}$ RPE and choroidal cells was similar to wild-type, whereas Oa1 could not be detected, as expected, in $Oa1^{-/-}$ RPE, and choroid.

immunofluorescence studies using antibodies to Cralbp, a specific marker for RPE cells[21] and confirmed that cells with elliptic big pigment granules were RPE cells (Fig. 2, inset). As expected, labeling with an Oa1-specific antibody demonstrated colocalization of Oa1 with pigmented granules in wild-type cell cultures, whereas no signal was detected in $Oa1^{-/-}$ cells. Oa1 was normally expressed and distributed in $Tyr^{c\text{-}2J}$ and $Matp^{uw}$ mutant RPE and choroidal melanocytes (Fig. 2).

We then analyzed expression of *Tyr* and *Matp* mRNA in Oa1 mutant eyes at birth by quantitative real-time PCR. *Tyr* and *Matp* expression was not impaired in the $Oa1^{-/-}$ genotype compared with the wild-type (Fig. 3A, 3B). Finally, we analyzed Tyr distribution in RPE and choroidal melanocyte primary cultures derived from $Oa1^{-/-}$ neonatal eyes. We found that Oa1 loss of function did not affect Tyr distribution (Figs. 3E,

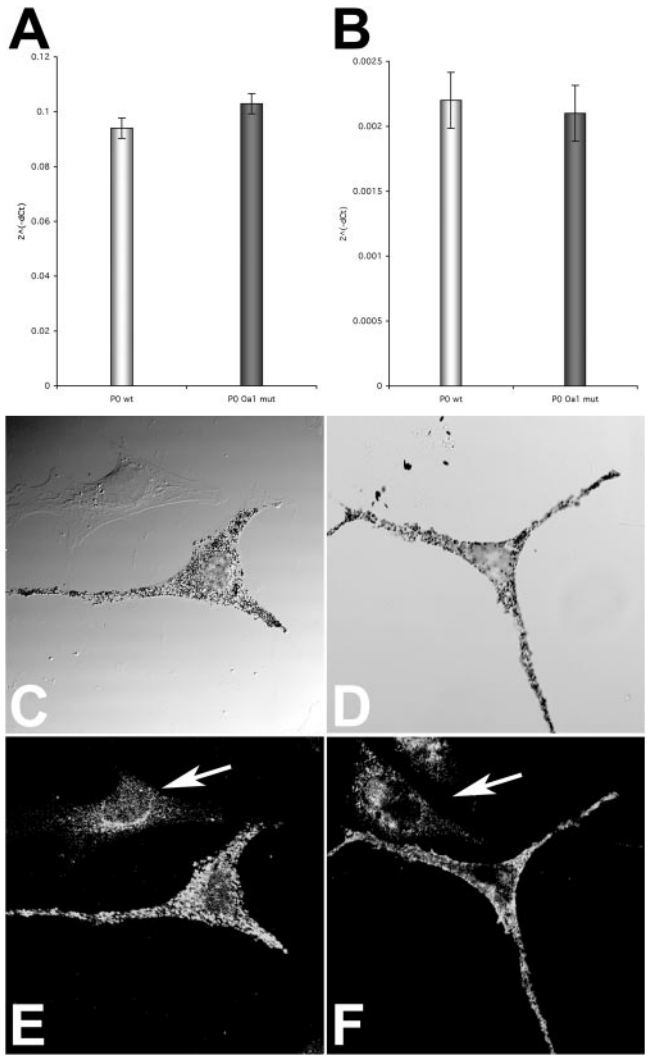

FIGURE 3. Tyrosinase and Matp expression in Oa1 mutant eyes. (**A**) Real-time quantitative RT-PCR of *Tyr* in neonatal (P0) wild-type (wt), and $Oa1^{-/-}$ (Oa1 mut) eyes. *y-Axis*: $2^{(-dCt)}$ value represents differences between the mean *Ct* (cycle threshold) values of tested genes and those of reference gene. (**B**) Real-time quantitative RT-PCR of *Matp* in neonatal (P0) wild-type (wt) and $Oa1^{-/-}$ (Oa1 mut) eyes. (**C**–**F**) Immunofluorescence analysis of Tyr distribution in RPE (*arrows*) and choroid-dissociated cells. (**C**, **E**) Micrographs of cells derived from wild-type mice, (**D**, **F**) micrographs of cells derived from $Oa1^{-/-}$ mice, (**C**) and (**D**) are bright-field phase images of the cells in (**E**) and (**F**), respectively.

TABLE 2. Size Distribution of Melanosomes in the RPE of Different Genotypes

	Diameter			
	<1 μm	1–1.5 μm	>1.5 μm	Mean Diameter (μm)
Stage IV				
Wild-type				
P7				
%	90	10	0	0.51
n	106	11	0	
3 months				
%	92	8	0	0.61
n	98	9	0	
Oa1$^{-/-}$				
P7				
%	63	14	23	0.90
n	30	7	11	
3 months				
%	44	40	16	1.00
n	21	19	8	
Stage II				
Tyr$^{c\text{-}2J}$/*Tyr*$^{c\text{-}2J}$				
P7				
%	100	0	0	0.56
n	118	0	0	
Oa1$^{-/-}$;*Tyr*$^{c\text{-}2J}$/*Tyr*$^{c\text{-}2J}$				
P7				
%	95	5	0	0.67
n	41	2	0	
Stage III				
Matp^{uw}/*Matp*^{uw}				
3 months				
%	87	13	0	0.54
n	14	2	0	
Oa1$^{-/-}$/*Matp*^{uw}/*Matp*^{uw}				
3 months				
%	97	3	0	0.56
n	40	1	0	

Data report the number (*n*) and the percentage (%) of the melanosomes counted in each condition and falling in each of the three ranges of diameter shown.

3F). Therefore, the absence of Oa1 does not interfere with the expression of Tyr and Matp.

Altogether, these results suggest that Oa1, Tyr, and Matp do not reciprocally influence each others expression and subcellular distribution.

Effect of Oa1 on Rate of Melanosome Biogenesis and Organelle Size

We generated *Oa1*$^{-/-}$;*Tyr*$^{c\text{-}2J}$/*Tyr*$^{c\text{-}2J}$ double-mutant mice and analyzed the melanosome phenotype in RPE at P7. At this time point, both the reduced number of melanosomes and the macromelanosome phenotype are easily detectable in Oa1-null mice (Tables 1, 2; Ref. 6). At P7, no melanin was deposited in the melanosomes of *Tyr*$^{c\text{-}2J}$/*Tyr*$^{c\text{-}2J}$ single-mutant or *Oa1*$^{-/-}$;*Tyr*$^{c\text{-}2J}$/*Tyr*$^{c\text{-}2J}$ double-mutant RPE, and melanosomes stopped their maturation at stage II (Fig. 4, Table 3). Of interest, the number of stage II melanosomes was reduced in the *Oa1*$^{-/-}$;*Tyr*$^{c\text{-}2J}$/*Tyr*$^{c\text{-}2J}$ double-mutant compared with the *Tyr*$^{c\text{-}2J}$/*Tyr*$^{c\text{-}2J}$ single-mutant RPE (Table 3).

We then evaluated whether the size of melanosomes was affected by the combination of the two mutations. To this purpose, we compared the diameter at P7 of the most mature stages in each genotype (i.e., stage II in *Tyr*$^{c\text{-}2J}$/*Tyr*$^{c\text{-}2J}$ and *Oa1*$^{-/-}$;*Tyr*$^{c\text{-}2J}$/*Tyr*$^{c\text{-}2J}$ and stage IV in *Oa1*$^{-/-}$). Stage II melanosomes had an average diameter of 0.56 μm in *Tyr*$^{c\text{-}2J}$/*Tyr*$^{c\text{-}2J}$ single mutant RPE and of 0.67 μm in the double mutant RPE (Table 2). These values were similar to those obtained from wild-type stage-IV melanosomes (average value, 0.51 μm; Table 2). On the contrary, they were smaller compared with *Oa1*$^{-/-}$ macromelanosomes (average value, 0.9 μm; Table 2).

The reduced number of stage-II melanosomes in double-mutant RPE demonstrates that Oa1 contributes to the rate of melanosome maturation at early stages and independently of melanin synthesis. However, we could not define yet whether melanin synthesis and/or melanosome maturation are necessary for the regulation of melanosomal size by Oa1.

Effect of Melanosome Maturation

To address whether melanin deposition and/or melanosome maturation are involved in the macromelanosome phenotype, we analyzed the RPE in P7 and 3 month old *Oa1*$^{-/-}$;*Matp*^{uw}/*Matp*^{uw} double-mutant mice. In fact *Matp*^{uw}/*Matp*^{uw} adult

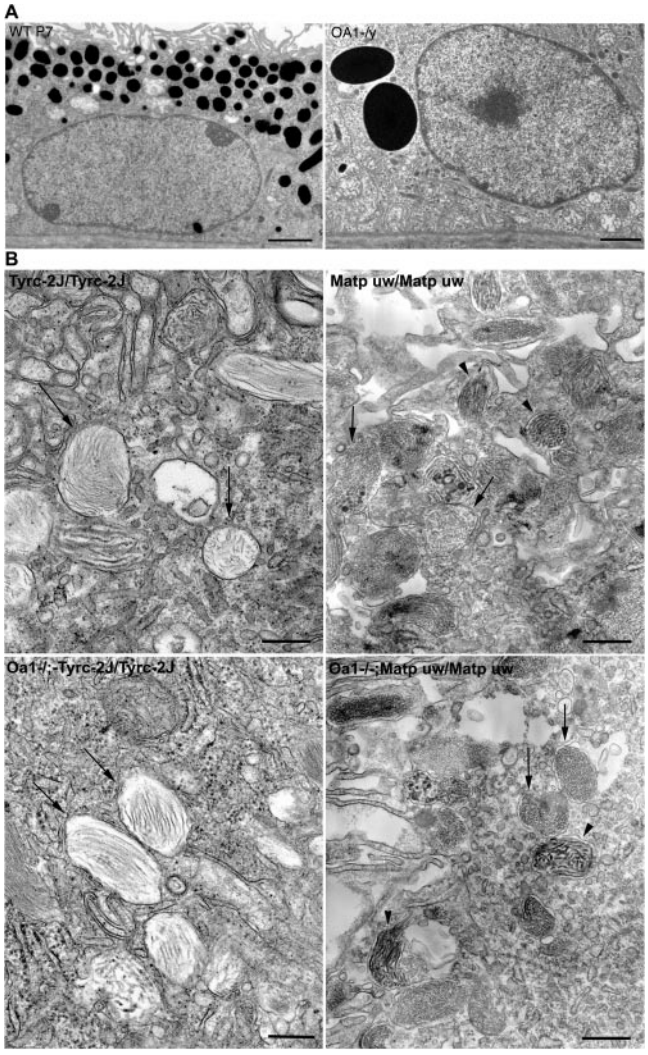

FIGURE 4. Ultrastructural analysis of RPE melanosomes in different genotypes. (**A**) Micrographs of RPE cells from wild-type and *Oa1*$^{-/-}$ mice at P7. Photographs are at the same magnification and show the difference in size of the melanosomes in the two animals. Bar, 2.55 μm. (**B**) Micrographs of RPE melanosomes from *Tyr*$^{c\text{-}2J}$/*Tyr*$^{c\text{-}2}$ and *Oa1*$^{-/-}$;*Tyr*$^{c\text{-}2J}$/*Tyr*$^{c\text{-}2}$ and *Matp*^{uw}/*Matp*^{uw} and *Oa1*$^{-/-}$;*Matp*^{uw}/*Matp*^{uw} mutant mice. *Arrows*: representative stage-II melanosomes. Different stages of melanosomes were found in RPE of *Matp*^{uw}/*Matp*^{uw} single and *Oa1*$^{-/-}$;*Matp*^{uw}/*Matp*^{uw} double-mutant mice. *Arrowheads*: stage III melanosomes. Bar, 0.47 μm.

TABLE 3. Number of Melanosomes in RPE of $Tyr^{c\text{-}2J}/Tyr^{c\text{-}2J}$ and $Oa1^{-/-}$; $Tyr^{c\text{-}2J}/Tyr^{c\text{-}2J}$ Mutant Mice, and $Matp^{uw}/Matp^{uw}$ and $Oa1^{-/-}$; $Matp^{uw}/Matp^{uw}$ Mutant Mice

	Stage			Area (μm^2)
	II	III	IV	
$Tyr^{c\text{-}2J}/Tyr^{c\text{-}2J}$				
P7	97	0	0	355
$Oa1^{-/-}$;$Tyr^{c\text{-}2J}/Tyr^{c\text{-}2J}$				
P7	62	0	0	355
$Matp^{uw}/Matp^{uw}$				
3 months	31	20	0	186
$Oa1^{-/-}$;$Matp^{uw}/Matp^{uw}$				
3 months	17	50	0	186

The total area of the cell analyzed (area) was determined by the point-intersection method and expressed in square micrometers.[29]

RPE was previously reported to display smaller but pigmented melanosomes.[14] Whereas at P7 we did not detect any melanosome in both $Matp^{uw}/Matp^{uw}$ and double-mutant mice (data not shown), at 3 months of age, in both genotypes RPE melanosomes did not proceed beyond stage III (Table 3). The $Matp^{uw}/Matp^{uw}$ single mutant showed a reduction in melanosome number compared with the $Oa1^{-/-}$;$Matp^{uw}/Matp^{uw}$ double mutant, though the difference is not significant. By morphometry, we measured similar diameters in the $Matp^{uw}/Matp^{uw}$ single mutant (0.54 μm) and in the $Oa1^{-/-}$;$Matp^{uw}/Matp^{uw}$ double mutant (0.56 μm) RPE (Table 2C). However, when analyzed in detail, the relative distribution of the different stages of melanosome showed a reduction in the number of stage-II melanosomes in the double-mutant compared with $Matp^{uw}/Matp^{uw}$ single-mutant RPE (Table 3). This event was accompanied by an increased percentage of stage-III melanosomes (75% of total melanosomes) in $Oa1^{-/-}$;$Matp^{uw}/Matp^{uw}$ double-mutant RPE when compared with $Matp^{uw}/Matp^{uw}$ single mutant RPE (40% of total melanosomes; Table 3). Therefore melanosome maturation increased ($P = 0.01$) in the absence of both Oa1 and Matp, although the block of melanosome maturation at stage III characterizing $Matp^{uw}/Matp^{uw}$ single-mutant RPE was retained.

Altogether these results suggested that Oa1 exerts a size control function only on fully developed stage-IV melanosomes, independent of melanin synthesis. Therefore, melanosome maturation and not melanin deposition has a direct influence on the formation of macromelanosomes.

DISCUSSION

Two main classes of albinism that affect pigmentation in the eye have been described: oculocutaneous albinism (OCA) and ocular albinism (OA). In OCA hypopigmentation is caused by inadequate melanization of an apparently normal number of melanosomes, whereas OA was suggested to result from reduced number of melanosomes.[25] Patients with OA1 have a severe reduction of visual acuity, horizontal and rotary nystagmus, photophobia, and lack of stereoscopic vision due to misrouting of the optic tract. A peculiar melanosome phenotype in these patients was characterized by the presence of pigmented melanosomes with a giant size,[23,25] suggesting that the absence of OA1 could interfere with the normal melanosome biogenesis. However, we still lack a comprehensive view of how this phenotype is acquired and how it relates with the albino phenotype observed in the RPE. In particular, it is unclear how the presence of pigmented melanosomes reconciles with the observed albino phenotype in the RPE, at which stage(s) of melanosome maturation OA1 exerts its function, and whether an impaired control of melanin synthesis and/or of rate of melanosome biogenesis is involved in giant melanosome formation. Our study addresses these important questions and allows defining the differences between OA (albinism isolated to the eye) and OCA. We focused our attention on two aspects of melanogenesis in the RPE: rate of melanosome formation and size control. We found that these events are both affected by lack of Oa1 activity.

We first characterized Oa1 interaction with Tyr and showed that there is no impairment in Tyr activity and expression in Oa1 mutant mice. This aspect of the phenotype differentiates Oa1 from other albino mice in which melanin production is affected.[22] However, the number of mature melanosomes in Oa1 mutant eyes was reduced by 50% in the RPE after birth. This reduction was in the number of stage IV melanosomes. It is possible that the effect on other melanosomal stages is masked by the lower number of stage-II and -III organelles after birth. In fact, a reduction in the number of stage-II melanosomes was detected both in mutants when melanosome maturation is impaired ($Oa1^{-/-}$;$Tyr^{c\text{-}2J}/Tyr^{c\text{-}2J}$ and $Oa1^{-/-}$;$Matp^{uw}/Matp^{uw}$ double mutants) and at embryonic stages in $Oa1^{-/-}$ RPE. These results demonstrate, for the first time, that the reduced pigmentation of the RPE observed in patients with ocular albinism type 1 is caused by reduced number of pigmented melanosomes.

A second relevant aspect of Oa1 function highlighted by our results is the specificity of Oa1 size control activity on stage-IV melanosomes. This conclusion is based on the absence of melanosome enlargement in the RPE of $Oa1^{-/-}$;$Tyr^{c\text{-}2J}/Tyr^{c\text{-}2J}$ and $Oa1^{-/-}$;$Matp^{uw}/Matp^{uw}$ double-mutant mice which lack stage-IV melanosomes and display either stage-II or -III, respectively. Therefore, in the absence of fully mature melanosomes Oa1 does not exert its size control function.

Whereas the Oa1 size control activity is specific for the most mature melanosomes, an additional Oa1 function appears to be exerted at earlier stages. In particular, in $Oa1^{-/-}$ single and double mutants, the number of stage-II melanosomes was reduced at the earliest stages of maturation analyzed: E15.5 for $Oa1^{-/-}$, and P7 or 3-month postnatal stages for $Oa1^{-/-}$; $Tyr^{c\text{-}2J}/Tyr^{c\text{-}2J}$ and $Oa1^{-/-}$;$Matp^{uw}/Matp^{uw}$ double mutants. In contrast, stage-III melanosomes were more abundant in $Oa1^{-/-}$;$Matp^{uw}/Matp^{uw}$ double mutants compared with $Matp^{uw}/Matp^{uw}$ single-mutant mice. This suggests that Oa1 may at the same time control the maturation rate of melanosomes and inhibit the overgrowth of the most mature ones. In agreement with this interpretation is our previous report of OA1 acting as a negative regulator of melanosome maturation.[26] We cannot exclude, however, that the phenotype observed in double-mutant mice could also be due to a specific interaction between the two genes.

Although we have not defined the mechanisms by which Oa1 may perform its double function, it is of note that heterotrimeric G-proteins associated with intracellular organelles have been described to participate in various steps of secretion and vesicular fusion[27] and organelle maturation,[28] even though no specific intracellular GPCR has yet been described for these functions. We suggest that Oa1 may act as a GPCR, either constitutively active, or activated by melanin or a byproduct of melanin synthesis that controls membrane delivery to the melanosomes. This interpretation could explain the reduction of early stage melanosomes and the macromelanosome phenotype.

Taken together, our findings indicate that Oa1 regulates melanosome maturation. Acting at early maturation stages, Oa1 controls the abundance of melanosomes in RPE cells, and, at later stages, Oa1 has a function in maintaining a correct melanosomal size. The dissection of these two Oa1 activities allows a better understanding of the albinism phenotype due to the

lack of this protein, and in the future it will be important in the design therapeutic approaches for this disease.

Acknowledgments

The authors thank Vittoria M. Schiaffino for collaborating in Oa1 antibody production, Salvatore Arbucci for confocal microscopy, Diego Di Bernardo, Graciana Diez-Roux, and Alberto Auricchio for discussion of the data; and Vincent J. Hearing and John Saari for the reagents.

References

1. Bassi MT, Schiaffino MV, Renieri A, et al. Cloning of the gene for ocular albinism type 1 from the distal short arm of the X chromosome. *Nat Genet.* 1995;10:13–19.
2. Surace EM, Angeletti B, Ballabio A, Marigo V. Expression pattern of the ocular albinism type 1 (OA1) gene in the murine retinal pigment epithelium. *Invest Ophthalmol Vis Sci.* 2000;41:4333–4337.
3. Schiaffino MV, Baschirotto C, Pellegrini G, et al. The Ocular albinism type 1 (OA1) gene product is a membrane glycoprotein localized to melanosomes. *Proc Natl Acad Sci USA.* 1996;93:9055–9060.
4. Samaraweera P, Shen B, Newton JM, Barsh GS, Orlow SJ. The mouse ocular albinism 1 gene product is an endolysosomal protein. *Exp Eye Res.* 2001;72:319–329.
5. Schiaffino MV, d'Addio M, Alloni A, et al. Ocular albinism: evidence for a defect in an intracellular signal transduction system. *Nat Genet.* 1999;23:108–112.
6. Incerti B, Cortese K, Pizzigoni A, et al. Oa1 knock-out: new insights on the pathogenesis of Ocular albinism type 1. *Hum Mol Genet.* 2000;9:2781–2788.
7. Marks MS, Seabra MC. The melanosome: membrane dynamics in black and white. *Nat Rev Mol Cell Biol.* 2001;2:738–748.
8. Orlow SJ. The biogenesis of melanosomes. In: Nordlund JJ, Boissy RE, Hearing VJ, King RA, Ortonne J-P, eds. *The Pigmentary system.* New York: Oxford University Press; 1998:97–106.
9. Jimbow K, Sugiyama S. Melanosomal translocation and transfer. In: Nordlund JJ, Boissy RE, Hearing VJ, King RA, Ortonne J-P, eds. *The Pigmentary System.* New York: Oxford University Press; 1998: 107–114.
10. Boissy RE. Extracutaneous melanocytes. In: Nordlund JJ, Boissy RE, Hearing VJ, King RA, Ortonne J-P, eds. *The Pigmentary System.* New York: Oxford University Press; 1998:59–73.
11. Schraermeyer U. Does melanin turnover occur in the eyes of adult vertebrates? *Pigment Cell Res.* 1993;6:193–204.
12. Newton JM, Cohen-Barak O, Hagiwara N, et al. Mutations in the human orthologue of the mouse underwhite gene (uw) underlie a new form of oculocutaneous albinism, OCA4. *Am J Hum Genet.* 2001;69:981–988.
13. Costin GE, Valencia JC, Vieira WD, Lamoreux ML, Hearing VJ. Tyrosinase processing and intracellular trafficking is disrupted in mouse primary melanocytes carrying the underwhite (uw) mutation: a model for oculocutaneous albinism (OCA) type 4. *J Cell Sci.* 2003;116:3203–3212.
14. Sweet HO, Brilliant MH, Cook SA, Johnson KR, Davisson MT. A new allelic series for the underwhite gene on mouse chromosome 15. *J Hered.* 1998;89:546–551.
15. Kwon BS, Haq AK, Pomerantz SH, Halaban R. Isolation and sequence of a cDNA clone for human tyrosinase that maps at the mouse c-albino locus. *Proc Natl Acad Sci USA.* 1987;84:7473–7477.
16. Du J, Fisher DE. Identification of *Aim-1* as the *underwhite* mouse mutant and its transcriptional regulation by MITF. *J Biol Chem.* 2002;277:402–406.
17. Chiu E, Lamoreux ML, Orlow SJ. Postnatal ocular expression of tyrosinase and related proteins: disruption by the *pink-eyed unstable* (p^{um}) mutation. *Exp Eye Res.* 1993;57:301–305.
18. Jimenez M, Kameyama K, Maloy WL, Tomita Y, Hearing VJ. Mammalian tyrosinase: biosynthesis, processing, and modulation by melanocyte-stimulating hormone. *Proc Natl Acad Sci USA.* 1988; 85:3830–3834.
19. Jimenez M, Tsukamoto K, Hearing VJ. Tyrosinases from two different loci are expressed by normal and by transformed melanocytes. *J Biol Chem.* 1991;266:1147–1156.
20. Tsukamoto K, Jackson IJ, Urabe K, Montague PM, Hearing VJ. A second tyrosinase-related protein, TRP-2, is a melanogenic enzyme termed DOPAchrome tautomerase. *EMBO J.* 1992;11:519–526.
21. Nawrot M, West K, Huang J, et al. Cellular retinaldehyde-binding protein interacts with ERM-binding phosphoprotein 50 in retinal pigment epithelium. *Invest Ophthalmol Vis Sci.* 2004;45:393–401.
22. LaVail JH, Nixon RA, Sidman RL. Genetic control of retinal ganglion cell projections. *J Comp Neurol.* 1978;182:399–421.
23. Wong L, O'Donnell FE Jr, Green WR. Giant pigment granules in the retinal pigment epithelium of a fetus with X-linked ocular albinism. *Ophthalmic Paediatr Genetics*. 1983;2:47–65.
24. Lehman AL, Silvers WK, Puri N, et al. The underwhite (uw) locus acts autonomously and reduces the production of melanin. *J Invest Dermatol.* 2000;115:601–606.
25. O'Donnell FEJ, Hambrick GWJ, Green WR, Iliff WJ, Stone DL. X-linked ocular albinism: an oculocutaneous macromelanosomal disorder. *Arch Ophthalmol.* 1976;94:1883–1892.
26. Schiaffino MV, Dellambra E, Cortese K, et al. Effective retrovirus-mediated gene transfer in normal and mutant human melanocytes. *Hum Gene Ther.* 2002;13:947–957.
27. Helms JB. Role of heterotrimeric GTP binding proteins in vesicular protein transport: indications for both classical and alternative G protein cycles. *FEBS Lett*. 1995;369:84–88.
28. Ahnert-Hilger G, Nurnberg B, Exner T, Schafer T, Jahn R. The heterotrimeric G protein Go_2 regulates catecholamine uptake by secretory vesicles. *EMBO J.* 1998;17:406–413.
29. Rabouille C. Quantitative aspects of immunogold labeling in embedded and nonembedded sections. *Methods Mol Biol.* 1999;117: 125–144.